5-2016

Computational Studies of Spin Trapping of Biologically Relevant Radicals by New Heteroaryl Nitrones

Eyram Asempa
East Tennessee State Universtiy

Computational Studies of Spin Trapping of Biologically Relevant Radicals by New Heteroaryl Nitrones

---

A thesis

presented to

the faculty of the Department of Chemistry

East Tennessee State University

In partial fulfillment

of the requirements for the degree

Master of Science in Chemistry

---

by

Eyram A. Asempa

May 2016

Dr. Scott J. Kirkby, Chair

Dr. Marina Roginskaya

Dr. David Close

Keywords: heteroaryl nitrones, FxBN, PBN, DMPO, biologically relevant radicals, Hartree-Fock Self-Consistent Field, Density Functional Theory

ABSTRACT

Computational Studies of the Spin Trapping of Biologically Relevant Radicals by New Heteroaryl Nitrones

by

Eyram A. Asempa

Heteroaryl nitrone spin traps have been suggested to act as free radical scavengers. The geometry optimizations and the single-point energies of the spin trapping reactions of the heteroaryl nitrones, 5,5-dimethylpyrroline-N-oxide (DMPO) and α-phenyl-N-*t*-butylnitrone (PBN) have been computationally studied using *ab initio* (Hartree-Fock (HF) and second-order Møller-Plesset (MP2)) methods and Density Functional Theory (DFT) methods. The effects of new heteroaryl substituents on a parent nitrone spin trap have been examined at the HF and MP2 levels with the 6-31G*, and cc-pVnZ (n=D, T, Q) basis sets. The thermodynamics of the spin trapping at the C-site and O-site with •H, •CH_3 and •OH radicals were studied at the HF/6-31G* and DFT/m06/6-31G* levels. The addition reactions favor at the C-sites and the double adducts are thermodynamically more stable than the mono adducts. The spin trapping of DMPO, PBN and α(Z)-(3-methylfuroxan-4-yl)-N-*tert*-butylnitrone (FxBN) with •OH have also been studied.

DEDICATION

I dedicate this work to My Almighty God for His deepest Love He has towards me.

ACKNOWLEDGEMENTS

"*The Lord is mine helper and my defender; and mine heart hoped in him, and I am helped.*
And my flesh flowered again; and (out) of my will I shall acknowledge to Him.
(The Lord is my helper and my defender; and my heart trusted Him, and I was helped.
And my heart full out joyed, or rejoiced; and I shall praise him with my song)"

~~ Psalm 28:7 (WYC).

My sincere appreciation goes to my Almighty God for His abundant Love He has towards me, His protection, guidance and grace through my graduate studies and research. I am grateful to the Lord for providing me with wonderful parents and siblings who love, support and sacrifice to see me soar higher in life.

I would like to express my gratitude to my advisor, Dr. Scott Kirkby for his immense guidance, support and useful critiques of this research work. I would also like to thank Drs. Roginskaya and Close (my thesis committee), Dr. Eagle (Chair of the Department of Chemistry), and all faculty members of department. Thank you to the Department of Chemistry, ETSU, for the graduate assistantship during my graduate studies and the ETSU School of Graduate Studies Student Research Grant for funds for my research work.

My appreciation also goes to Ms. Libby Tipton, Disability Services, and Vital Signs for the accommodations.

Not forgetting Bread of Life Ministries, Duke Debrah, Martha Essandoh, Constance Warden, Faisal Ibrahim, Isaac Addo, Angelica Bridges and her family, and all loved ones in the Department of Chemistry who have been supportive and kind during my studies.

Benedicite omnes, God bless you all!

TABLE OF CONTENTS

Page

ABSTRACT....2

DEDICATION....3

ACKNOWLEDGMENTS....4

LIST OF TABLES....7

LIST OF FIGURES....8

LIST OF ABBREVIATIONS....11

Chapter

1. INTRODUCTION....13

Free Radicals....13

Nitrone Spin Traps....14

2. QUANTUM MECHANICS....19

General Introduction to Computational Chemistry....19

The Schrödinger Equation....22

The Hamiltonian Operator....23

Atomic Units....24

The Born-Oppenheimer Approximation....25

The Hartree-Fock Self Consistent Field Method....27

Hartree's Procedure....29

The Wave Function as a Slater Determinant....33

The Variational Principle 33

The Roothaan-Hall Equations 35

Restricted and Unrestricted Hartree-Fock Methods 37

Møller-Plesset Perturbation Theory 38

Density Functional Theory 39

Basis Sets 44

3. RESULTS AND DISCUSSION 48

Computational Details 48

Discussion of the Results 48

4. CONCLUSIONS 80

REFERENCES 81

APPENDIX: Tables of Additional Data from the Calculations 95

VITA 144

LIST OF TABLES

Table Page

1. Calculated bond lengths for formaldonitrone and the new heteroaryl nitrones at HF/6-31G* 50

2. Energies of selected biologically relevant radicals and their dipole moments 52

3. Energies of formaldonitrone and the new heteroaryl nitrones at the HF/6-31G*, MP2/cc-pVDT, MP2/cc-pVTZ, MP2/cc-pVQZ, the MP2 CBS limit, and DFT/m06/6-31G* levels of theory. The dipole moments were calculated at the HF/6-31* level 55

4. Energies of the spin trapping reactions of selected radicals with formaldonitrone and the new heteroaryl nitrones at the C-site for (a) HF/6-31G* and (b) DFT/m06/6-31G*.....57

5. Energies of the spin trapping reactions of biologically relevant radicals with the new heteroaryl nitrones the O-site for (a) HF/6-31G* and (b) DFT/m06/6-31G* 58

6. Energies of the spin trapping reactions of •H with formaldonitrone and the new heteroaryl nitrones at both C- and O-sites at (a) HF/6-31G* and (b) DFT/6-31G*.....67

7. Energies of the spin trapping reactions of •CH_3 with formaldonitrone and the new heteroaryl nitrones at both C- and O-sites at (a) HF/6-31G* and (b) DFT/m06/6-31G* 68

8. Energies of the spin trapping reactions of •OH with formaldonitrone and the new heteroaryl nitrones at both C- and O-sites at (a) HF/6-31G* and (b) DFT/m06/6-31G* 69

9. Energies of the addition of •OH to DMPO, PBN and FxBN at the DFT/m06/6-31G* and HF/6-31* levels of theory.....75

LIST OF FIGURES

Figure Page

1. The addition of a nitrone spin trap to a free radical to produce a nitroxide.....14

2. The resonance stabilization of nitroxide.....15

3. Chemical structures of linear PBN, cyclic DMPO, and several derivatives commonly used as spin traps.....16

4. The reaction of a prototype nitrone with a radical to form a spin adduct.....17

5. The chemical structures of the proposed novel heteroaryl nitrone spin traps.....18

6. Algorithm for self-consistent field theory.....32

7. A flowchart summary of the procedure for solving the Roothaan-Hall equations.....36

8. A graphical representation of the orbital treatment for the RHF, UHF and ROHF methods.....38

9. The optimized geometry of formaldonitrone and the new heteroaryl nitrones. All bond lengths are measured in Å.....51

10. NWChem optimized geometries of biologically relevant radicals.....53

11. ChemDraw® representations of the new heteroaryl spin adducts with •H added at the C-site carbon.....59

12. ChemDraw® representations of the new heteroaryl spin adducts with •CH_3 added at the C-site carbon.....60

13. ChemDraw® representations of the new heteroaryl spin adducts with •OH added at the C-site carbon.....61

14. ChemDraw® representations of the new heteroaryl spin adducts with •H at added at the O-site oxygen.....62

15. ChemDraw® representations of the new heteroaryl spin adducts with •CH_3 added at the O-site oxygen 63

16. ChemDraw® representations of the new heteroaryl spin adducts with •OH added at the O-site oxygen 64

17. NWChem Optimized Geometries of new heteroaryl spin adducts at C- and O- sites. The colors follow standard colors: red - oxygen, hydrogen - white, grey - carbon, blue - nitrogen, and yellow - sulfur 65

18. ChemDraw® representations of the new heteroaryl diadducts with •H added at both the C-site carbon and the O-site oxygen 70

19. ChemDraw® representations of the new heteroaryl diadducts with •CH_3 added at both the C-site carbon and the O-site oxygen 71

20. ChemDraw® representations of the new heteroaryl diadducts with •OH added at both the C-site carbon and the O-site oxygen 72

21. NWChem optimized geometry of the most stable diadduct thermodynamically of 1,2,3-thiadiazol-5-yl nitrone with di •OH at both the C- and O-sites. The colors follow standard colors: red - oxygen, hydrogen - white, grey - carbon, blue - nitrogen, and yellow - sulfur ... 73

22. ChemDraw® representations of 5,5-dimethylpyrroline-N-oxide, phenyl-N-t-butylnitrone and (Z)-(3-methylfuroxan-4-yl)-N-tert-butylnitrone 76

23. NWChem optimized geometry of the spin adduct of PBN with •OH radical at C- site. The colors follow standard colors: red - oxygen, hydrogen - white, grey - carbon, and blue - nitrogen 77

24. NWChem optimized geometry of diadduct of DMPO with di •OH at both the C- and O-sites. The colors follow standard colors: red - oxygen, hydrogen - white, grey - carbon, and blue - nitrogen 78

25. NWChem optimized geometries of a) the spin adduct of FxBN with •OH at C-site and b) the diadduct of FxBN with di •OH at both C- and O- sites. The intramolecular

hydrogen bonds are present in both a) and b). The colors follow standard colors: red - oxygen, hydrogen - white, grey - carbon, and blue - nitrogen.....79

LIST OF ABREVIATIONS

ROS:	Reactive Oxygen Species
I-R:	Ischemia-Reperfusion
EPR:	Electron Spin Resonance
DFT:	Density Functional Theory
a.u.:	Atomic Units
E_h:	hartree
PBN:	*α*-phenyl-N-*t*-butylnitrone
DMPO:	5,5-dimethylpyrroline-N-oxide
DEMPO:	5-Diethoxyphosphoryl-5-methyl-1-pryrroline N-oxide
EMPO:	2-ethoxycarboonyl-2-methyl-3,4-dihydro-2H-pyrrole-1-oxide
BocMPO:	5-tert-butoxycarbonyl-5-methyl-1-pyrroline N-oxide
AMPO:	5-carbamoyl-5-methyl-1-pyroroline N-oxide
FxBN:	*α*(Z)-(3-methylfuroxan-4-yl)-N-*tert*-butylnitrone
HSCF:	Hartree Self-Consistent Field
HF:	Hartree-Fock
HF-SCF:	Hartree-Fock Self-Consistent Field
RHF:	Restricted Hartree-Fock
ROHF:	Restricted Open-shell Hartree-Fock
UHF:	Unrestricted Hartree-Fock
BO:	Born-Oppenheimer

MPPT: Møller-Plesset Perturbation Theory

RSPT: Rayleigh-Schrödinger Perturbation Theory

STO: Slater-Type Orbital

CBS: Complete Basis Set

CHAPTER 1

INTRODUCTION

Free Radicals

A free radical is any species that contains one or more unpaired electrons in the outermost (valence) shell of an atom or molecule.[1] The unpaired electrons change the chemical reactivity of the molecule,[2] which makes it more reactive and unstable than the corresponding diamagnetic specie. Free radicals are classified by different criteria and these include reactive oxygen species (ROS, *e.g.* superoxide radical anion ($O_2^{\bullet -}$) and hydroxyl radical (OH•)), reactive nitrogen species (nitric oxide (NO•), peroxynitrite ($ONOO^-$)), sulfur-centered radicals (thiyl radicals (RS•)), and carbon-centered radicals (trichloromethyl (CCl_3•)). They are produced in a wide variety of chemical and biological systems including the formation of plastics, the ageing of paints, the combustion of fuels, and in the human body.[3] Human bodies generate free radicals through the action of internal and external factors.[4] Internal factors include metabolic processes that generate free radicals in the biological systems such as mitochondria and phagocytes.[5] External factors generating free radicals include exposure to X-rays, ozone, cigarette smoking, air pollutants, and industrial chemicals.[6] Psychological factors, like stress and emotion, can also generate free radicals through physiological responses.[7]

Most of the radicals of interest in biological systems are short-lived molecules with half-lives ranging from 10^{-3} to 10^{-9} s.[8] They are required for normal cell function in controlled amounts, but when in excess, can cause damage to cell membranes and other tissue leading to cancer, cardiovascular disease, neurological disorders, ischemia-reperfusion (I-R), and other diseases.[9-12]

Nitrone Spin Traps

Spin traps are diamagnetic compounds that have the ability to trap and stabilize free radicals in chemical and biological systems. Spin trapping was named by E.G. Janzen and is a chemical reaction in which free radicals add to diamagnetic compounds (spin traps) to produce more stable radical products (spin adducts).[13,14] Franchi *et al*.[15] and Spulber *et al*.[16] have stated that the use of spin trapping for the detection of radicals has contributed significantly to the understanding of some of the fundamental free-radical-mediated processes in chemical and biological systems.

Nitrones are organic compounds that are used as spin traps in both chemical and biological systems. The simplest chemical formula for a nitrone is given as X–CH=NO–Y where X and Y are alkyl or aryl substituents.[17] They are used as a key synthetic precursor,[18] therapeutic agent,[19,20] and a spin trapping agent for the detection and characterization of free radicals.[21-24] The design of the nitrone spin traps plays an important role in determining how informative and sensitive the spin trapping technique may be for a particular free radical.[25] The addition of a nitrone spin trap to a free radical leads to the formation of a stable nitroxide.

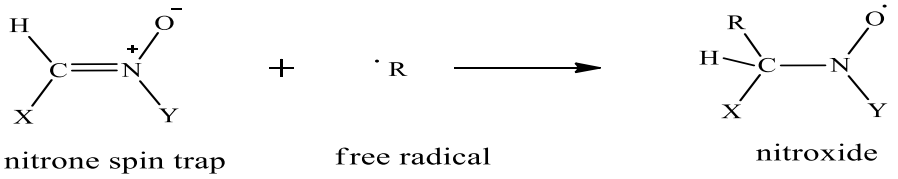

Figure 1: The addition of a nitrone spin trap to a free radical to produce a nitroxide

A nitroxide is a stable free radical because of resonance stabilization of the unpaired electron between the nitrogen and the oxygen of the nitroxyl functional group.[26]

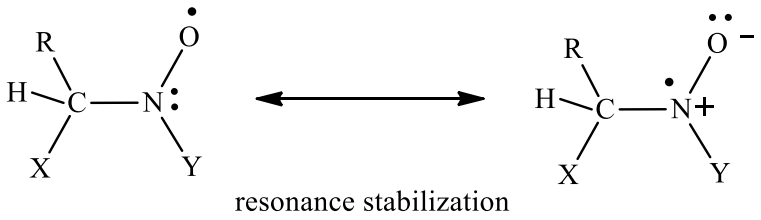

Figure 2: The resonance stabilization of nitroxide

Novelli *et al*.[27-29] proposed the use of nitrones as potential pharmacological agents. They are mostly non-toxic and are used as nitrone-based therapeutics in the treatment of oxidation stress-mediated diseases such as neurodegeneration, cardiovascular disease, and cancer. They are able to survive long enough in biological systems to allow detection of the radicals. Nitrone spin traps can also be used as reagents for the detection of radicals in fuel cell research,[30-32] nanotechnology,[33,34] catalysis,[35] environmental remediation,[36] and photodynamic therapy.[37-39] Basically, there are two classes of nitrone spin traps. There are the linear nitrones: α-phenyl-N-t-butylnitrone (PBN, see Figure 3) and its derivatives and the pyrroline-based cyclic nitrones: 5,5-dimethyl pyrroline-N-oxide (DMPO) and its derivatives.[40-43] The linear nitrones are mostly used as spin traps in *in-vitro*, *in-vivo* and *ex-vivo* systems[44,45] and have shown neuroprotective and antioxidant activities as well as free radical scavenger properties.[46-50] The pyrroline based cyclic nitrones, DMPO and its derivatives have shown to have better ability to trap oxygen-centered radicals and reactive nitrogen species. These are 5-diethoxyphosphoryl-5-methyl-1-pryrroline N-oxide (DEPMPO),[51] and 2-ethoxycarboonyl-2-methyl-3,4-dihydro-2H-pyrrole-1-oxide (EMPO),[52] 5-tert-butoxycarbonyl-5-methyl-1-pyrroline N-oxide (BocMPO).[53] However, these spin traps are not effective for all free radical species. A new family of spin traps of EMPO derivatives has been synthesized and their spin adducts have shown to give reasonable stability.[54,55] Also, research has shown that an amido derivative, 5-carbamoyl-5-methyl-1-pyrroline N-oxide (AMPO) has the highest rate constant of superoxide trapping, followed by

EMPO, with both DEPMPO and DMPO having the slowest reactivity.[56,57] The advantages of using nitrone spin traps are: they are less sensitive to light, oxygen, and water vapor; they are soluble in a large number of solvents at fairly high concentrations (~0.1M); and the spin adducts are considerably more stable because a carbon atom separates the nitroxide functional group from the trapped radical species.[24,58] However, the available nitrone spin traps present many disadvantages such as low water solubility, sensitivity to nucleophilic attack by water, and low stability of the spin adduct formed. Also, the information regarding the nature and structure of the trapped species is difficult to obtain from the Electron Paramagnetic Resonance (EPR) spectrum of the spin adduct.[58-61]

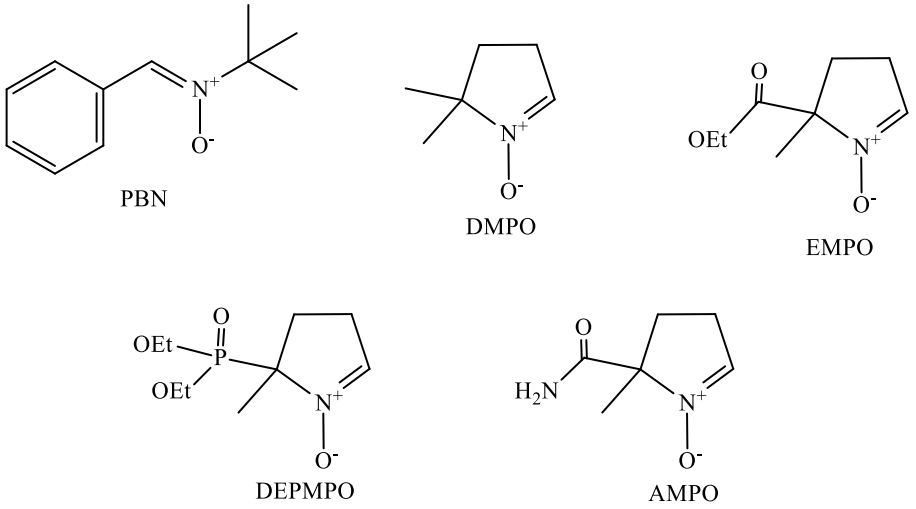

Figure 3: The chemical structures of linear PBN, cyclic DMPO, and several derivatives commonly used as spin traps

Heteroaryl nitrones consist of a heteroaromatic substituent on the carbon atom of the nitrone function.[62] New heteroaryl nitrones were synthesized through the condensation reaction between heteroaromatic aldehyde and N-monosubstituted hydroxylamines.[63] Porcal *et al.* [63] synthesized thiadiazolyl and furanoxyl nitrone derivatives and found that these new heteroaryl

nitrones have an excellent ability to add free radicals to produce stable products. The EPR spectroscopy demonstrated their ability to scavenge different free radicals. They also stated that these heteroaryl nitrones showed a therapeutic potential as neuroprotective agents in preventing the death of cells from oxidative stress and damage in biological systems. Barriga *et al.*[64] experimentally studied new heteroaryl nitrones with spin trap properties. They stated that the physicochemical characterization of new heteroaryl nitrones by EPR demonstrated their capability to trap and stabilize oxygen-, carbon-, sulfur-, and nitrogen- centered free radicals.

Although, the parent nitrone spin trap (H_2C=NHO) with radicals (•H, •CH_3, •OH, and •OOH) were computationally examined by Boyd and Boyd[65] to determine the most probable site of radical addition, the minimum-energy geometries of the spin adducts, and the energy changes involved in the addition reaction; the effects of heteroaryl (furoxanyl and thiadiazolyl) substituents on this parent nitrone spin trap (see Figure 5) have not been computationally studied to understand the chemical and physical basis that can influence the spin trapping efficiency of these nitrones and the corresponding stability of their spin adducts. Hence this work aims to computationally study the spin trapping of selected biologically relevant radicals (•H, •CH_3, and •OH) using these novel heteroaryl (furoxanyl and thiadiazolyl) nitrones (suggested by the work of Porcal *et al.* [63]) using *ab initio* and Density Functional Theory (DFT) methods.

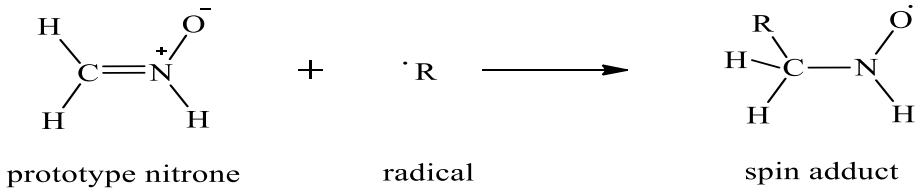

Figure 4: The reaction of a prototype nitrone with a radical to form a spin adduct

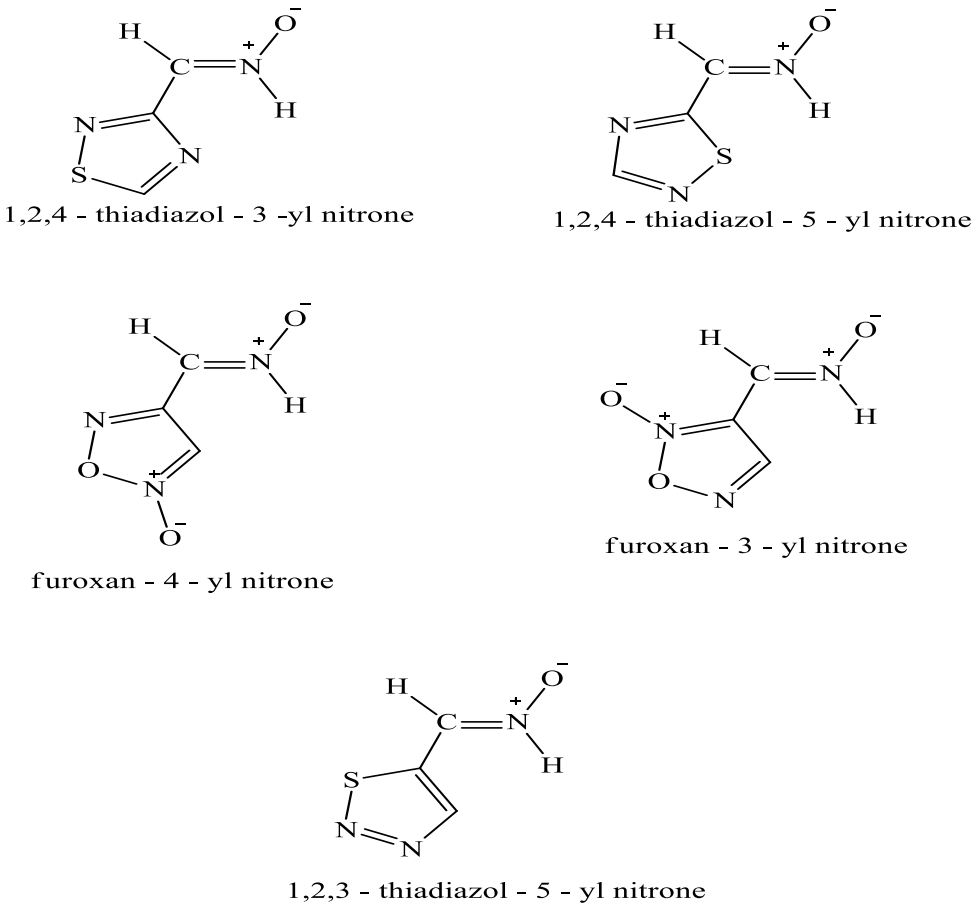

Figure 5: The chemical structures of the proposed novel heteroaryl nitrone spin traps

CHAPTER 2

QUANTUM MECHANICS

General Introduction to Computational Chemistry

Theoretical chemistry is the mathematical description of chemistry. Currently, there are two ways to approach theoretical chemistry problems, namely computational theoretical chemistry and non-computational theoretical chemistry. Computational theoretical chemistry deals with the numerical computation of molecular electronic structures and interactions while non-computational theoretical chemistry deals with the formulation of analytical expressions for the properties of molecules and their reactions.[66] Theoretical chemistry is further divided into two categories based on the methodology. These are static methods (based on the solution of the time independent Schrödinger Equation) and dynamic methods (based on the time dependent Schrödinger Equation).[67]

Computational chemistry is a natural outgrowth of theoretical chemistry, the traditional role of which involves the creation and dissemination of a penetrating conceptual infrastructure for the chemical sciences, particularly at the atomic and molecular levels. Serious attempts have been made to obtain highly accurate quantitative information about the chemical behavior of molecules through numerical approximations to the solution of the Schrödinger equation since the appearance of digital computers.[68]

There have been revolutionary expansions in the breadth and capability of computational chemistry, with an equal rise in optimism regarding the ability of computational chemistry to resolve challenging problems both of a fundamental scientific character and of clearly practical interest.[68] Computational chemistry is central to rational drug design; it contributes to the

selection and synthesis of new compounds, and guides the design of catalysts.[68] New quantum mechanical techniques have provided an understanding of the electronic properties of materials and have advanced the level of precision at which molecules, of at least moderate size, can be modeled.[69] Such techniques are used for electronic structure determination, geometry optimization and the calculation of potential energy surfaces, frequency calculations, definition of transition-state structures and reaction pathways, protein folding, electron charge distribution calculations, calculations of rate constants for chemical reactions, thermodynamics calculations such as heat of reaction and energy of activation, and calculations of many molecular bulk physical and chemical properties.[70] Computational chemistry studies may be carried out to find a starting point for a laboratory synthesis or to assist in understanding experimental data such as the position and source of spectroscopic peaks. Hence, computational chemistry is an important field of chemistry that may be applied in many areas such as material science, pharmaceutics, nanoscience, polymer science and in the petroleum industry.

The most important tools of computational chemistry are:[71]

Molecular mechanics (MM): This is a purely empirical scheme based on a model of a molecule as a collection of balls (atoms) held together by springs (bonds). It is used to calculate the energy of a given molecule and the geometry for the molecule (geometry optimization). It is fast and can be used to study small molecules as well as large biological systems such as proteins and DNA.[72] Examples of molecular mechanics methods are the Molecular Mechanics, MM2 and MM3[73] and the Universal Force Field (UFF) of Rappè.[74]

Ab initio calculations: These are based on solutions of the Schrödinger equation from first principles without introducing empirical parameters. *Ab initio* calculations describe how

electrons in a molecule behave. The *ab initio* methods solve the Schrödinger equation to give a molecule's energy and wave functions (a mathematical function used to calculate the electron distribution of a molecule). Examples of *ab initio* methods are the Hartree–Fock (HF) method, Møller-Plesset Perturbation Theory (MPPT) methods and Configuration Interaction (CI) methods.[75]

Semi-empirical calculations: These are based on the Schrödinger equation, but parameterized with empirical data to reproduce experimental observables. Examples of semi–empirical methods are AM1 of Dewar, PM3 of Stewart and PM3 of Hehre.[76]

Density Functional Theory (DFT) calculations: Like *ab initio* and other semi-empirical calculations, DFT is also based on the Schrödinger equation. However, it calculates the electron density of a molecule instead of the wave function. Examples of DFT functionals are Becke, three-parameter, Lee-Yang-Parr (B3LYP), and Perdew-Burke-Ernzerhof (PBE).[77]

Molecular dynamics calculations: Molecular dynamics is the computer simulation of the physical movement of atoms and molecules. It applies Newton's laws of motion to molecules by numerically solving the equations for a system of interacting particles where the forces between the particles and the potential energy are defined by molecular mechanics force fields. Thus, the motion of an enzyme can be simulated as it changes shape on binding to a substrate, or the motion of a swarm of water molecules around a molecule of solute can be modeled.[78]

The Schrödinger Equation

The time dependent Schrödinger equation for one spatial dimension is of the form: [79,80]

$$\frac{-\hbar^2}{2m}\frac{\partial^2\Psi(x,t)}{\partial x^2} + V(x)\Psi(x,t) = i\hbar\frac{\partial\Psi(x,t)}{\partial t} \tag{2-1}$$

The equation describes the time dependence of any quantum chemical system, where $\hbar$ is Planck's constant, h, divided by 2π, m is the mass of the system, V is the potential energy operator, i is the imaginary operator ($\sqrt{-1}$) and $\Psi(x, t)$ is the wave function of the system, which is a function of position (including possibly spin), x, and time, t. The wave function originated from classical mechanics. The time-dependent Schrödinger equation may be used to derive the time-independent equation. The potential energy operator in the time-dependent Schrödinger equation serves to set conditions on the spatial part of the wave function and it is helpful to separate the equation into the time-independent Schrödinger equation for one dimension and the relationship for time evolution of the wave function.

$$\hat{\mathrm{H}}\Psi = i\hbar\frac{\partial\Psi}{\partial t} \qquad\qquad \frac{-\hbar^2}{2m}\frac{\partial^2\Psi(x)}{\partial x^2} + V(x)\Psi(x) = E\Psi(x) \tag{2-2}$$

Time evolution Time independent equation

Solving the time evolution of the system yields the Hamiltonian operator, $\hat{H}$, formed from the classical Hamiltonian. E represents the energy of the system, which gives the time independent Schrödinger equation. $\psi(x)$ represents the state function, which provides information on the physical properties of the system. The time-independent Schrödinger equation may be generalized to three dimensions as:

$$\frac{-\hbar^2}{2m}\left[\frac{\partial^2\Psi}{\partial x^2} + \frac{\partial^2\Psi}{\partial y^2} + \frac{\partial^2\Psi}{\partial z^2}\right] + V(x,y,z)\Psi(x,y,z) = E\Psi(x,y,z) \tag{2-3}$$

and in spherical polar coordinates as:

$$\frac{-\hbar^2}{2m}\nabla^2\Psi + V(r,\theta,\phi)\Psi(r,\theta,\phi) = E\Psi(r,\theta,\phi) \tag{2-4}$$

where ∇^2 is a second-order differential operator known as the Laplacian:

$$\nabla^2 = \frac{\partial^2\Psi}{\partial x^2} + \frac{\partial^2\Psi}{\partial y^2} + \frac{\partial^2\Psi}{\partial z^2} \tag{2-5}$$

Schrödinger's equation is currently not solvable for any system larger than that of the hydrogen atom because of interelectronic repulsion creating a three-body problem. However, a number of assumptions and approximations may be used to yield an approximate solution.

The Hamiltonian Operator

A quantum mechanical operator is associated with each measurable parameter in a physical system and the operator associated with the system energy is called the Hamiltonian. The Hamiltonian operator, $\hat{H}$ is the sum of the kinetic energy, T and potential energy, V

$$\hat{H} = T + V \tag{2-7}$$

where

$$T = \frac{-\hbar^2}{2m}\left[\frac{\partial^2\Psi}{\partial x^2} + \frac{\partial^2\Psi}{\partial y^2} + \frac{\partial^2\Psi}{\partial z^2}\right] \tag{2-7a}$$

$$V = \frac{1}{4\pi\varepsilon_0}\sum_l \sum_{m<l} \frac{q_l q_m}{r_{lm}} \tag{2-7b}$$

and where q_l and q_m are the charges on the l^{th} and m^{th} particle with a separation distance of r_{lm}, and ε_o is the permittivity of free space.

A molecule is considered as a system of interacting nuclei and electrons; hence, the Hamiltonian operator for such a system is constructed as follows:

$$\hat{\mathrm{H}} = -\sum_{i=1}^{N}\frac{\hbar^2}{2m_e}\nabla_i^2 - \sum_{A=1}^{M}\frac{\hbar^2}{2M_A}\nabla_A^2 - \sum_{i=1}^{N}\sum_{A=1}^{M}\frac{1}{4\pi\varepsilon_0}\frac{Z_A e^2}{r_{iA}} + \sum_{i=1}^{N-1}\sum_{j=i+1}^{N}\frac{1}{4\pi\varepsilon_0}\frac{e^2}{r_{ij}} + \sum_{A=1}^{M}\sum_{B>A}^{M}\frac{1}{4\pi\varepsilon_0}\frac{Z_A Z_B e^2}{R_{AB}}$$

$$\hat{\mathrm{H}} = \hat{\mathrm{H}}_{elec}^{kin} + \hat{\mathrm{H}}_{nuc}^{kin} + \hat{\mathrm{H}}_{elec-nuc}^{pot} + \hat{\mathrm{H}}_{elec-elec}^{pot} + \hat{\mathrm{H}}_{nuc-nuc}^{pot} \quad (2\text{-}8)$$

The equations shown for the Hamiltonian operators of a molecule correspond to the operators for kinetic energy contribution of the electrons, $\hat{\mathrm{H}}_{elec}^{kin}$, the kinetic energy contribution of the nuclei, $\hat{\mathrm{H}}_{nuc}^{kin}$, the potential energy contribution from electron-nuclei interaction, $\hat{\mathrm{H}}_{elec-nuc}^{pot}$, the potential energy contribution from electron-electron interaction, $\hat{\mathrm{H}}_{elec-elec}^{pot}$, and the potential energy contribution from nuclei-nuclei interaction, $\hat{\mathrm{H}}_{nuc-nuc}^{pot}$.

Atomic Units

The results of accurate quantum-mechanical calculations on atoms and molecules are obtained using atomic units (a. u.). Atomic units form a system of natural units, which is used for calculations. They are based on Gaussian units in which the three defining base units are the fundamental natural constants *e* (electronic charge), m_e (electronic mass), and $\hbar$. The advantage of using these units is that they bring the electronic Schrödinger equation to its intrinsically

simplest form such that the key atomic properties will have the values of one.[81,82] In order to obtain a less complicated expression for the Hamiltonian:

$$\hat{\mathrm{H}} = -\frac{1}{2}\sum_{i=1}^{N}\nabla_i^2 - \frac{1}{2}\sum_{A=1}^{M}\nabla_A^2 - \sum_{i=1}^{N-1}\sum_{j=i+1}^{N}\frac{1}{r_{ij}} + \sum_{A=1}^{M}\sum_{B>A}^{M}\frac{Z_A Z_B}{R_{AB}} \qquad (2\text{-}9)$$

The atomic unit of energy, $\frac{e^2}{a_o}$, is the hartree (E_h),

$$E_h = \frac{e^2}{4\pi\varepsilon_o a_o} = 27.21138602\ eV \qquad (2\text{-}10a)$$

$$a_o = \frac{\hbar^2}{m_e e^2} = 0.5291177\ \text{Å} \qquad (2\text{-}10b)$$

where one hartree is the Coulombic repulsion between two electrons separated by a distance of one Bohr radius, or 0.52911725 Å. It is equivalent to 27.21138602 eV or $4.359744650 \times 10^{-18}$ J.

Born-Oppenheimer Approximation

The Born-Oppenheimer (BO) approximation is one of the basic concepts underlying the description of the quantum states of molecules. The physical idea behind the BO approximation is that the nuclei are much heavier than electrons. As electrons move much faster than nuclei, the nuclei can be considered as fixed with respect to the motion of the electrons. So ignoring relativistic interactions, the molecular Hamiltonian may be written as:

$$\hat{\mathrm{H}} = -\frac{\hbar}{2}\sum_i m_i\nabla_i^2 - \frac{\hbar^2}{2m_e}\sum_l \nabla^2 + \sum_i\sum_{j>i}\frac{Z_i Z_j e^2}{r_{ij}} - \sum_i\sum_l\frac{Z_l e^2}{r_{li}} + \sum_m\sum_{l>m}\frac{e^2}{r_{lm}} \qquad (2\text{-}11)$$

where *i* and *j* are nuclei and *l* and *m* are electrons. The first term of the equation is the kinetic energy operator for the nuclei, and the second term is the kinetic energy operator for electrons.

The third term is the electrostatic energy of repulsion between the nuclei separated by a distance r_{ij}. The fourth is the electrostatic energy for attraction between nucleus *i* and electron *l* separated by a distance r_{li}. By separating the nuclear and electronic motions, the problem can be simplified to the electronic Schrödinger equation:

$$\hat{\mathrm{H}}_{el}\psi_{el}(q_l q_i) = E_{el}\psi_{el}(q_l q_i) \tag{2-12}$$

The nuclear kinetic energy terms in the molecular Hamiltonian are neglected and the Schrödinger equation for the electronic motion is written as:

$$\left(\hat{\mathrm{H}}_{el} + V_{NN}\right)\psi_{el} = U\psi_{el} \tag{2-13}$$

where the electronic Hamiltonian is

$$\hat{\mathrm{H}}_{el} = -\frac{\hbar^2}{2m_e}\sum_i \nabla_i^2 - \sum_i \sum_l \frac{Z_i e^2}{r_{il}} + \sum_m \sum_{l>m} \frac{e^2}{r_{lm}} \tag{2-14}$$

Also, the nuclear repulsion term V_{NN} is given as

$$V_{NN} = \sum_i \sum_{j>i} \frac{Z_i Z_j e^2}{r_{ij}} \tag{2-15}$$

The total energy inclusive of the internuclear repulsion experienced by the nuclei *i* and *j* is the energy *U*. The internuclear distance r_{ij} is fixed at a constant value and hence the electronic wave functions and energies depend parametrically on the nuclear coordinates:

$$\psi_{el} = \psi_{el,n}(q_l, q_i) \tag{2-16}$$

$$U = U_n(q_n) \tag{2-17}$$

The electronic Hamiltonian is dependent on the electronic coordinates and parameterizes the nuclear coordinates. The nuclear repulsion term V_{NN} is constant for a particular nuclear configuration. Hence, V_{NN} can be neglected from the electronic Schrödinger equation giving:

$$\hat{\mathrm{H}}_{el}\psi_{el} = E_{el}\psi_{el} \tag{2-18}$$

The purely electronic energy E_{el} is related to the total energy as

$$U = E_{el} + V_{NN} \tag{2-19}$$

The approximation yields reasonable results for the ground electronic states of diatomic molecules.

The Hartree-Fock Self Consistent Field Method

The Hartree-Fock Self-Consistent Field (HF-SCF) method is the basis for the use of atomic and molecular orbitals in many-electrons system. In many-electron systems such as Helium or Lithium, the HF-SCF method is employed to determine the accurate wave functions. The exact wave function for hydrogen can be calculated, however, the wave functions of larger systems can only be obtained if approximations are made. For an n-electron system, the Hamiltonian operator is given as:

$$\hat{\mathrm{H}} = -\frac{\hbar^2}{2m_e}\sum_{i=1}^{n}\nabla_i^2 - \sum_{i=1}^{n}\frac{Ze^2}{r_1} + \sum_{i=1}^{n-1}\sum_{j=i+1}^{n}\frac{e^2}{r_{ij}} \tag{2-20}$$

where the first term represents the sum of the kinetic energy for n-electrons, the second term represents the sum of the potential energy for the attractions between the electrons and the nucleus of charge *Ze*. *Z* = n for neutral atoms and the third term represents the interelectronic

repulsion term. The restriction $j>i$ rejects counting the same interelectronic repulsion twice and avoids terms like $\frac{e^2}{r_{ii}}$. As an initial approximation, the interelectronic repulsion term may be neglected to obtain a zeroth-order wave function. The zeroth-order wave function may be expressed as a product of n hydrogen-like (one-electron) orbitals:

$$\psi^{(o)} = f_1(r_1\theta_1\phi_1)f_2(r_2\theta_2\phi_2)\ldots f_n(r_n\theta_n\phi_n) \tag{2-21}$$

The hydrogen-like wave functions are given as:

$$f = R_{nl}(r)Y_l^m(\theta,\phi) \tag{2-22}$$

R_{nl} (r) represents the radial component of the hydrogen-like orbitals and is given by:[83]

$$R_{nl}(r) = \left\{\frac{n-l-1}{2n[n+1]}\right\}^{\frac{1}{2}}\left(\frac{2}{na_o}\right)^{\frac{l+3}{2}} r^l e^{-\frac{r}{na_o}} L_{n+1}^{2l+1}\left(\frac{2r}{na_o}\right) \tag{2-23}$$

The $L_{n+1}^{2l+1}\left(\frac{2r}{na_o}\right)$ term is associated Laguerre polynomials, while *n* and *l* terms are quantum numbers. The spherical harmonic, $Y_l^m(\theta,\phi)$, terms are given by:[84]

$$Y_l^m(\theta,\phi) = \left[\frac{(2l+1)}{4\pi}\frac{l-|m|!}{(l+|m|!}\right]^{\frac{1}{2}} P_l^{|m|}\cos(\theta)e^{im\phi} \tag{2-24}$$

where $P_l^{|m|}\cos(\theta)$ is the associated Legendre polynomials.

The approximate wave function is qualitatively useful; however, it is quantitatively inaccurate because all electrons experience the same nuclear charge. Therefore, the approximation can be made quantitatively accurate by employing different effective atomic numbers for different orbitals for the screening effect. Hence, there is the need to use a variational function that is not restricted to any form of orbitals. Such a function is written as:

$$\phi = g_1(r_1\theta_1\phi_1)g_2(r_2\theta_2\phi_2) \dots g_n(r_n\theta_n\phi_n) \quad (2\text{-}25)$$

The variational integral is then minimized by the functions g_i as shown below:

$$E_1 \leq \frac{\int \phi * \hat{\mathrm{H}} \phi d\tau}{\int \phi * \phi d\tau} \quad (2\text{-}26)$$

where E_1 is the ground state energy for the system.

Generally, an approximation is made in the atomic calculations as:

$$g_i = h_i(r_i)Y_{li}^m(\theta_i\phi_i) \quad (2\text{-}27)$$

Hartree introduced the procedure for calculating g_i and it is termed as the Hartree Self-Consistent field (HSCF) method.[85,86]

Hartree's Procedure

The product wave function is the first step to guess in Hartree's procedure.

$$\phi = s_1(r_1\theta_1\phi_1)s_2(r_2\theta_2\phi_2) \dots s_n(r_n\theta_n\phi_n) \quad (2\text{-}28)$$

s_i in the above equation is the normalized function of r multiplied by a spherical harmonic. The primary approximation is the central field approximation where the electrostatic electron-electron repulsion term is averaged. Each electron is considered to interact with a continuous charge distribution where by each electron sees the other electrons as being smeared out to form a static distribution of electric charges through which it moves. The potential energy of interactions between two charges q_1 and q_2 is given as

$$V_{12} = \frac{1}{4\pi\varepsilon_o}\frac{q_1 q_2}{r_{12}} \tag{2-29}$$

By considering a charge density (charge per unit volume) ρ and the infinitesimal charge in the infinitesimal volume (*dv*), the potential energy of interaction of any electron carrying a charge Q with the static continuum is given as

$$V = \frac{Q}{4\pi\varepsilon_o}\int \frac{\rho}{r} dv \tag{2-30}$$

where r is the distance between Q and ρ.

The probability density for electron *i* is $|s_i|^2$, hence

$$\rho = -e|s_i|^2 \tag{2-31}$$

The probability density function of the second electron with $|s_2|$ is

$$V_{12} = \frac{e^2}{4\pi\varepsilon_o}\int \frac{|s_2|^2}{r_{12}} dv_2 \tag{2-32}$$

By adding the interaction with other electrons gives

$$V_{12} + V_{13} + \cdots + V_{1n} = \sum_{j=2}^{n} \frac{e^2}{4\pi\varepsilon_o}\int \frac{|s_j|^2}{r_{1j}} dv_j \tag{2-33}$$

The potential energy of interaction between an electron and the nucleus gives

$$V(r_1\theta_1\phi_1) = \sum_{j=2}^{n} \frac{e^2}{4\pi\varepsilon_o}\int \frac{|s_j|^2}{r_{1j}} dv_j - \frac{Ze^2}{4\pi\varepsilon_o r_1} \tag{2-34}$$

The effective potential acting on an electron, from the central field approximation, is considered as a function of r only. $V(r_1\theta_1\phi_1)$ is averaged over the angles θ and ϕ to give

$$V_1(r_1) = \frac{\int_0^{2\pi}\int_0^{\pi} V(r_1\theta_1\phi_1) sin\theta_1 d\theta_1 d\phi_1}{\int_0^{2\pi}\int_0^{\pi} sin\theta d\theta d\phi} \tag{2-35}$$

Therefore, $V_1(r_1)$ is substituted in a one electron Schrödinger equation to give:

$$\varepsilon_1 t(1) = \left[-\frac{\hbar^2}{2m_e}\nabla_1^2 + V_1(r_1)\right] t_1(1) \tag{2-36}$$

where ε_1 is the energy of the orbital of electron one and $t(1)$ is the improved orbital of electron one. This procedure is repeated iteratively to improve the orbitals for each electron until the final sets of orbitals give the HSCF wave function. The general form of the differential equation for finding the Hartree-Fock orbitals is given as:

$$\mathcal{F} t_i(i) = \mathcal{E}_i t_i(i) \tag{2-37}$$

$\mathcal{F}$ is the Hartree-Fock operator where

$$\mathcal{F} = \left[-\frac{\hbar^2}{2m_e}\nabla_1^2 + V_1(r_1)\right] \tag{2-38}$$

The orbital energy in the SCF approximation is calculated by iteratively solving the one electron Schrödinger equation where by the energy of the atom is the sum of the orbital energies minus a correction term. The correction term is introduced to avoid the double counting of the repulsion terms. Hence, the corrected energy is given as

$$E = \sum_{i=1}^{n} \varepsilon_i - \sum_{i=1}^{n-1}\sum_{j=i+1}^{n} \iint \frac{e^2}{4\pi\varepsilon_o} \frac{|g_i(i)|^2 |g_i(i)|^2}{r_{ij}} dv_i dv_j \tag{2-39}$$

In the equation, the first term is the sum of orbital's energies and the second term is the sum of potential energy terms counted twice.

There is an improvement on Hartree's method by using the properly antisymmetrized wave function (Slater determinant) instead of simple one-electron wavefunctions.[87] The method is ideal for a computer, because it is easily written as an algorithm as shown below:

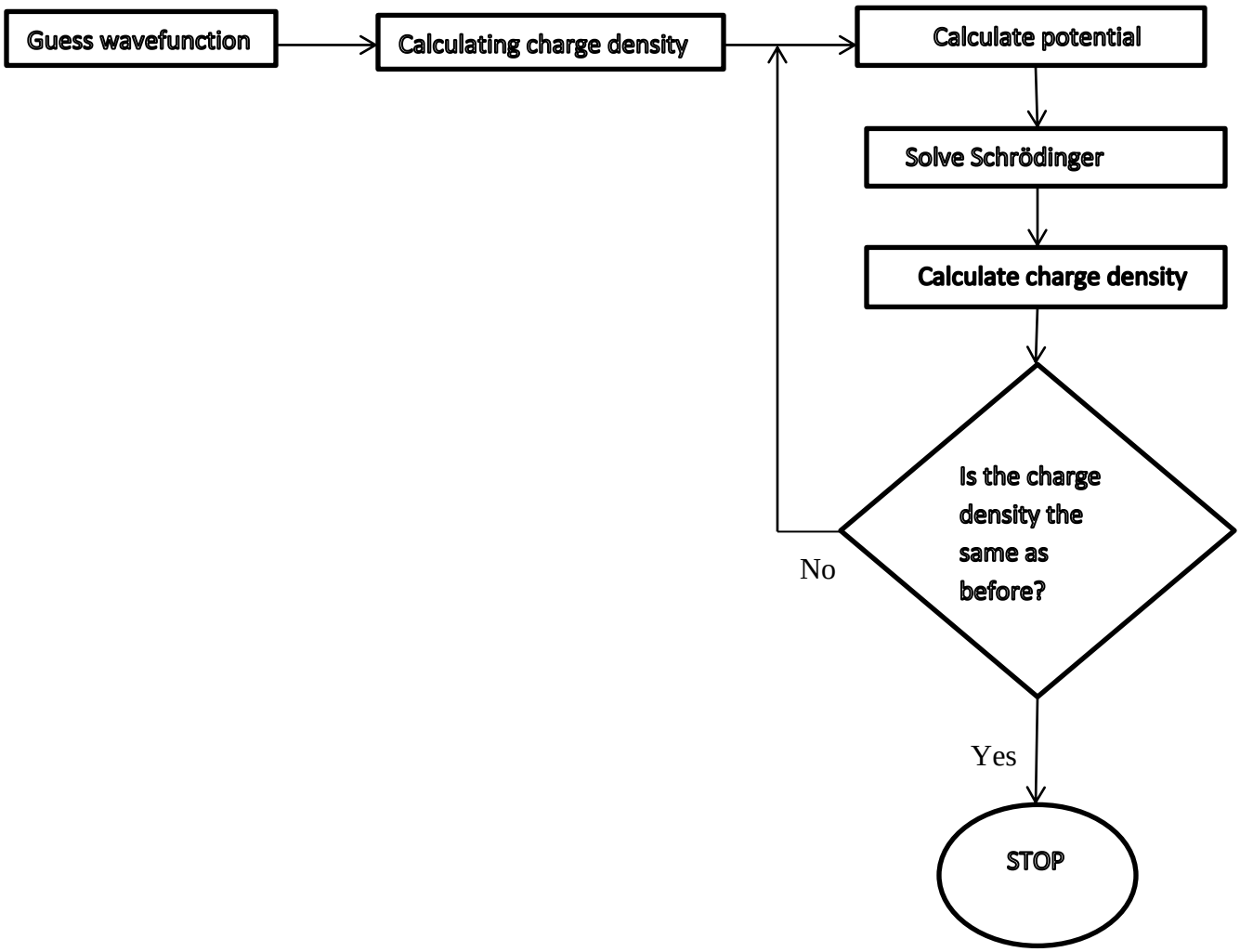

Figure 6: Algorithm for self-consistent field theory

The Wave Function as a Slater Determinant

The two important properties of the electronic wave function Ψ are that the wave function must be normalized and the electron wave function must be anti-symmetric (it changes sign when two electrons are interchanged) because electrons are fermions. The molecular Hartree-Fock (HF) wave function is written as anti-symmetrized and normalized products of spin orbitals, where each spin-orbital being a product of a spatial orbital ϕ_i and a spin function (either α or β).[88]

$$\Psi = \frac{1}{\sqrt{N!}} \begin{vmatrix} \phi_1(1)\alpha_1 & \phi_1(1)\beta_1 & \cdots & \phi_N(1)\alpha_1 & \phi_N(1)\beta_1 \\ \phi_1(1)\alpha_2 & \phi_1(1)\beta_2 & \cdots & \phi_N(1)\alpha_2 & \phi_N(1)\beta_2 \\ \vdots & \vdots & & \vdots & \vdots \\ \phi_1(1)\alpha_N & \phi_1(1)\beta_N & \cdots & \phi_N(1)\alpha_N & \phi_N(1)\beta_N \end{vmatrix} \tag{2-40}$$

The vital assumption in the HF method is that the wave function of an electron, which is not a physical observable, can be represented mathematically as an anti-symmetric product of molecular orbitals. Each electron is assumed to experience an average charge distribution due to other electrons in the system, and not interact explicitly with other electrons.

The Variational Principle

The variational principle is a starting point for almost all methods that seek to find an approximate solution to the Schrödinger equation. The Variational theorem states that the energy determined from any approximate wavefunction will always be greater than the energy for the exact wavefunction. It gives the expression for the HF molecular electronic energy E_{HF} as

$$E_{HF} = < \psi | \hat{\mathrm{H}}_{el} + V_{NN} | \psi > \tag{2-41}$$

where ψ is the Slater determinant HF wave function, $\hat{H}_{el}$ is the electronic Hamiltonian operator and V_{NN} is the potential energy for nuclear repulsion.

The electronic Hamiltonian gives the sum of one-electron Hamiltonians as

$$f_i = -\frac{1}{2}\nabla_i^2 - \sum_\alpha \frac{Z_\alpha}{r_{i\alpha}} \tag{2-42}$$

and the two electron operator as

$$g_{ij} = \frac{1}{r_{ij}} \tag{2-43}$$

The HF energy of a diatomic or polyatomic molecule with closed shells only is:[89]

$$E_{HF} = 2\sum_{i=1}^{n/2} H_{ii}^{core} + \sum_{i=1}^{n/2}\sum_{i=1}^{n/2}(2J_{ij} + K_{ij}) + V_{NN} \tag{2-44}$$

where H_{ii}^{core} is the core Hamiltonian for one-electron, J_{ij},the coulomb integral and K_{ij}, the exchange integral. The HF method seeks to minimize the variational integral E_{HF} for the orbitals ϕ_i. The orbitals are assumed orthogonal and must satisfy the equation as:

$$\mathcal{F}(1)\phi_i(1) = \varepsilon_i\phi_i(1) \tag{2-45}$$

The orbital energy ε_i for normalized ϕ_i is given as:

$$\varepsilon_i = \int \phi(1)\mathcal{F}(1)\phi_i(1)dv_i \tag{2-46}$$

and by simplifying the equation gives:

$$\varepsilon_i = H_i^{core} + \sum_{j=1}^{n/2}(2J_{ij} - K_{ij}) \tag{2-47}$$

Then, the HF energy is finally obtained as:

$$E_{HF} = 2\sum_{i=1}^{n/2}\varepsilon_i + \sum_{i=1}^{n/2}\sum_{i=1}^{n/2}(2J_{ij} + K_{ij}) + V_{NN} \quad (2\text{-}48)$$

The Roothaan-Hall Equations

Roothaan and Hall independently formulated the HF equations by using non-orthonormal Gaussian type or Slater type basis sets.[90,91] The Roothaan-Hall equations are obtained as:

$$\sum_{v=1}^{Nbasis}\left(F_{\mu v} - \varepsilon_i S_{\mu v}\right)C_{vi} = 0; \qquad \mu = 1,2 \ldots Nbasis \quad (2\text{-}49)$$

The electronic energy is calculated from the core Hamiltonian matrix $H_{\mu v}^{core}$, the Fock matrix $F_{\mu v}$ and the one electron density matrix $P_{\mu v}$. The Hartree-Fock energy is obtained by adding E_{elec} to the nuclear repulsion energy:

$$E_{HF} = \frac{1}{2}\sum_{\mu=1}^{Nbasis}\sum_{v=1}^{Nbasis} P_{\mu v}(F_{\mu v} + H_{\mu v}^{core}) + \sum_{A=1}^{M}\sum_{A<B}^{M}\frac{Z_A Z_B}{R_{AB}} \quad (2\text{-}50)$$

Figure 7 gives the flowchart summary of the procedure for solving the Roothaan-Hall equations.

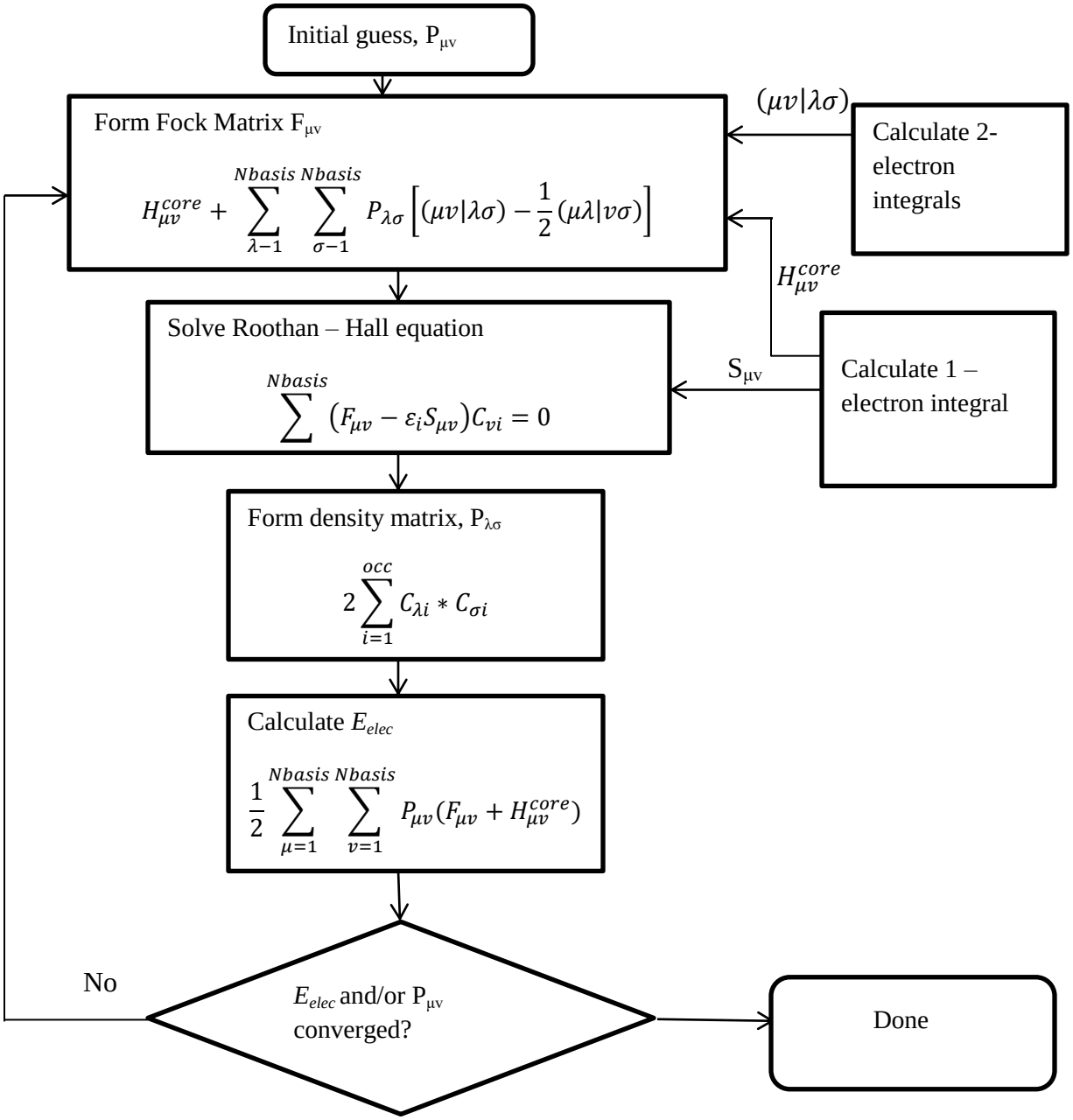

Figure 7: A flowchart summary of the procedure for solving the Roothaan-Hall equations

Restricted and Unrestricted Hartree-Fock Methods

The Restricted Hartree-Fock (RHF) method is a HF-SCF method where an atom or a molecule is a closed-shell system with all spatial orbitals (atomic or molecular) doubly occupied. The RHF method is thus not suitable for an open-shell system. Therefore, to solve this problem, two methods are used; the Restricted Open-Shell Hartree-Fock (ROHF) and the Unrestricted Hartree-Fock method (UHF). The UHF method is the common one used to treat open-shell systems to separate α and β electrons into singly occupied spatial orbitals. It is also used to solve two sets of Roothaan-Hall equations, known as the Pople-Nesbet equations:[92]

$$F^{\alpha}C^{\alpha} = SC^{\alpha}\varepsilon^{\alpha} \tag{2-51a}$$

$$F^{\beta}C^{\beta} = SC^{\beta}\varepsilon^{\beta} \tag{2-51b}$$

where F^{α} and F^{β} are the Fock matrices for the α and β orbitals, C^{α} and C^{β} are the coefficient matrices for the α and β orbitals, S is the overlap matrix of the basis functions, and ε^{α} and ε^{β} are the matrices of orbital energies for the α and β orbitals. However, the disadvantage of using the UHF method is that one-electron Slater determinants for α and β electrons are not satisfactory eigenfunctions of the total spin operator, $\hat{S}^2$. As a result, wave functions of higher states contaminate the total wave function. The spin contamination, which is the deviation of the expectation value of the total spin operator, $\langle\hat{S}^2\rangle$, from $S(S+1)$ gives an indication of the contamination from higher spin states. ROHF uses doubly occupied molecular orbitals as far as possible and then singly occupied orbitals for the unpaired electrons. The ROHF method, unlike UHF, gives a satisfactory eigenfunction of the total spin operator $\hat{S}^2$, (that is, it has no spin contamination from higher spin states).

Figure 8 shows a graphical representation of the orbital treatment for RHF, UHF and ROHF methods

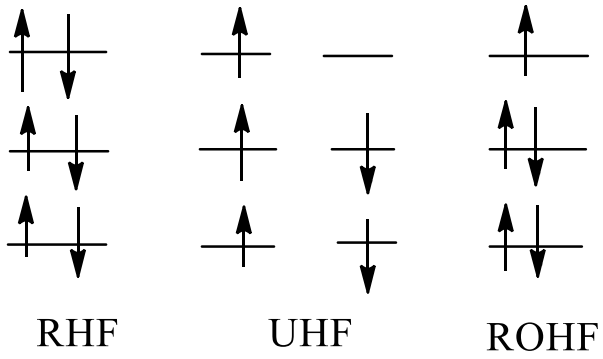

Figure 8: A graphical representation of the orbital treatment for the RHF, UHF and ROHF methods

Møller-Plesset Perturbation Theory (MPPT)

Møller-Plesset Perturbation Theory (MPPT) plays a unique role in quantum chemistry because of its treatment of dynamic electron correlation.[93] It is a particular formulation of many body perturbation theory (MBPT) which takes $\hat{H}_0$ to be the sum of the one-electron Fock operators, and treats electron correlation as the perturbation to the zeroth-order Hamiltonian.

The Hamiltonian operator, $\hat{H}$ in MPPT is divided into two parts:

$$\hat{H} = \hat{H}_0 + \lambda V \tag{2-52}$$

where λV is a small perturbation.

Rayleigh-Schrödinger Perturbation Theory (RSPT) can be used to find the ground state wave function and energy of the system as a power series:

$$\Psi = \Psi^{(0)} + \lambda\Psi^{(1)} + \lambda^2\Psi^{(2)} + \lambda^3\Psi^{(3)} \ldots \quad (2\text{-}53)$$

$$E = E^{(0)} + \lambda E^{(1)} + \lambda^2 E^{(2)} + \lambda^3 E^{(3)} \ldots \quad (2\text{-}54)$$

By substituting these equations into the time-independent Schrödinger equation gives:

$$\left(\hat{\mathrm{H}}_0 + \lambda\tilde{\mathrm{V}}\right)\left(\sum_i^n \lambda^i \Psi^{(i)}\right) = \left(\sum_i^n \lambda^i E^{(i)}\right)\left(\sum_i^n \lambda^i \Psi^{(i)}\right) \quad (2\text{-}55)$$

The HF energy, $E_{\mathrm{HF}} = E_{(0)} + E_{(1)}$ and the HF wave function $\Psi(0)$ are obtained for $n = 1$ and for $n = 0$, the sum of the electronic orbital energies $\sum_i$ is also obtained. The corresponding MP*n* energies are obtained when these equations are used to solve to the *n*th order, for example, MP2, MP3 and MP4.

Density Functional Theory

The basic principle of Density Functional Theory (DFT) is that the energy of a molecule may be determined from the electron density $\rho(r)$ instead of the approximate many electron wave function ψ.[94] They are extremely popular and are one of the most used methods in computational chemistry, computational physics, and condensed-matter physics.[95] In 1927, DFT found its root in the works of Thomas and Fermi. They proposed that "electrons are distributed uniformly in the six dimensional phase space for the motion of an electron at the rate of two for each of volume" and that there is an effective potential field that "is itself determined by the nuclear charge and this distribution of electrons," the kinetic energy of the system of electrons is approximated in the Thomas-Fermi method as an explicit functional of the density, but neglects exchange and correlation among electrons.[96] Dirac extended the approximation of Thomas and

Fermi, by formulating the local approximation for exchange, giving rise to the energy functional for electrons in an external potential:

$$E_{TF}[\rho] = E_T[\rho] + E_V[\rho] + E_J[\rho] + E_{XC}[\rho] \quad (2\text{-}56)$$

where E_T is the kinetic energy of the electron, E_V is the external potential energy from electron-nuclear interaction and nuclear-nuclear repulsion. E_J and E_{XC} are the electron repulsion term and the exchange correlation term respectively.

Current DFT methods originate from the Hohenberg-Kohn theorem,[97] which states that all properties of a system defined by an external potential are uniquely determined by the ground state electron density. Hence, the state electron density that gives the minimum total energy is the ground state electron density because of the variational principle.

The Hamiltonian of a given system, and its electronic energy, is divided using the Kohn-Sham approach[98]

$$E[\rho(r)] = E_{Ne}[\rho(r)] + T[\rho(r)] + E_{ee}[\rho(r)] \quad (2\text{-}57)$$

$$= \int \rho(r) V_{Ne} dr + F[\rho(r)]$$

where $F[\rho(r)]$ is a functional of the electron density, $\rho(r)$.

The factors of $F[\rho(r)]$ are: the kinetic energy of the non-interacting system with density $T_s[\rho(r)]$, the classical electrostatic electron-electron repulsion energy, $J[\rho(r)]$, and the exchange-correlation energy $E_{xc}[\rho(r)]$.

The DFT approach in Equation 2-57 gives the following expression for the calculation of energy:

$$E[\rho(r) =$$

$$-\frac{1}{2}\sum_i^N \langle\varphi_i|\nabla^2|\varphi_i\rangle + \frac{1}{2}\sum_i^N \sum_j^N \iint |\varphi_i(r)|^2 \frac{1}{r_{12}} \left|\varphi_j(r_2)\right|^2 dr_1 dr_2 - \sum_i^N \int \sum_A^M \frac{Z_A}{r_{1A}} |\varphi_i(r_i)|^2 dr_1 +$$

$$E_{XC}[\rho(r)] \tag{2-58}$$

However, the exact form of the exchange correlation energy, $E_{XC}[\rho(r)]$, is unknown. Finding the accurate form of $E_{XC}[\rho(r)]$ is still an agendum of modern research in quantum chemical methods.

Logically, E_{XC} is approximated as a local or nearly local functional of the density with[99]

$$E_{XC} = \int dr\rho(r)\, \varepsilon^{xc}([\rho], r) \tag{2-59}$$

where ε^{xc} is the energy per electron at point r that depend on only ρ. The equation shows that E_{XC} can be calculated locally at a position r and exclusively from the positional value of ρ.

The local density and the Dirac exchange energy produce the exchange energy of a uniform free electron gas as:[100]

$$E_{LDA}^X[\rho] = -\frac{3}{2}\alpha K_D = -\frac{9}{8}\alpha \left(\frac{3}{\pi}\right)^{\frac{1}{3}} \int \rho^{\frac{4}{3}}(r) dr \tag{2-60}$$

where K_D represents the Dirac exchange-energy formula and α , an empirical constant which has a value of 2/3 for a uniform free electron gas.

The Kohn-Sham Local-Spin-Density Approximation (KS-LSDA) can correct the shortcomings of the Kohn-Sham Local Density Approximation (KS-LDA) where the LDA for exchange energy functional gives the equation:[101]

$$E_{LSDA}^X\left[\rho^\alpha \rho^\beta\right] = 2^{\frac{1}{2}} C_X \int ((\rho^\alpha)^{\frac{4}{3}} + \left(\rho^\beta\right)^{\frac{4}{3}}) dr \tag{2-61}$$

When the spin polarization energy is defined as:

$$\varsigma = \frac{\rho^{\alpha}-\rho^{\beta}}{\rho} = \frac{\rho^{\alpha}-\rho^{\beta}}{\rho^{\alpha}+\rho^{\beta}} \tag{2-62}$$

then the exchange energy becomes:

$$E_{LSD}^{X} = \int \rho \varepsilon^{x}(\rho, \varsigma) dr \tag{2-63}$$

with

$$\varepsilon^{x}(\rho, \varsigma) = \varepsilon_{x}^{0} + [\varepsilon_{x}^{1}(\rho) - \varepsilon_{x}^{0}(\rho)] f(\varsigma) \tag{2-64}$$

where ε_{x}^{0} is the exchange energy density for the spin-compensated homogeneous electron gas and ε_{x}^{1} is the exchange energy for spin-completely-polarized homogeneous electron gas.

Since the exchange energy is the major source of error in LDA, this model has been simplified to give the generalized gradient approximation (GGA).

$$E_{GGA}^{X} = -\frac{3}{4}\left(\frac{3}{\pi}\right)^{\frac{1}{3}} \int dr \rho^{\frac{1}{3}} F(s) \tag{2-65}$$

with

$$S = \frac{|\nabla \rho(r)|}{2K_F \rho} \tag{2-66}$$

$$K_F = (3\pi^2 \rho)^{\frac{1}{3}} \tag{2-67}$$

and

$$F(s) = (1 + 1.296S^2 + 14S^4 + 0.2S^6)^{\frac{1}{15}} \tag{2-68}$$

When the exchange function combines with the correlation functional, it reduces the error on the exchange correlation energy through the exchange functional. An example of a hybrid functional is Becke's three parameter exchange functional combined with the correlation functional of Lee, Yang and Parr (B3LYP)[102,103] and it is written as:

$$E_{B3LYP}^{XC} = (1-a)E_{LSDA}^{X} + aE_{HF}^{X} + bE_{B88}^{X} + (1-c)E_{LSDA}^{C} + cE_{LYP}^{C} \quad (2\text{-}69)$$

where B88 is the Becke's exchange functional and LYP is the Lee-Young-Parr correlation functional.[102,103]

The Kohn-Sham theory solves the equation:

$$F(1)\psi = \varepsilon\psi \quad (2\text{-}70)$$

where

$$F(1) = -\frac{1}{2}\nabla_1^2 - \sum_\alpha \frac{Za}{r_{1\alpha}} + \sum_j J_j(1) + V^{XC} \quad (2\text{-}70a)$$

$$V^{XC} = \frac{\partial E^{XC}}{\partial \rho} \quad (2\text{-}70b)$$

The electron density is obtained from the sum over the occupied orbitals when the Kohn-Sham orbitals are determined:

$$\rho = \sum_i |\psi_i|^2 \quad (2\text{-}71)$$

Hybrid functionals such as BLYP; Becke exchange, Perdew and Wang correlation(B3PW91) and Becke exchange, Perdew correlation (B3P86) have attained great success in the computational chemistry.[104] This is due to the accuracy of the results they give for a large variety of

compounds, particularly organic molecules,[105] the prediction of molecular geometries, and harmonic vibrational frequencies.[104]

Basis Sets

A basis set is defined as a set of functions (called basis functions) which are combined in linear combinations to create molecular orbitals. Basis functions are atomic orbitals described by a mathematical function based on spherical or Cartesian coordinates.

$$\varphi_i = \sum_{\mu=1}^{Nbasis} C_{\mu i} X_\mu \tag{2-72}$$

The two most common basis functions are Slater-type orbitals and Gaussian-type orbitals. Historically, Slater-type orbitals (STOs) were used as basis functions of molecular orbitals due to their similarity to the atomic orbitals of the hydrogen atom.

$$\chi_i(\varsigma, n, l, m; r, \theta, \phi) = N r^{n-1} e^{-\varsigma r} Y_{lm}(\theta, \phi) \tag{2-73}$$

where ς is an exponent, Y_{lm} is a spherical-harmonic function that describes the shape (the angular momentum part); N is a normalization constant; r, θ, and ϕ are the spherical coordinates and n, l, m are the principal, angular momentum, and magnetic quantum numbers respectively. $e^{-\varsigma r}$, the exponential term, represents the energy of electrons near the nucleus. STOs are no longer used because they are difficult to evaluate the resulting secular determinants. Multicenter integrals, which involve more than one nuclear center, are difficult to calculate. This problem may be overcome by using Gaussian-type functions (GTFs)

$$g(\alpha, l, m, n; x, y, z) = N e^{-\alpha(x^2+y^2+z^2)} x^l y^m z^n \tag{2-74}$$

$$= N e^{-\alpha r^2} x^l y^m z^n \tag{2-75}$$

where *x*, *y*, and *z* are spherical coordinates; *n*, *l*, *m* are integral exponents of Cartesian coordinates, and α is the exponent instead.

STO-nG, where n is an integer, is the most common minimal basis set. The *n* value gives the number of Gaussian primitive functions, which comprise a single basis function. Minimal basis sets give rough results that are insufficient for research-quality publication; however they are much cheaper than their larger counterparts. Examples of commonly used minimal basis sets are: STO-3G, STO-4G, STO-6G and STO-3G*.

The split-valence basis sets describe the inner-shell electron using a single Slater orbital and the valence shell by a sum of Slater orbitals. They have a larger number of basis functions per atom. Two or more sizes of basis functions are given to the valence shells of each atom, which allow the orbitals to change size. The notation for the split-valence basis sets is X-YZg. X represents the number of primitive Gaussians, comprising each core atomic orbital basis function. the Y and Z represent the valence orbitals that are composed of two basis functions each, the first one is a linear combination of Y primitive Gaussian functions and the second one is a linear combination of *Z* primitive Gaussian functions. The presence of two numbers after the hyphen indicates that the basis set is a split-valence double-zeta basis set. X-YZWg and X-YZWVg are split-valence triple- and quadruple-zeta basis sets respectively.

Polarized basis sets add orbitals with a higher angular momentum than the ground state electronic configuration of each atom at the Hartree-Fock level. These could improve the split valence basis sets by adding orbitals with different shapes. The 6-31G(d) (also called 6-31G*) and the 6-311G(d, p) basis sets are the examples of polarized basis sets.

Basis sets with added diffuse functions are important for systems where electrons are far from the nucleus such as anions, and molecules with lone pairs of electrons. These allow diffuse orbitals to occupy larger regions in space. An example of a diffuse basis set is the 6-311+G(d, p) basis set.

Polarization effects occur when orbitals of higher orbital quantum number are added to the mathematical expression of a given orbital, for example 3d orbital and the 2p orbital. When 3d orbitals are added to the 2p orbital functions for second row elements of the periodic table, an asterisk (*) alternative used to indicate the basis set (as above). Also, a double asterisk indicates that polarization is being added on hydrogen 1s orbitals. 3-21G* is an exception to this in which the asterisk denotes the addition of a d-orbital to the second row atoms, that is, 3-21G(d). Also, when different orbitals are added, the added orbitals are given in parenthesis, that is, 6-31G(d,p) means that extra sets of p and d functions are added to non-hydrogen atoms and p extra functions are added to hydrogen, thus denoting 6-31G**. Examples of commonly used split-valence basis sets are 3-21G, 3-21G* and 6-311G*.

Dunning and coworkers[106] developed the correlation consistence (cc) basis sets such as cc-pVDZ, cc-pVTZ, cc-pVQZ, cc-pV5Z, and cc-pV6Z. They are denoted as cc-pVnZ, where n ranges from 2 to 6. The 'cc-p', stands for ‘correlation-consistent polarized’, the ‘V’ indicate that they are valence-only basis sets while Z represents zeta. The Complete Basis Set methods were developed by Petersson and co-workers as a model chemistry.[107-109] They make use of a complete basis set (CBS) extrapolation of the correlation energy based on the asymptotic convergence of pair natural orbital expansions.[110-114] CBS methods are important in that, at higher and higher levels of correlation, the contribution of the correction to the total energy can be determined to less accuracy than at lower levels of theory. Thus, these methods use relatively

large basis sets for the structure calculation, medium sized basis sets for the second-order correlation correction, and small sized basis sets for higher order correlation corrections. Also, empirical corrections are added as necessary.[115]

CHAPTER 3

RESULTS AND DISCUSSION

Computational Details

All calculations were carried out using NWChem from the Molecular Sciences Laboratory Software Group of Pacific Northwest National Laboratory.[116,117] Extensible Computational Chemistry Environment software was used to manage the calculations and generate pictorial representations.[118] All geometries of the nitrones were fully optimized at Hartree-Fock (self-consistent field) (HF-SCF) and Density Functional Theory (DFT) with the 6-31G* basis set levels of theory, and the single point calculations were done on the HF-SCF optimized geometries at second–order Møller-Plesset Perturbation Theory (MP2) with the cc-pVDZ, cc-pVTZ and cc-pVQZ basis sets to obtain energies. All equilibrium geometries were characterized by the absence of imaginary frequencies. The geometries of DMPO, PBN and FxBN were fully optimized at DFT/m06/6-31G* and HF/6-31G*. In addition, Milliken population analyzes were used to obtain spin and charge populations.

Discussion of the Results

Table 1 shows calculated bond lengths and bond angles for formaldonitrone and the new heteroaryl nitrones at HF/6-31G*. Formaldonitrone is a parent nitrone and has a planar geometry. It has C=N and N-O bond lengths of 1.269 Å and 1.254 Å, respectively. The C-H bond length is 1.083 Å. The CNO bond angle for formaldonitrone is 128.3º. The new heteroaryl substituents considered in this work are 1,2,3-thiadiazol-5-yl, 1,2,4-thiadiazol-3-yl, 1,2,4-thiadiazol-5-yl, furoxan-3-yl, and furoxan-4-yl. When the hydrogen, H attached to the nitrone is substituted by these heteroaryl substituents, the bond lengths and the bond angles shorten or

lengthen depending on the nature of the substituents. The C=N bonds lengthen by 0.006 Å - 0.010 Å while the N-O bond lengths shorten by 0.003 Å – 0.013 Å. The C-$C_{heteroaryl}$ bond lengths lengthen in the range of 1.428 Å – 1.440 Å. In addition, there is a decrease in the CNO bond angle in the range of 127.3º - 127.8º. The O atom in the nitrones is highly electronegative because of its higher charge population than the N atom and the C atom. Figure 9 shows the optimized geometry of formaldonitrone and the new heteroaryl nitrones.

Table 1: Calculated bond lengths for formaldonitrone and the new heteroaryl nitrones at HF/6-31G*

Nitrone Spin Trap	Calculated bond lengths (Å)			Calculated bond angles (deg.)
	C=N	N-O	C-$C_{heteroaryl}$	CNO
Formaldonitrone	1.269	1.254	1.083	128.3
1,2,4-thiadiadozol-3-yl nitrone	1.277	1.244	1.440	127.8
1,2,4-thiadiazol-5-yl nitrone	1.279	1.241	1.433	127.5
Furoxan-4-yl nitrone	1.277	1.242	1.436	127.5
Furoxan-3-yl nitrone	1.275	1.251	1.428	127.3
1,2,3-thiadiazol-5-yl nitrone	1.278	1.246	1.433	127.3

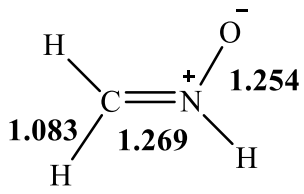

formaldonitrone

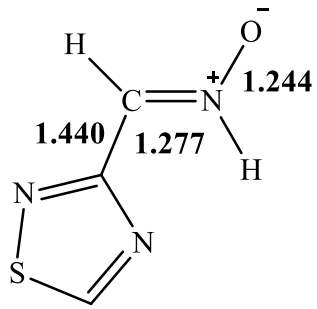

1,2,4 - thiadiazol - 3 -yl nitrone

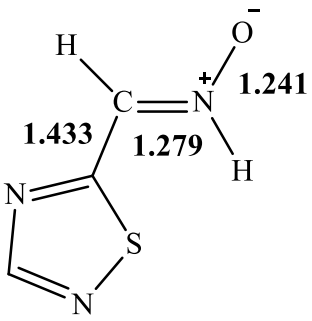

1,2,4 - thiadiazol - 5 - yl nitrone

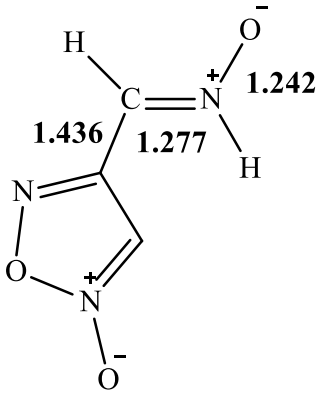

furoxan - 4 - yl nitrone

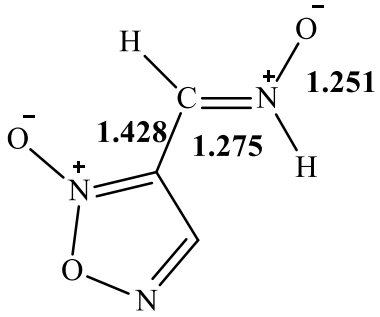

furoxan - 3 - yl nitrone

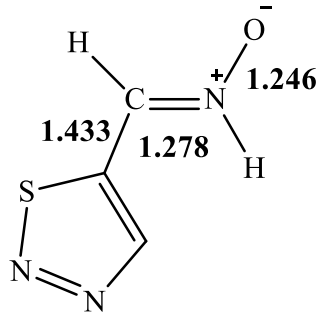

1,2,3 - thiadiazol - 5 - yl nitrone

Figure 9: The optimized geometry of formaldonitrone and the new heteroaryl nitrones. All bond lengths are in Å

Table 2 shows the total energies of selected biologically relevant radicals, •H, •CH_3, •OH, and their dipole moments. Among the three radicals, •OH radical has the highest polarity of 1.94 D. It also has the lowest energy. The •CH_3 radical has no polarity because its molecular geometry is trigonal planar. The optimized geometries for the radicals are shown in Figure 10. The order of increasing reactivity for radical addition to nitrones is •H < •CH_3 < •OH, which correlates with the inductive effect of each radical as well as the radical's reduction potential.[119] The spin and charge populations of each radical give insights into the reactivity to nitrones.

Table 2: Energies of selected biologically relevant radicals and their dipole moments

Radical	Energy (E_h) HF/6-31G*	Energy (E_h) DFT/m06/6-31G*	Dipole Moment (D)	Reduction Potential (V)
•H	-0.49820	-0.49792	0	0
•CH_3	-39.63860	-39.79542	0	1.90
•OH	-75.22340	-75.64294	1.94	2.31

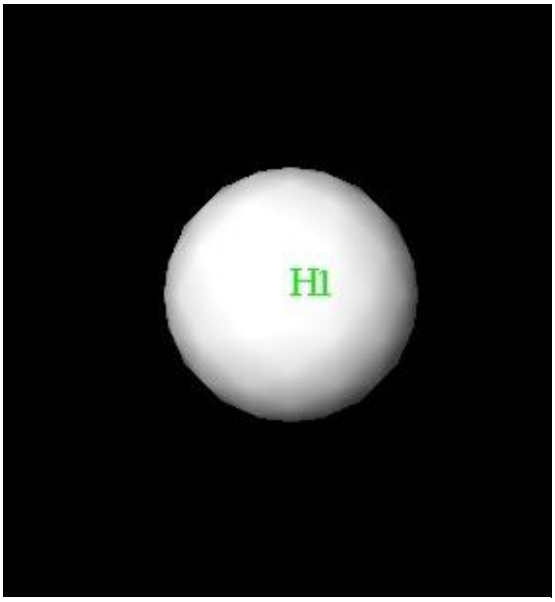

Hydrogen Radical

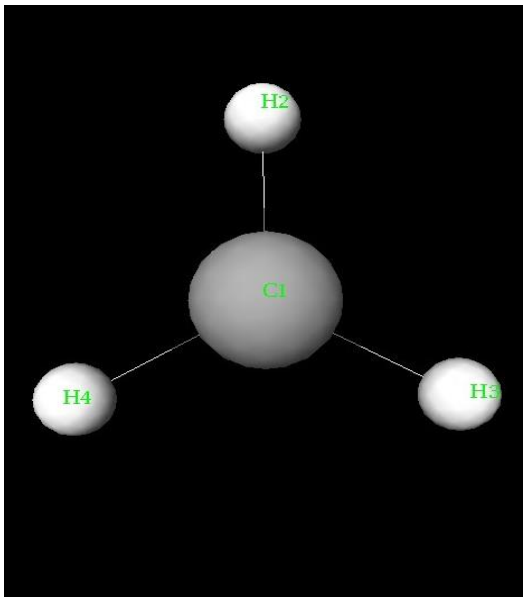

Methyl Radical

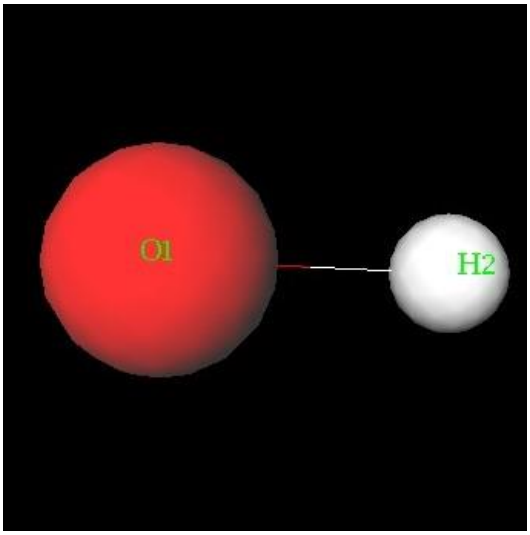

Hydroxyl Radical

Figure 10: NWChem optimized geometries of biologically relevant radicals

Table 3 shows the relative energies of formaldonitrone and new heteroaryl nitrones at the HF/6-31G*, MP2/cc-pVDT, MP2/cc-pVTZ, MP2/cc-pVQZ, the MP2 CBS limit, and DFT/m06/6-31G* levels of theory (from HF/6-31G* optimized structures), as well as the dipole moments obtained at HF/6-31G*. The relative energies show that the new heteroaryl nitrones are more stable due to the electronic effects of new heteroaryl substituents. Because of the high stability of the new heteroaryl nitrones, the nitrones show a great capacity to scavenge free radicals.[63,64] Thus the order of increasing stability of the spin traps is formaldonitrone < furoxanyl nitrone < thiadiazoyl nitrone. Also, the polarity of the spin traps is decreasing in the order: 1,2,4-thiadiazol-3-yl nitrone > furoxan-3-yl nitrone > 1,2,4-thiadiazol-5-yl nitrone > furoxan-4-yl nitrone > 1,2,3-thiadiazol-5-yl nitrone.

Table 3: Energies of formaldonitrone and the new heteroaryl nitrones at the HF/6-31G*, MP2/cc-pVDT, MP2/cc-pVTZ, MP2/cc-pVQZ, the MP2 CBS limit, and DFT/m06/6-31G* levels of theory. The dipole moments were calculated at the HF/6-31* level

Nitrone Spin Trap	HF/6-31G* (E_h)	MP2/ cc-pVDT (E_h)	MP2/ cc-pVTZ (E_h)	MP2/ cc-pVQZ (E_h)	E_{CBS} (E_h)	DFT/m06/ 6-31G* (E_h)	Dipole moment (D)
Formaldonitrone	-168.80921	-169.32379	-169.50071	-169.55895	-169.59220	-169.69089	4.47
1,2,4-thiadiazol-3-yl nitrone	-750.95291	-752.19826	-752.60343	-752.73909	-752.81677	-753.46128	5.65
1,2,4-thiadiazol-5-yl nitrone	-750.94373	-752.1917	-752.59696	-752.73268	-752.81040	-753.45461	1.97
Furoxan-4-yl nitrone	-502.97481	-504.49516	-504.96856	-505.13299	-505.22777	-505.53385	1.76
Furoxan-3-yl nitrone	-502.97470	-504.47422	-504.96811	-505.13295	-505.22729	-505.53513	4.26
1,2,3-thiadiazol-5-yl nitrone	-750.89840	-752.15743	-752.56122	-752.69673	-752.77436	-753.41851	0.26

As may be seen in Tables 4 and 5, the reaction of biologically relevant radicals with the new heteroaryl nitrones at the C- and O-sites shows that, generally, the spin trapping of biologically relevant radicals by the new heteroaryl nitrones at the C-sites is more exothermic than the spin trapping at the O-sites. This is because the N-O bond of the spin adducts at the C-site serves as a resonance contributor. This is due to the high spin populations of N and O for the spin adducts at the C-sites. However, at the O-sites of the spin adducts, the C atom of the spin adduct carries the higher spin population than N and O, hence the N-O bond does not serve as a resonance contributor. From Table 4, thermodynamically, the reactions of •OH with the new heteroaryl nitrones have the highest exothermicities as compared to the reactions of •H and •CH_3. Hence, the spin adducts formed from the spin trapping reactions with •OH have the highest stability. The furoxan-3-yl spin adduct with •OH has the largest energy change (most negative) of -671.99673 kJ/mol and it is the most stable spin adduct for HF/6-31G*, while furoxan-4-yl has the largest change (-379.41101 kJ/mol) for DFT/m06/6-31G*.

Also from Table 5, the spin trapping reactions of •CH_3 are endothermic in contrast to those for •H and •OH. However, from Table 5b, the spin trapping reactions of •OH with the new heteroaryl nitrones, except 1,2,4-thiadiazol-3-yl nitrone, are less exothermic as compared to the spin trapping reactions of •H and •CH_3. Thus, the spin trapping reactions of •H by the new heteroaryl nitrones at the O-sites give the highest exothermicities, hence the reactions produce the most stable spin adducts.

Table 4: Energies of the spin trapping reactions of selected radicals with formaldonitrone and the new heteroaryl nitrones at the C-site for (a) HF/6-31G* and (b) DFT/m06/6-31G*

(a)

Spin Trap	ΔE (kJ/mol)[a]		
	•H	•CH_3	•OH
Formaldonitrone	-305.66071	-39.96011	-641.40965
1,2,4-thiadiadozol-3-yl nitrone	-273.83965	-13.62635	-615.33844
1,2,4-thiadiazol-5-yl nitrone	-302.35258	-32.81875	-647.00197
Furoxan-4-yl nitrone	-330.78675	-60.62280	-670.63147
Furoxan-3-yl nitrone	-335.40763	-63.79965	-671.99673
1,2,3-thiadiazol-5-yl nitrone	-303.06147	-33.71142	-654.09082

(b)

Spin Trap	ΔE (kJ/mol)[a]		
	•H	•CH_3	•OH
Formaldonitrone	-274.86360	-241.23094	-372.08586
1,2,4-thiadiadozol-3-yl nitrone	-235.27106	-207.62454	-336.56285
1,2,4-thiadiazol-5-yl nitrone	-250.05262	-222.45862	-377.67818
Furoxan-4-yl nitrone	-265.88439	-230.28261	-379.41101
Furoxan-3-yl nitrone	-261.63108	-230.67643	-378.25579
1,2,3-thiadiazol-5-yl nitrone	-247.95222	-317.23917	-367.17618

[a]ΔE = energy change for gas phase species at equilibrium bond lengths at 0K

$$\Delta E = E_{adduct} - [E_{spin} + E_{radical}]$$

Spin trap and adduct energies are listed in the Appendix.

Table 5: Energies of the spin trapping reactions of biologically relevant radicals with the new heteroaryl nitrones the O-site for (a) HF/6-31G* and (b) DFT/m06/6-31G*

(a)

Spin Trap	ΔE (kJ/mol)[a]		
	•H	•CH_3	•OH
Formaldonitrone	-125.18384	158.71148	-214.63463
1,2,4-thiadiadozol-3-yl nitrone	-180.81819	54.584145	-337.14046
1,2,4-thiadiazol-5-yl nitrone	-261.44729	31.007155	-351.13437
Furoxan-4-yl nitrone	-293.11082	-0.84016	-387.94388
Furoxan-3-yl nitrone	-241.70353	55.266775	-311.06924
1,2,3-thiadiazol-5-yl nitrone	-280.29838	12.261085	-[b]

(b)

Spin Trap	ΔE (kJ/mol)[a]		
	•H	•CH_3	•OH
Formaldonitrone	-102.31574	-51.03972	26.93763
1,2,4-thiadiadozol-3-yl nitrone	-159.23658	-134.24182	-164.04124
1,2,4-thiadiazol-5-yl nitrone	-216.91881	-148.55079	-107.01538
Furoxan-4-yl nitrone	-206.15426	-143.74613	-98.95510
Furoxan-3-yl nitrone	-171.99651	-111.11116	-24.18086
1,2,3-thiadiazol-5-yl nitrone	-217.44391	-154.37940	-107.96056

[a]ΔE = energy change for gas phase species at equilibrium bond lengths at 0K

$$\Delta E = E_{adduct} - [E_{spin} + E_{radical}]$$

Spin trap and adduct energies are listed in the Appendix.

[b]Structure optimized with an O-O bond length beyond accepted covalent bond length

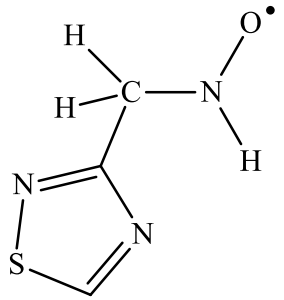

1,2,4-thiadiazol-3-yl spin adduct

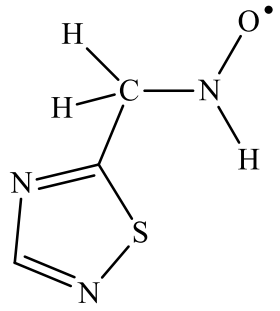

1,2,4-thiadiazol-5-yl spin adduct

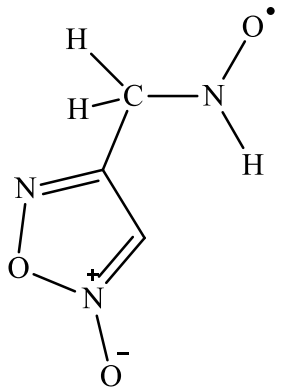

furoxan-4-yl spin adduct

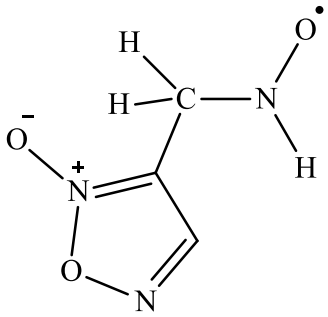

furoxan-3-yl spin adduct

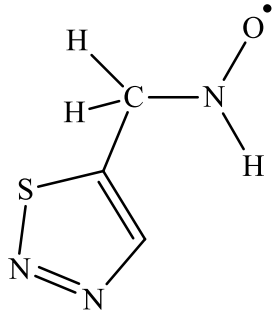

1,2,3-thiadiazol-5-yl spin adduct

Figure 11: ChemDraw® representations of the new heteroaryl spin adducts with •H added the C-site carbon

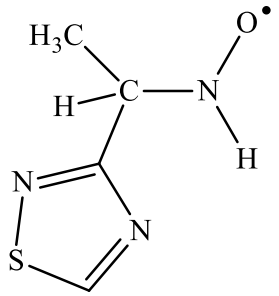

1,2,4-thiadiazol-3-yl spin adduct

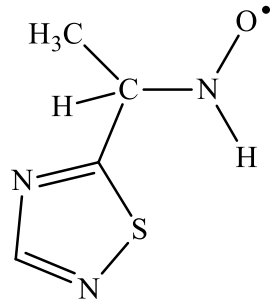

1,2,4-thiadiazol-5-yl spin adduct

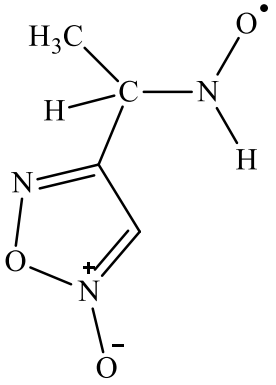

furoxan-4-yl spin adduct

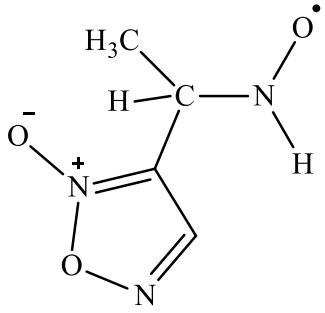

furoxan-3-yl spin adduct

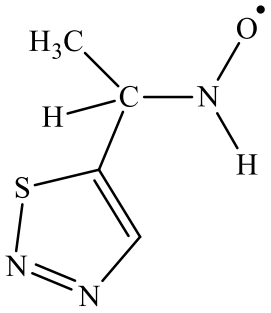

1,2,3-thiadiazol-5-yl spin adduct

Figure 12: ChemDraw® representations of the new heteroaryl spin adducts with •CH_3 added at the C-site carbon

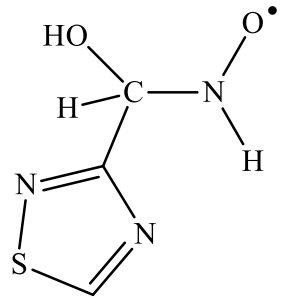

1,2,4-thiadiazol-3-yl spin adduct

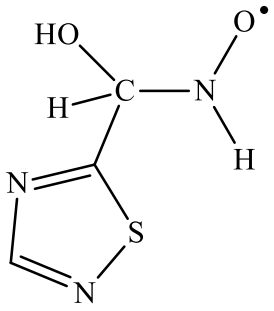

1,2,4-thiadiazol-5-yl spin adduct

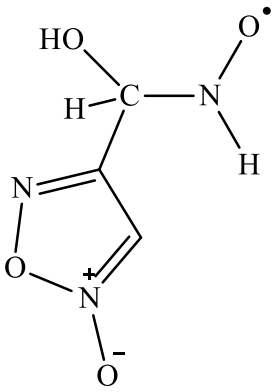

furoxan-4-yl spin adduct

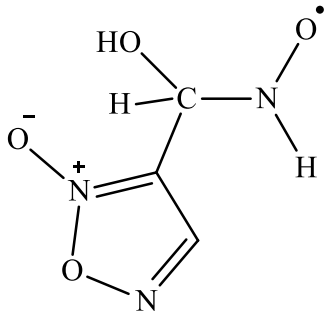

furoxan-3-yl spin adduct

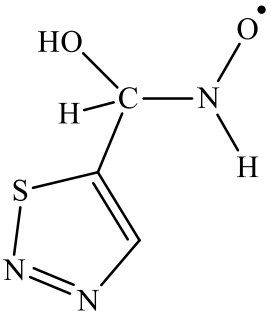

1,2,3-thiadiazol-5-yl spin adduct

Figure 13: ChemDraw® representations of the new heteroaryl spin adducts with •OH added at the C-site carbon

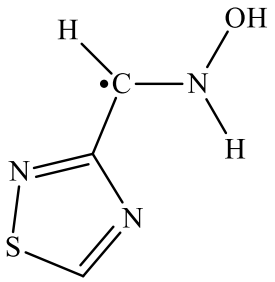

1,2,4-thiadiazol-3-yl spin adduct

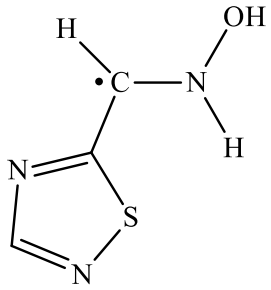

1,2,4-thiadiazol-5-yl spin adduct

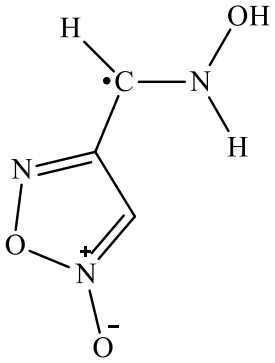

furoxan-4-yl spin adduct

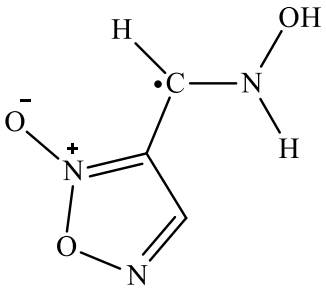

furoxan-3-yl spin adduct

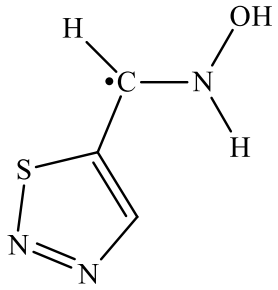

1,2,3-thiadiazol-5-yl spin adduct

Figure 14: ChemDraw® representations of the new heteroaryl spin adducts with •H added at the O-site oxygen

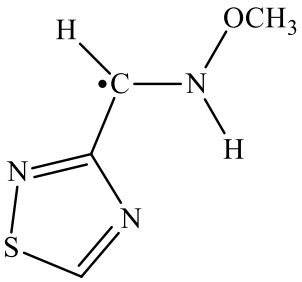

1,2,4-thiadiazol-3-yl spin adduct

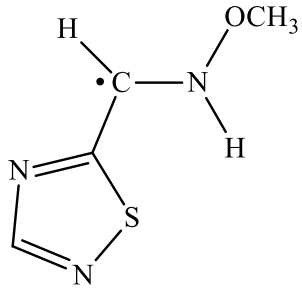

1,2,4-thiadiazol-5-yl spin adduct

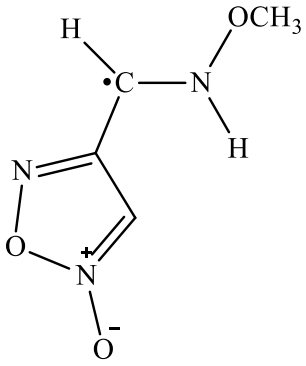

furoxan-4-yl spin adduct

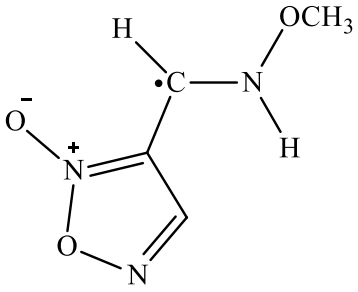

furoxan-3-yl spin adduct

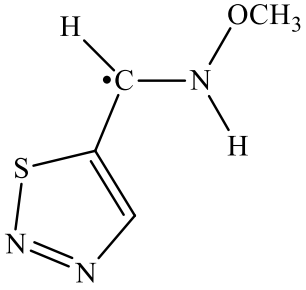

1,2,3-thiadiazol-5-yl spin adduct

Figure 15: ChemDraw® representations of the new heteroaryl spin adducts with •CH_3 added at the O-site oxygen

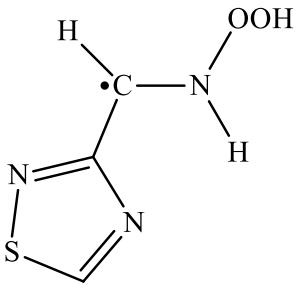

1,2,4-thiadiazol-3-yl spin adduct

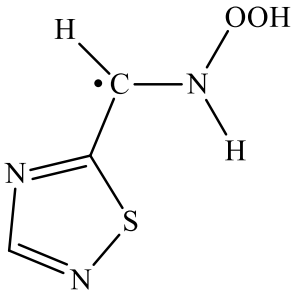

1,2,4-thiadiazol-5-yl spin adduct

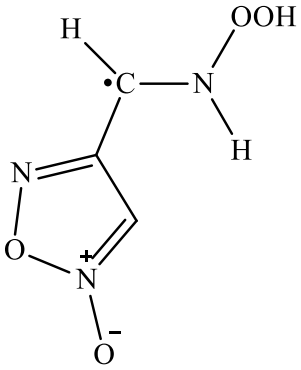

furoxan-4-yl spin adduct

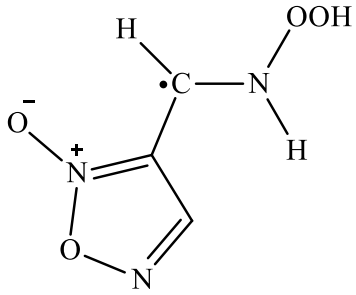

furoxan-3-yl spin adduct

Figure 16: ChemDraw® representations of the new heteroaryl spin adducts with •OH added at the O-site oxygen

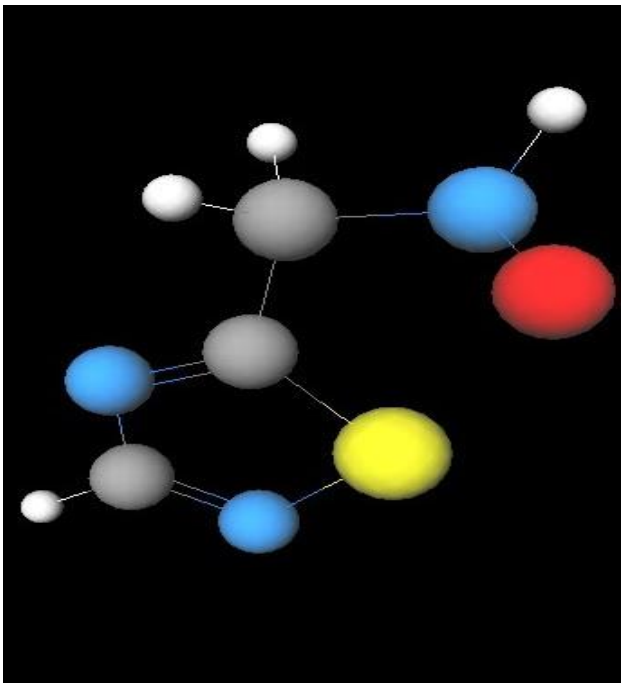

a) Hydrogen radical at the C-site of 1,2,4-thiadiazol-5-yl nitrone

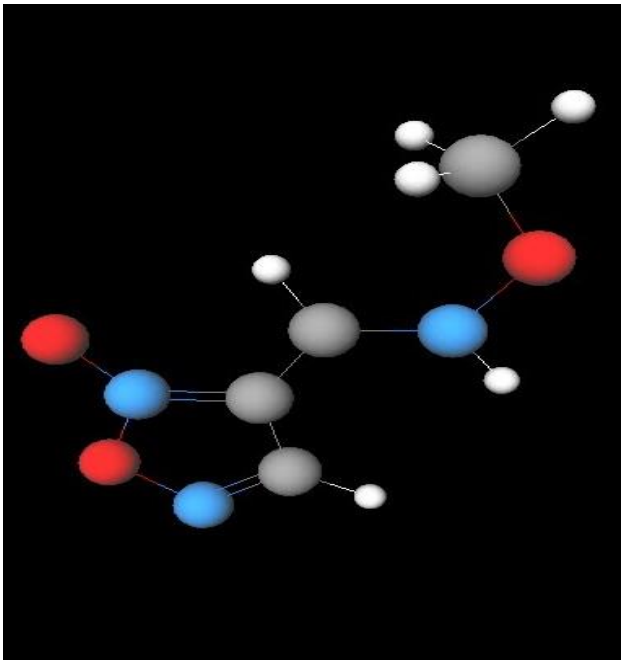

b) Methyl radical at the O-site of furoxan-3-yl nitrone

Figure 17: NWChem optimized geometries of example new heteroaryl spin adducts at the C- and O-sites. The colors follow standard colors: red - oxygen, hydrogen - white, grey - carbon, blue - nitrogen, and yellow - sulfur

The energetics of the spin trapping reactions of biologically relevant radicals with the new heteroaryl nitrones at both the C- and O-sites are shown in Tables 6, 7, and 8. Thermodynamically, the spin trapping reactions of di •OH are highly exothermic, hence their diadducts are very stable. The spin trapping reactions of di $•CH_3$ with the new heteroaryl nitrones have the least exothermicities as compared to di •H and di •OH. In addition, the diadducts are more stable than the mono spin adducts at the C-sites and the mono spin adduct at the O-sites. The double spin adducts are known to occur experimentally[120,121] having been observed using liquid chromatography and mass spectroscopy.[122] Even though the double spin adducts are generally stable, they are EPR inactive because they are diamagnetic.

Table 6: Energies of the spin trapping reactions of •H with formaldonitrone and the new heteroaryl nitrones at both C- and O-sites at (a) HF/6-31G* and (b) DFT/m06/6-31G*

(a)

Spin Trap	Energy (E_h)		ΔE	
	Parent	Diadduct	E_h	kJ/mol
Formaldonitrone	-168.80921	-170.01157	-0.20596	-540.74798
1,2,4-thiadiadozol-3-yl nitrone	-750.95291	-752.14573	-0.19642	-515.70071
1,2,4-thiadiazol-5-yl nitrone	-750.94373	-752.14639	-0.20626	-541.53563
Furoxan-4-yl nitrone	-502.97481	-504.17685	-0.20564	-539.90782
Furoxan-3-yl nitrone	-502.97470	-504.17701	-0.20591	-540.61671
1,2,3-thiadiazol-5-yl nitrone	-750.89840	-752.10158	-0.20678	-542.90089

(b)

Spin Trap	Energy (E_h)		ΔE	
	Parent	Diadduct	E_h	kJ/mol
Formaldonitrone	-168.80921	-170.91393	-0.22720	-596.51360
1,2,4-thiadiadozol-3-yl nitrone	-750.95291	-754.67003	-0.21291	-558.99521
1,2,4-thiadiazol-5-yl nitrone	-750.94373	-754.67160	-0.22115	-580.62933
Furoxan-4-yl nitrone	-502.97481	-506.75566	-0.22597	-593.28424
Furoxan-3-yl nitrone	-502.97470	-506.75056	-0.21959	-576.53355
1,2,3-thiadiazol-5-yl nitrone	-750.89840	-754.63406	-0.21971	-576.84861

Table 7: Energies of the spin trapping reactions of •CH_3 with formaldonitrone and the new heteroaryl nitrones at both C- and O-sites at (a) HF/6-31G* and (b) DFT/m06/6-31G*

(a)

Spin Trap	Energy (E_h)		ΔE	
	Parent	Diadduct	E_h	kJ/mol
Formaldonitrone	-168.80921	-248.0778	0.00861	22.60556
1,2,4-thiadiadozol-3-yl nitrone	-750.95291	-830.21125	0.01886	49.51693
1,2,4-thiadiazol-5-yl nitrone	-750.94373	-830.21313	0.00780	20.47890
Furoxan-4-yl nitrone	-502.97481	-582.24307	0.00894	23.47197
Furoxan-3-yl nitrone	-502.97470	-582.24686	0.00504	13.23252
1,2,3-thiadiazol-5-yl nitrone	-750.89840	-830.16683	0.00877	23.02564

(b)

Spin Trap	Energy (E_h)		ΔE	
	Parent	Diadduct	E_h	kJ/mol
Formaldonitrone	-168.80921	-249.47214	-0.19041	-499.92146
1,2,4-thiadiadozol-3-yl nitrone	-750.95291	-833.22912	-0.17700	-464.71350
1,2,4-thiadiazol-5-yl nitrone	-750.94373	-833.23218	-0.18673	-490.25962
Furoxan-4-yl nitrone	-502.97481	-585.30874	-0.18405	-483.22328
Furoxan-3-yl nitrone	-502.97470	-585.31344	-0.18747	-492.20249
1,2,3-thiadiazol-5-yl nitrone	-750.89840	-833.19462	-0.18527	-486.42639

Table 8: Energies of the spin trapping reactions of •OH with formaldonitrone and the new heteroaryl nitrones at both C- and O-sites at (a) HF/6-31G* and (b) DFT/m06/6-31G*

(a)

Spin Trap	Energy (E_h)		ΔE	
	Parent	Diadduct	E_h	kJ/mol
Formaldonitrone	-168.80921	-319.62732	-0.37131	-974.87441
1,2,4-thiadiadozol-3-yl nitrone	-750.95291	-901.76282	-0.36311	-953.345305
1,2,4-thiadiazol-5-yl nitrone	-750.94373	-901.76535	-0.37482	-984.08991
Furoxan-4-yl nitrone	-502.97481	-653.79778	-0.37617	-987.63434
Furoxan-3-yl nitrone	-502.97470	-653.79602	-0.37452	-983.30226
1,2,3-thiadiazol-5-yl nitrone	-750.89840	-901.72202	-0.37682	-989.34091

(b)

Spin Trap	Energy (E_h)		ΔE	
	Parent	Diadduct	E_h	kJ/mol
Formaldonitrone	-168.80921	-320.2125	-0.23573	-618.90912
1,2,4-thiadiadozol-3-yl nitrone	-750.95291	-904.965539	-0.21838	-573.35406
1,2,4-thiadiazol-5-yl nitrone	-750.94373	-904.96419	-0.22370	-587.32435
Furoxan-4-yl nitrone	-502.97481	-657.04745	-0.22772	-597.87886
Furoxan-3-yl nitrone	-502.97470	-657.04763	-0.22662	-594.99081
1,2,3-thiadiazol-5-yl nitrone	-750.89840	-904.92959	-0.22520	-591.26260

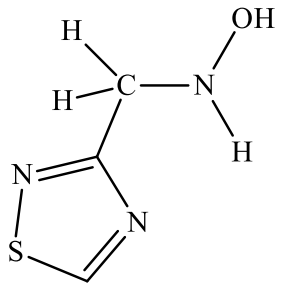

1,2,4-thiadiazol-3-yl double adduct

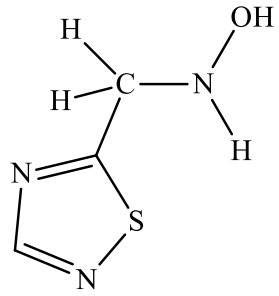

1,2,4-thiadiazol-5-yl double adduct

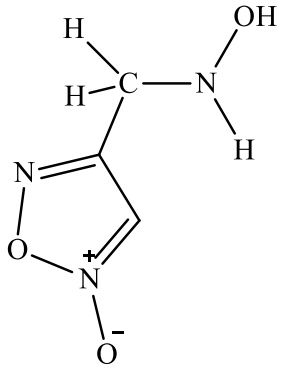

furoxan-4-yl double adduct

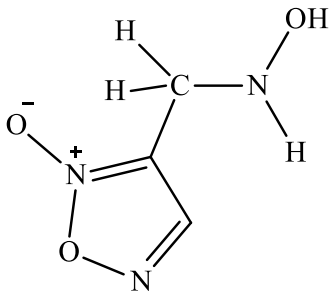

furoxan-3-yl double adduct

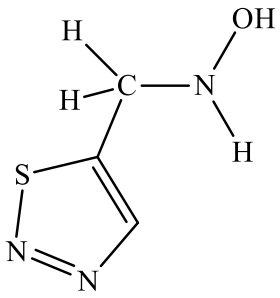

1,2,3-thiadiazol-5-yl double adduct

Figure 18: ChemDraw® representations of the new heteroaryl diadducts with •H added at both the C-site carbon and the O-site oxygen

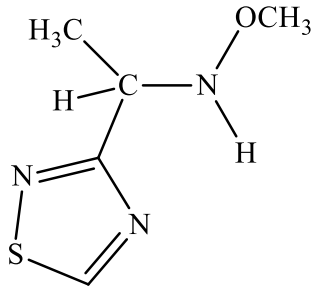

1,2,4-thiadiazol-3-yl double adduct

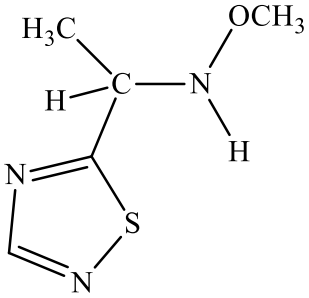

1,2,4-thiadiazol-5-yl double adduct

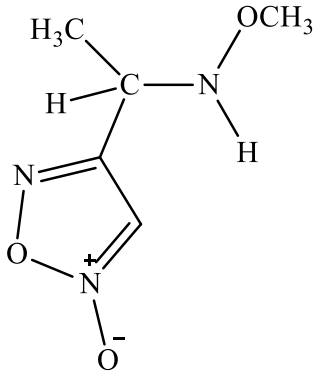

furoxan-4-yl double adduct

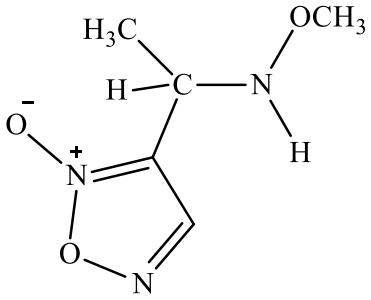

furoxan-3-yl double adduct

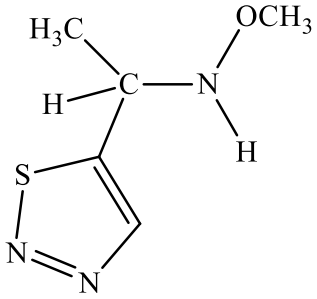

1,2,3-thiadiazol-5-yl double adduct

Figure 19: ChemDraw® representations of the new heteroaryl diadducts with •CH_3 added at both the C-site carbon and the O-site oxygen

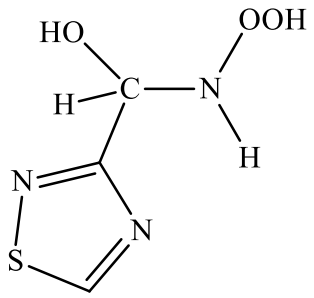

1,2,4-thiadiazol-3-yl spin adduct

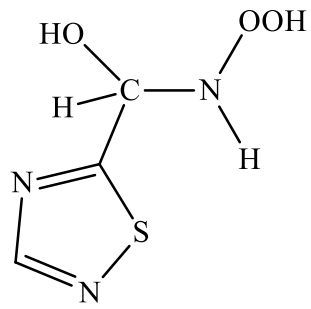

1,2,4-thiadiazol-5-yl spin adduct

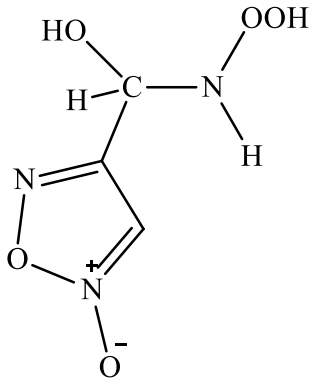

furoxan-4-yl spin adduct

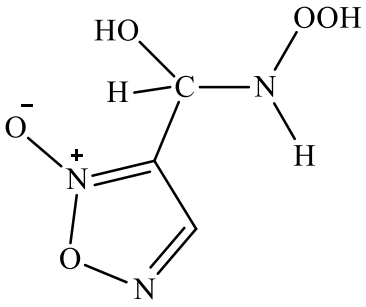

furoxan-3-yl spin adduct

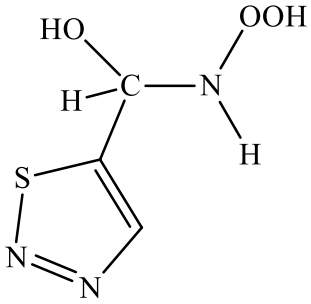

1,2,3-thiadiazol-5-yl spin adduct

Figure 20: ChemDraw® representations of the new heteroaryl diadducts with •OH added at both the C-site carbon and the O-site oxygen

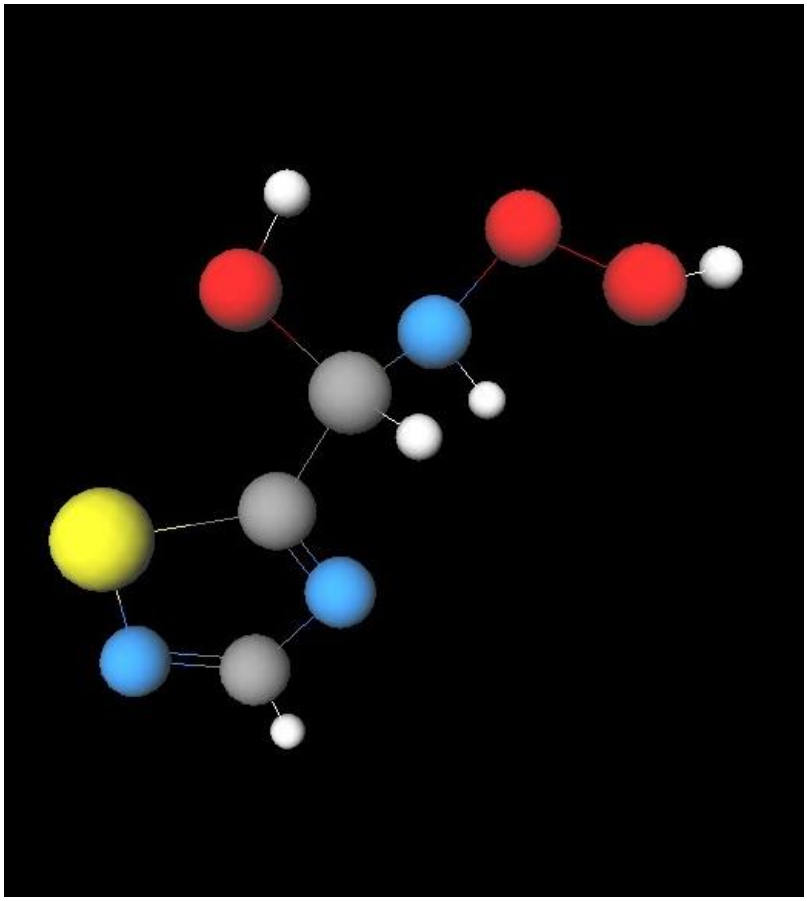

Figure 21: NWChem optimized geometry of the most stable diadduct thermodynamically of 1,2,3-thiadiazol-5-yl nitrone with di •OH at added both the C- and O-sites. The colors follow standard colors: red - oxygen, hydrogen - white, grey - carbon, blue - nitrogen, and yellow - sulfur

From Table 9, the reaction of PBN with •OH is highly endothermic for both the mono spin adduct and the diadduct while the reactions of DMPO and FxBN with •OH are exothermic. The reactivity of FxBN with •OH is highly exothermic and shows the highest stability for both the mono and diadduct, with the diadduct being the most stable all the spin adducts. This is rationalized by the presence of intramolecular hydrogen bonding in both the mono and diadduct of FxBN with •OH, which makes them very stable. The order of increasing stability of the spin

adducts of PBN, DMPO, and FxBN follows the same trend with the experimental half-lives and the spin trapping rate constants, obtained by Barriga *et al*.[64] Experimental studies have shown that the new heteroaryl nitrone, FxBN, is more sensitive to trapping the hydroxyl radical than DMPO in competition assays and is known to possess spin trapping capability in biological system because of its low toxicity.[64] The EPR experiments have also shown that the presence of a heteroaryl substituent in the nitrone increases the stability of the spin adduct formed.[62]

Data obtained for the new heteroaryl nitrones, mono spin adducts, and diadducts at the DFT/m06/6-31G* level of theory provide lower energies than data obtained at HF/6-31G*. DFT is well known to be a reliable method for the computation of molecular structures, vibrational frequencies and energy studies. The energy changes from DFT and HF are comparable. Thermodynamically, DFT indicates that the monoadduct of DMPO is more stable than the diadduct. However, from HF, the diadduct of DMPO is more stable than the mono spin. The mono spin adduct and diadduct of PBN at HF/6-31G* are more stable than at DFT/mo6/6-31G*. The present results by DFT and HF all indicate that FxBN for both the mono spin adduct and the diadduct are highly exothermic and are more stable than those of DMPO and PBN. In addition, the energy changes of the mono spin adduct and diadduct of FxBN at DFT/m06/6-31G* are lower than the energy changes of at HF/6-31G*.

Table 9: Energies of the addition of •OH to DMPO, PBN and FxBN at the DFT/m06/6-31G* and HF/6-31* levels of theory

Nitrone	ΔE (kJ/mol)				$t_{1/2}$ (s)	$k_{ST}*10^9$ ($dm^3mol^{-1}s^{-1}$)
	DFT		HF			
	Monoadduct	Diadduct	Monoadduct	Diadduct		
DMPO	-1123.81	-571.73	-628.14	-935.92	3300.0	3.6
PBN	+5940.85	+5739.95	+5471.65	+5195.04	36.0	2.6
FxBN	-1548.71	-1847.18	-698.44	-979.83	7560.0	12.2

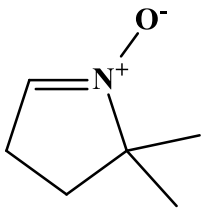

DMPO - 5,5-dimethylpyrroline-N-oxide

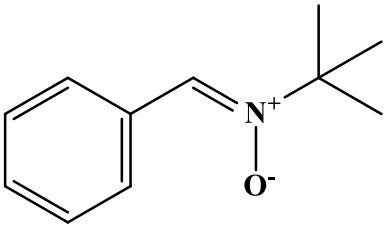

PBN - phenyl-N-t-butylnitrone

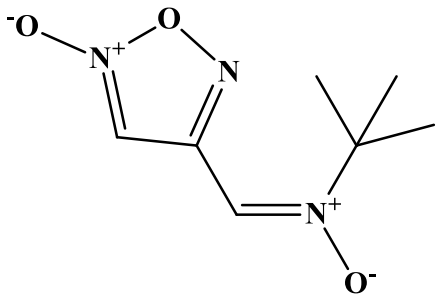

FxBN - (Z)-(3-methylfuroxan-4-yl)-N-tert-butylnitrone

Figure 22: ChemDraw® representations of 5,5-dimethylpyrroline-N-oxide, phenyl-N-t-butylnitrone and (Z)-(3-methylfuroxan-4-yl)-N-tert-butylnitrone

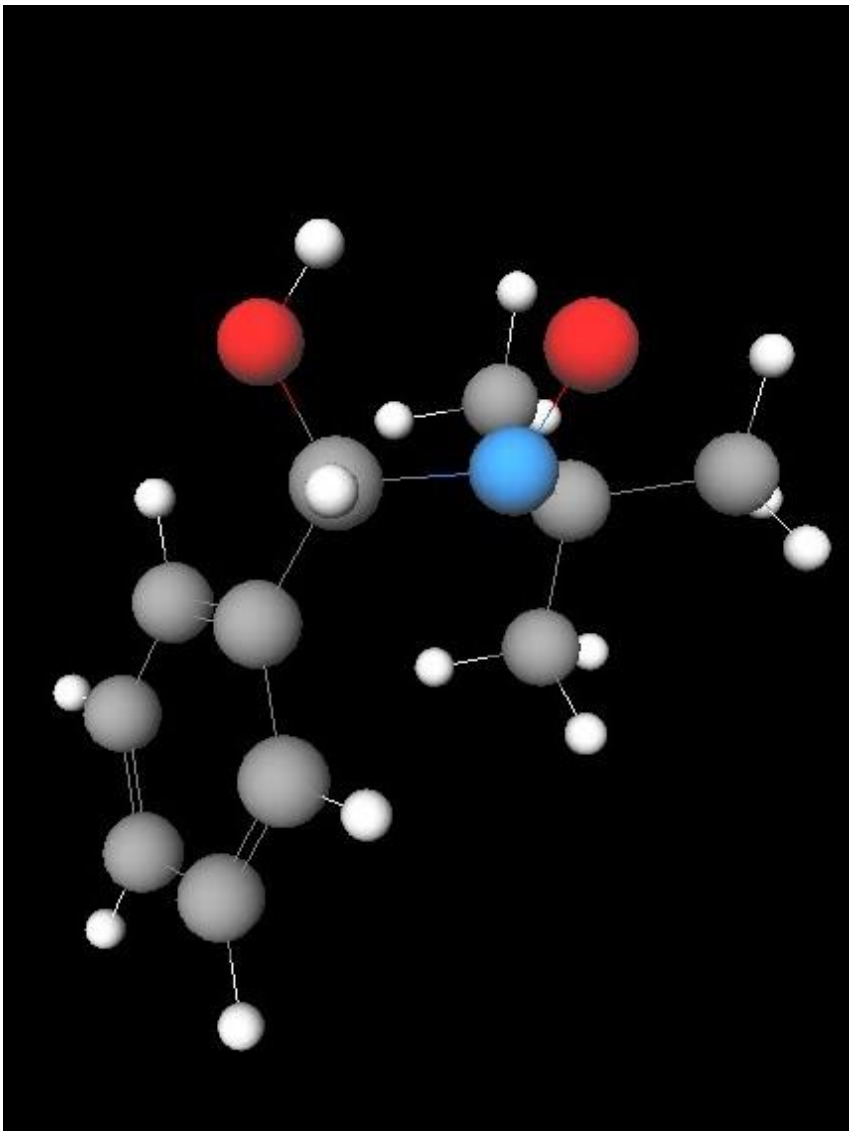

Figure 23: NWChem optimized geometry of the spin adduct of PBN with •OH radical at C- site. The colors follow standard colors: red - oxygen, hydrogen - white, grey - carbon, and blue - nitrogen

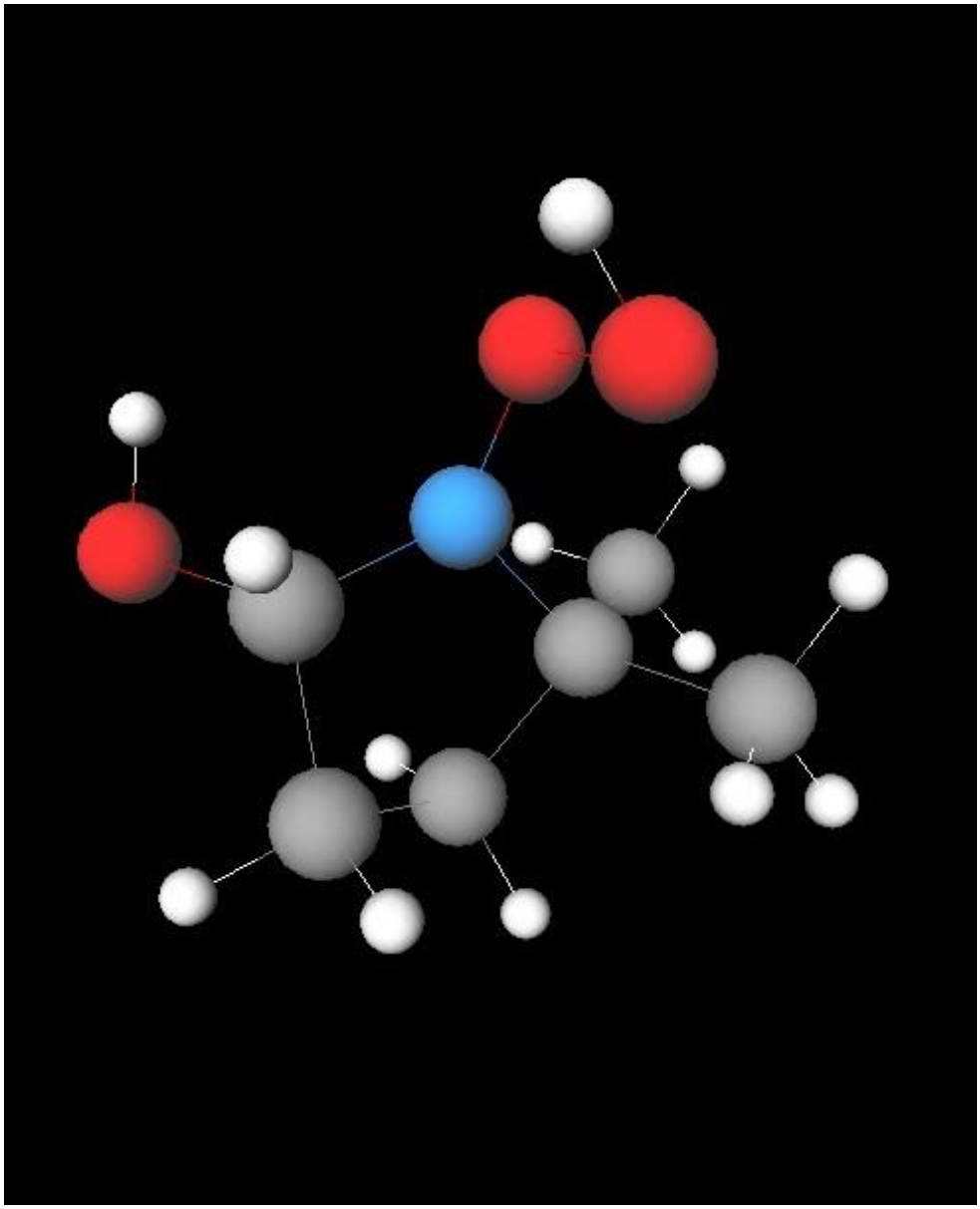

Figure 24: NWChem optimized geometry of diadduct of DMPO with di •OH at both the C- and O- sites. The colors follow standard colors: red - oxygen, hydrogen - white, grey - carbon, and blue - nitrogen

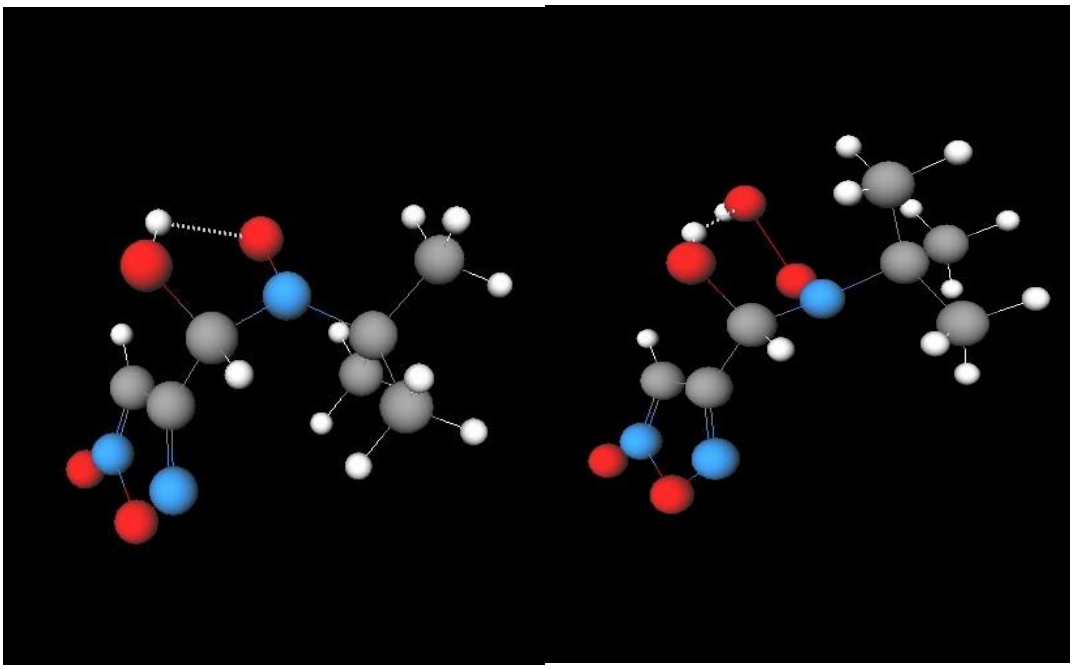

a b

Figure 25: NWChem optimized geometries of a) the spin adduct of FxBN with •OH at C-site and b) the diadduct of FxBN with di •OH at both C- and O- sites. The intramolecular hydrogen bonds are present in both a) and b). The colors follow standard colors: red - oxygen, hydrogen - white, grey - carbon, and blue - nitrogen

CHAPTER 4

CONCLUSIONS

The connectivity, the nature, and the position of the new heteroaryl substituents in the parent nitrone may affect the chemical and biological properties of the nitronyl group. New heteroaryl nitrones are the most stable spin traps due to the electronic effects of new heteroaryl substituents. The addition reaction between the new heteroaryl nitrones and the radicals at the C-site is more exothermic than at the O-site. This is due to the presence of resonance stabilization occurring at the C-site adduct. Generally, diadducts are thermodynamically more stable than mono spin adducts. The reactions of di •OH with the nitrones at both the C- and O- sites show the highest exothermicities with 1,2,3-thiadiazol-5-yl diadduct being the most thermodynamically stable compound. The new heteroaryl nitrone, FxBN, is the most stable spin trap adducts for the •OH radical compared to DMPO and PBN.

REFERENCES

1. Karlsson, J. Introduction to Nutraology and Radical Formation. In *Antioxidants and Exercise;* Illinois: Human Kinetics Press, 1997, 1-143.
2. Betteridge, D. J. What is Oxidative Stress? *Metabolism* **2000,** *49,* 3-8.
3. Halliwell, B. Free Radicals and Other Reactive Species in Disease. *Encyclopedia of Life Sciences* **2015**, 1–9.
4. Tegeli, V.; Karpe, P.; Katve V. Importance of Free Radical and Antioxidant on Human Health. *International Journal of Pharmaceutical, Chemical and Biological sciences* **2014**, *4*, 1038-1050.
5. Ebadi M. Antioxidants and Free Radicals in Health and Disease: An Introduction to Reactive Oxygen Species, Oxidative Injury, Neuronal Cell Death and Therapy in Neurodegenerative Diseases. **2001**, 13-5.
6. Bagchi, K.; Puri, S. Free Radicals and Antioxidants in Health and Disease. *East Mediterranean Health Journal* **1998**, *4*, 350-360.
7. Halliwell, B.; Erchabach, R. A.; Lologer, J.; Aruoma, O. I. The Characterization of Antioxidants. *Food Chem Toxicol.* **1995,** *33*, 601-617.
8. Buettner, G. R.; Jurkiewicz, B. A. Ascorbate free radical as a marker of oxidative stress: an ERR study. *Free Radical Biology and Medicine* **1993**, *14*, 49-55
9. Esme, H.; Cemek, M.; Sezer, M.; Soglam, H.; Demir, A.; Melek, H.; Unlu, M. High Levels of Oxidative Stress in Patients with Advanced Lung Cancer. *Respirology* **2008,** *13*,112-116.

10. Weisel, R. D.; Mickle, D. A.; Finkle, C. D.; Tumiati, L. C.; Madonik, M.; Ivanov, J.; Burtaon, G. W.; Ingold, K. U. Myocardial Free-Radical Injury after Cardioplegia. *Circulation* **1989**, *80*, III14-8.
11. Kenhrer, J. P. Free Radicals as Mediators of Tissue Injury and Disease. *Critical reviews in toxicology* **1993**, *23*, 21-48.
12. Droge, W. Free Radicals in the Physiological Control of Cell Function. *Physiological reviews* **2002,** *82*, 47-95
13. Janzen, E. G. Spin trapping. *Acc. Chem. Res*. **1971**, *4*, 31-40.
14. Eaton, G. R.; Eaton S. S.; Salikhov, K. M. *Foundations of modern EPR: World Scientific;* Singapore, **1998**.
15. Zweier, J. L.; Flaherty, J. T.; Weisfeldt, M. L. Direct Measurement of Free Radical Generation following Reperfusion of Ischemic Myocardium. *Proc. Natl. Acad. Sci.* **1987**, *84*, 1404.
16. Zweier, J. L.; Kuppusamy, P.; Lutty, G. A. Measurement of Endothelial Cell Free Radical Generation: Evidence for A Central Mechanism of Free Radical Injury in Postischemic Tissues. *Proc. Natl. Acad. Sci.* **1988**, *85*, 4046.
17. Floyd, R. A.; Kopke, R. D.; Choi, C-H; Foster, S. B.; Doblas, S.; Towner, R. A. Nitrones as Therapeutics. *Free Radical Biology and Medicine* **2008**, *45*, 1361.
18. Feuer H., Ed. Nitrile Oxides, Nitrones and Nitronates. In *Organic Synthesis: Novel Strategies in Synthesis.* John Wiley & Sons: Hoboken, N.J., 2008.
19. Floyd, R. A.; Towner, R. A.; He, T.; Hensley, K.; Maples, K. R. Theory and Biological Application of the Electron Spin Resonance Technique of Spin Trapping. *Free Radical Biol. Med.* **2011**, *51*, 931.

20. Villamena, F. A.; Zweier, J. L. Detection of Reactive Oxygen and Nitrogen Species by EPR Spin Trapping. *Antioxidant Redox Signaling* **2004**, *6*, 619.

21. Rosen, G. M.; Britigan, B. E.; Halpern, H. J.; Pou, S.; Biology and Detection by Spin Trapping: Free Radicals; Oxford University Press, N.Y., 1999.

22. Rhodes, C. J. *The Critical Role of Free Radicals: Toxicology of the human environment*; Taylor & Francis, London, 2000.

23. Thornalley, P. J. Theory and biological Application of the Electron Spin Resonance Technique of Spin Trapping. *Life Chemistry Reports* **2010**, 1–56.

24. Janzen, E. G. Critical Review of Spin Trapping in Biological Systems In: *Free Radicals in Biology* Academic Press, New York, **1980**, 115–154.

25. Novelli, G.; Angiolini, P.; Cansales, G.; Lippi, R.; Tani, R.; Anti-Shock Action of Phenyl-t-butyl-nitrone, A Spin trapper **1986**, 119–124.

26. Novelli, G. P.; Angiolini, P.; Tani, R.; Consales, G.; Bordi, L. Phenyl-t-butyl-nitrone is Active against Traumatic Shock in Rats. *Free Radic. Res. Commun.* **1985**, *1*, 321–327.

27. Novelli, G. P.; Anglolini, P.; Tani, R. The Spin Trap Phenyl Butyl Nitrone Prevents Lethal Shock in the Rat. In Free Radicals in Liver Injury; Poll, G.; Cheeseman, K. H.; Dianzani, M. U.; Slater T. F., Eds. IRL Press Limited: Oxford, 1986, pp 225–228.

28. Bosnjakovic, A.; Kadirov, M. K.; Schlick, S. Using ESR Spectroscopy to Study Radical Intermediates in Proton-Exchange Membranes Exposed to Oxygen Radicals. *Res. Chem. Intermed*. **2007**, *33*, 677.

29. Bosnjakovic, A.; Schlick, S. Spin Trapping by 5, 5-dimethylpyrroline-N-oxide in Fenton Media in the Presence of Nafion Perfluorinated Membranes: Limitations and Potential. *J. Phys. Chem. B.* **2006**, *110*, 10720 –10728.

30. Danilczuk, M.; Bosnjakovic, A.; Kadirov, M. K.; Schlick, S. J. Direct ESR and Spin Trapping Methods for the Detection and Identification of Radical Fragments in Nafion Membranes and Model Compounds exposed to Oxygen Radicals. *Power Sources* **2007**, *172*, 78.

31. Dodd, N. J.; Jha A. N. Photoexcitation of Aqueous Suspensions of Titanium Dioxide Nanoparticles: An Electron Spin Resonance Spin Trapping Study of Potentially Oxidative Reactions. *Photochem. Photobiol*. **2011**, 87, 632-640.

32. Ionita, P.; Conte, M.; Gilbert, B. C.; Chechik, V. Gold Nanoparticle-Initiated Free Radical Oxidations and Halogen Abstractions. *Org. Biomol. Chem*. **2007**, *5,* 3504-3509

33. Fu, H.; Zhang, L.; Zhang, S.; Zhu, Y.; Zhao, J. Electron Spin Resonance Spin-trapping Detection of Radical Intermediates in N-doped TiO2-assisted Photodegradation of 4-Chlorophenol. *J. Phys. Chem. B.* **2006**, *110*, 3061-3065.

34. Xiao, G.; Wang, X.; Li, D.; Fu, X. InVO 4-sensitized TiO 2 Photocatalysts for Efficient Air Purification with Visible Light. *J. Photochem. Photobiol., A*. **2008**, *193,* 213-221.

35. Mroz, P.; Pawlak, A.; Satti, M.; Lee, H.; Wharton, T.; Gali, H.; Sarna, T.; Hamblin, M. R. Functionalized Fullerenes Mediate Photodynamic Killing of Cancer Cells: Type I versus Type II Photochemical Mechanism. *Free Radical Biol. Med*. **2007**, *43*, 711.

36. Rajendran, M.; Inbaraj, J. J.; Gandhidasan, R.; Murugesan, R. Photogeneration of Reactive Oxygen Species by 3-arylcoumarin and flavanocoumarin derivatives. *J. Photochem. Photobiol. A.* **2006**, *182*, 67.

37. Zeng, Z.; Zhou, J.; Zhang, Y; Qiao, R.; Xia, S.; Chen, J.; Wang, X.; Zhang, B. Photodynamic Properties of Hypocrellin A, Complexes with Rare Earth Trivalent Ions: Role of the Excited State Energies of the Metal Ions. *J. Phys. Chem. B.* **2007**, *111*, 2688.

38. Janzen, E. G.; Liu, J. I.-P. J. Radical Addition Reactions of 5, 5-dimethyl-1-pyrroline-1-oxide. ESR Spin Trapping with A Cyclic Nitrone. *Magn. Reson.* **1973,** *9*, 510.

39. Timmins, G. S.; Liu, K. J.; Bechara, E. J.; Kotake, Y.; Swartz, H. M. Trapping of Free Radicals with Direct in vivo EPR Detection: A Comparison of 5, 5-dimethyl-1-pyrroline-N-oxide and 5-diethoxyphosphoryl-5-methyl-1-pyrroline-N-oxide as Spin Traps for HO• and $SO_4^{\bullet -}$. *Free Radical Biol. Med.* **1999**, *27*, 329.

40. Kotake, Y.; Janzen, E. G. Decay and Fate of the Hydroxyl Radical Adduct of alpha-phenyl-N-tert-butylnitrone (PBN) in Aqueous Media. *J. Am. Chem. Soc.* **1991**, *113*, 9503.

41. Floyd, R. A.; Hensley, K.; Forster, M. J.; Kelleher-Andersson, J. A.; Wood, P. L. Nitrones, Their Value as Therapeutics and Probes to Understand Aging. *Mech. Ageing Dev.* **2002**, *123*, 1021.

42. Dikalova, A.E.; Kadiiska, M.B.; Mason, R.P. An In Vivo ESR Spin-Trapping Study: Free Radical Generation in Rats from Formate Intoxication—Role of the Fenton Reaction. *Proc. Natl. Acad. Sci.* **2001**, *98*, 13549-13553.

43. Kadiiska, M. B.; Burkitt, M. J.; Xiang, Q. H.; Mason, R. P. Iron Supplementation generates Hydroxyl Radical In Vivo. An ESR Spin-Trapping Investigation. *J. Clin. Invest.* **1995,** *96*, 1653-1657.

44. Hensley, K.; Carney, J. M.; Stewart, C. A.; Tabatabaie, T.; Pye, Q.; Floyd, R. A. *Int. Rev. Neurobiol.* **1997**, *40*, 299.

45. Kotake, Y. Pharmacologic Properties of Phenyl N-tert-butylnitrone. *Antioxid. Redox Signal.* **1999,** *1*, 481.

46. Li, P. A.; He, Q. P.; Nakamura, L.; Csiszar, K. Free Radical Spin Trap α-phenyl-N-tert-butyl-nitrone inhibits Caspase-3 Activation and reduces Brain Damage following A Severe Forebrain Ischemic Injury. *Free Radical Biol. Med.* **2001**, *31*, 1191.

47. Durand, G.; Polidori, A.; Salles, J. P.; Prost, M.; Durand, P.; Pucci, B. Synthesis and Antioxidant Efficiency of A New Amphiphilic Spin-Trap derived from PBN and Lipoic Acid. *Bioorg. Med. Chem. Lett.* **2003**, *13*, 2673.

48. Floyd, R. A.; Kopke, R. D.; Choi, C.-H.; Foster, S. B.; Doblas, S.; Towner, R. A. Nitrones as Therapeutics. *Free Radical Biol. Med.* **2008**, *45*, 1361.

49. Fréjaville, C.; Karoui, H; Tuccio, B.; Moigne, F. L.; Culcasi, M.; Pietri, S.; Lauricella, R.; Tordo, P. 5-(Diethoxyphosphoryl)-5-methyl-1-pyrroline N-oxide: A New Efficient Phosphorylated Nitrone for the In Vitro and In Vivo Spin Trapping of Oxygen-Centered Radicals. *J. Med. Chem.*, **1995**, *38* 258-265.

50. Olive, G.; Mercier, A.; Moigne, F..; Rockenbauer, A.; Tordo, P. 2-ethoxycarbonyl-2-methyl-3, 4-dihydro-2H-pyrrole-1-oxide: Evaluation of the Spin Trapping Properties. *Free Radical Biol. Med*. **2000** *28*, 403-408.

51. Zhao, H.; Joseph, J.; Zhang, H.; Karoui, H.; Kalyanaraman, B. Synthesis and Biochemical Applications of a Solid Cyclic Nitrone Spin Trap: A Relatively Superior Trap for Detecting Superoxide Anions and Glutathiyl Radicals. *Free Radical Biol. Med.* **2001**, *31* 599-606.

52. Stolze, K.; Rohr-Udilova, N.; Rosenau, T.; Hofingerc, A.; Nohl, H. Free Radical Trapping Properties of Several Ethyl-substituted derivatives of 5-ethoxycarbonyl-5-methyl-1-pyrroline N-oxide (EMPO). *Bioorg. Med. Chem*. **2007**, *15*, 2827.

53. Stolze, K.; Rohr-Udilova, N.; Hofinger, A.; Rosenau, T. Spin Trapping Experiments with Different Carbamoyl-substituted EMPO derivatives. *Bioorg. Med. Chem.* **2008**, *16*, 8082.

54. Villamena, F. A.; Rockenbauer, A.; Gallucci, J.; Velayutham, M.; Hadad, C. M.; Zweier, J. L. Spin Trapping by 5-carbamoyl-5-methyl-1-pyrroline N-oxide (AMPO): Theoretical and Experimental Studies. *J. Org. Chem.,* **2004,** *69*, 7994-8004.

55. Villamena, F. A.; Xia, S.; Merle, J. K.; Lauricella, R.; Tuccio, B.; Hadad, C. M.; Zweier, J. L. Reactivity of Superoxide Radical Anion with Cyclic Nitrones: Role of Intramolecular H-bond and Electrostatic Effects. *J. Am. Chem. Soc.* **2007,** *129*, 8177-8191.

56. Terabe, S.; Konaka, R. Electron Spin Resonance Studies on Oxidation with Nickel Peroxide. Spin Trapping of Free-Radical Intermediates." *J. Am. Chem. Soc.* **1969,** *91*, 5655–5657.

57. Bardelang, D.; Charles, L.; Finet, J.P.; Jicsinszky, L.; Karoui, H.; Marque, S.R., et al. α-Phenyl-N-tert-butylnitrone-Type Derivatives Bound to β-Cyclodextrins: Syntheses, Thermokinetics of Self-Inclusion and Application to Superoxide Spin-Trapping. *Chemistry* **2007,** *13* 9344–9354.

58. Terabe, S.; Konaka, R. Electron Spin Resonance Studies on Oxidation with Nickel Peroxide. Spin Trapping of Free-Radical Intermediates. *J. Am. Chem. Soc.* **1969**, *91*, 5655– 5657.

59. Bardelang, D.; Charles, L.; Finet, J. P.; Jicsinszky, L.; Karoui, H.; Marque, S. R.; et al. Alpha-phenyl-N-tertbutylnitrone-type derivatives bound to beta-cyclodextrins: Syntheses, Thermokinetics of Selfinclusion and Application to Superoxide Spin-Trapping. *Chemistry.* **2007**, *13*, 9344–9354.

60. Sankuratri, N.; Kotake, Y.; Janzen, E. G. Studies on the Stability of Oxygen Radical Spin Adducts of a New Spin Trap: 5-methyl-5-phenylpyrroline-1-oxide (MPPO).*Free Radical Biol. Med.* **1996**, *21*, 889.

61. Tsai, P.; Ichikawa, K.; Mailer, C.; Pou, S.; Halpern, H. J.; Robinson, B. H.; Nielsen, R.; Rosen, G. M. Esters of 5-carboxyl-5-methyl-1-pyrroline N-oxide: A Family of Spin Traps for superoxide. *J. Org. Chem.* **2003**, *68*, 7811.

62. Goldstein, S.; Lestage, P. Chemical and Pharmacological Aspects of Heteroaryl-nitrones. *Current Medicinal Chemistry* **2000**, *7*, 1255-1267.

63. Porcal, W.; Hernández, P.; González, M.; Ferreira, A.; Olea-Azar, C.; Cerecetto, H.; Castro, A. Heteroarylnitrones as Drugs for Neurodegenerative Diseases: Synthesis, Neuroprotective Properties, and Free Radical Scavenger Properties. *J. Med. Chem.* **2008**, *51*, 6150–6159.

64. Barriga, G.; Olea-Azar, C.; Norambuena, E.; Castro, A.; Porcal, W.; Gerpe, A.; González, M.; Cerecetto, H. New Heteroaryl Nitrones with Spin Trap Properties: Identification of a 4-furoxanyl derivative with Excellent Properties to be used in Biological Systems. *Bioorganic & Medicinal Chemistry* **2010**, *18*, 795–802.

65. Boyd, S. L.; Boyd, R. J. A Theoretical Study of Spin Trapping by Nitrone: Trapping of Hydrogen, Methyl, Hydroxyl, and Peroxyl Radicals. *J. Phys. Chem*. **1994**, *98*, 11705 – 11713.

66. Young, D. *Computational Chemistry: A Practical Guide for Applying Techniques to Real World Problems*, John Wiley & Sons, **2001.**

67. Pacheco, B. A. *Introduction to Computational Chemistry*, LONI workshop series, Tulane University, New Orleans, **2011**, 4.

68. Lavery, D. R. “Mathematical Challenges from Theoretical/Computational Chemistry.” National Academy of Sciences – National Research Council 2101 Constitution Avenue 20418

69. Mathematical Challenges from Theoretical/Computational Chemistry, Committee on Mathematical Challenges from Computational Chemistry, National Research Council, **1995,** 1-144.

70. Leach, A. R. Principles and Applications: In *Molecular Modelling,* Ed., Prentice Hall: Harlow, England. 2001.

71. Lewars E. *Introduction to the Theory and Applications of Molecular and Quantum Mechanics,* Klumer Academic Publishers, **2004,** 2-3.

72. Anslyn, E. V.; Dennis, A. D. *Modern Physical Organic Chemistry,* University Science Books, **2006**

73. Allinger, N. L. Conformational Analysis. 130. MM2. A Hydrocarbon Force Field Utilizing V1 and V2 Torsional Terms. *J. Am. Chem. Soc.* **1997**, *99*, 8127-8134

74. Rappe, K. A.; Casewit C. J.; Colwell K. S.; Goddardlii, W. A.; Skiff, W. M. UFF, A Full Periodic Table Force Field for Molecular Mechanics and Molecular Dynamics Simulations. *J. Am. Chem. Soc.* **1992**, 114, 10024-10035.

75. Levine, I. N. *Quantum Chemistry.* Prentice Hall: Englewood Cliffs, N. J., **1991**, 455–544.

76. Dewar, J. S.; Zoebisch, E. G.; Healy, E. F.; Stewart, J. P. Development and Use of Quantum Mechanical Molecular Models. 76. AM1: A New General Purpose Quantum Mechanical Molecular Model. *J. Am. Chem. Soc.* **1985**, *107*, 3902.

77. Kohn, W.; Becke, A. D.; Parr, R. G. Density Functional Theory of Electronic Structure. *J. Phys. Chem.* **1996**, *100*, 12974.

78. Alder, B. J.; Wainwright, T. E. Studies in Molecular Dynamics. I. General Method. *J. Chem. Phys.* **1959**, *31*, 459

79. Schrödinger, E. Quantisierung als eigenwertproblem. *Ann. Phys.* **1926**, *79*, 361.

80. Schrödinger, E. An Undulatory Theory of the Mechanics of Atoms and Molecules. *Phys. Rev*. **1926**, *28*, 1049.

81. Hartree, D. R. The Wave Mechanics of an Atom with a Non-Coulomb Central Field II: Some Results and Discussion. *Proc. Cambridge Phil. Soc.* **1927**, *24*, 111.

82. McWeeny, R. Natural Units in Atomic and Molecular Physics. *Nature* **1973**, *243*, 196.

83. Teschl, G. Mathematical Methods in Quantum Mechanics; With Applications to Schrödinger Operators, American Mathematical Society, **2009.**

84. Courant, R.; Hilbert, D. Methods of Mathematical Physics, **1962**, Volume I, Wiley-Interscience.

85. Fock, V. Näherungsmethode zur Lösung des Quantenmechanischen Mehrkörperproblems. *Z. Phys*. **1930**, *61*, 126.

86. Hartree, D. R. The Wave Mechanics of an Atom with a Non-Coulomb Central Field. Part I. Theory and Methods. *Proc. Cambridge Phil. Soc.* **1928**, 24, 426.

87. Slater, J.; Verma, H. C. The Theory of Complex Spectra. *Physical Review*, **1929**, *34*, 1293-1322.

88. Atkins, P.W. An Introduction to Quantum Chemistry: In *Molecular Quantum Mechanics Parts I and II*, Oxford University Press. 1977.

89. Levine, I. N. *Quantum Chemistry*. Eds., Pearson Education Inc., 2014, 409-411.

90. Roothaan, C. C. J. New Developments in Molecular Orbital Theory. *Rev. Mod. Phys.* **1951**, *23*, 69.

91. Hall, G. G. The Molecular Orbital Theory of Chemical Valency. VIII. A Method of Calculating Ionization Potentials. *Proc. Roy. Soc.* **1951**, *A205*, 541.

92. Pople, J. A.; Nesbet, R. K. Self-Consistent Orbitals for Radicals. *J. Chem. Phys.* **1954**, *22*, 571.

93. Møller, C.; Plesset, M. S. Note on an Approximation Treatment for Many-Electron Systems. *Phys. Rev.* **1934**, *46*, 618.

94. Kohn, W.; Becke, A. D.; Parr, R. G. Density Functional Theory of Electronic Structure. *J. Phys. Chem.* **1996**, *100*, 12974.

95. Geerlings, P.; De Proft F.; Langenaeker, W. Conceptual Density Functional Theory. *Chem. Rev.* **2003**, *103*, 1793-1874.

96. Parr R. G., Yang, W; *Density Functional Theory of Atoms and Molecules*, Oxford New York, **1989**, 185-187.

97. Hohenberg, P.; Kohn, W. Inhomogeneous electron gas. *Phys. Rev*. **1964**, *136*, B864.

98. Kohn, W.; Sham, L. J. Self-Consistent Equations including Exchange and Correlation Effects. *Phys. Rev*. **1965**, *140*, A1133.

99. Levine, I. N. *Quantum Chemistry*. Eds.; Pearson Education Inc., 2014, 559.

100. Levine, I. N. *Quantum Chemistry*. Eds.; Pearson Education Inc.,**2014,** 560.

101. Kohn, W.; Sham, J. L. Self-Consistent Equations including Exchange and Correlation Effects. *Phys. Rev*., **1965**, *140*, A1133.

102. Kim, K.; Jordan, K. D. Comparison of Density Functional and MP2 Calculations on the Water Monomer and Dimer. *J. Phys. Chem.* **1994.** *98*, 10089–10094.

103. Stephens, P. J.; Devlin, F. J.; Chabalowski, C. F.; Frisch, M. J. *Ab initio* Calculation of Vibrational Absorption and Circular Dichroism Spectra using Density Functional Force Fields. *J. Phys. Chem.*, **1994,** *98*, 11623–11627.

104. Raghavachari, K. Perspective on "Density Functional Thermochemistry. III. The Role of Exact Exchange. *Theor. Chem. Acc.* **2000**, *103*, 361.

105. Young, D. C, A Practical Guide for Applying Techniques to Real World Problem: In *Computational Chemistry;* John Wiley & Sons Inc., **2001,** 45.

106. Dunning, T. H. Gaussian Basis Sets for Use in Correlated Molecular Calculations. I. The Atoms Boron through Neon and Hydrogen. *J. Chem. Phys.* **1989,** *90*, 1007–1023.

107. Peterson, G. A.; Malick, D. K., Wilson, G. W., Ochterski, J. W., Montgomery, J. J. A.; Frisch, M. J. Calibration and Comparison of the Gaussian-2, Complete Basis Set, and Density Functional Methods for Computational Thermochemistry. *J. Chem. Phys.* **1998**, *109*, 10570.

108. Peterson, G. A.; Al-Laham, M. A. A Complete Basis Set Model Chemistry. II. Open-Shell Systems and the Total Energies of the First-Row Atoms. *J. Chem. Phys*. **1991**, *94*, 6081.

109. Peterson, G. A.; Bennett, A.; Tensfeldt, T. G.; Al-Laham, M. A.; Shirley, W. A.; Mantzaris, J. A Complete Basis Set Model Chemistry. I. The Total Energies of Closed-Shell Atoms and Hydrides of the First-Row Elements. *J. Chem. Phys*. **1988**, *89*, 2193.

110. Lowdin, P. O. Quantum Theory of Many-Particle Systems. I. Physical Interpretations by Means of Density Matrices, Natural Spin-Orbitals, and Convergence Problems in the Method of Configurational Interaction. *Phys. Rev.* **1955**, *97*, 1474.

111. Shull, H.; Lowdin, P. O. Role of the Continuum in Superposition of Configurations. *J. Chem. Phys.* **1955**, *23*, 1362.

112. Lowdin, P. O.; Shull, H. Natural Orbitals in the Quantum Theory of Two-Electron Systems. *Phys. Rev.* **1956**, 101, 1730.

113. Shull, H.; Lowdin, P. O. Superposition of Configurations and Natural Spin Orbitals. Applications to the He Problem. *J. Chem. Phys.* **1959**, *30*, 617.

114. Shull, H. Natural Spin Orbital Analysis of Hydrogen Molecule Wave Functions. *J. Chem. Phys.* **1959**, 30, 1405.

115. Ochterski, J. W.; Petersson, G. A.; Montgomery Jr, J. A.; A Complete Basis Set Model Chemistry. V. Extensions to Six or More Heavy Atoms. *J. Chem. Phys.* **1996,** *104*, 2598-2619.

116. Valiev, M. ; Bylaska, E.J. ; Govind, N.; Kowalski, K.; Straatsma, T.P.; van Dam, H.J.J.; Wang, D.; Nieplocha, J.; Apra, E.; Windus, T. L.; de Jong, W.A.; "NWChem: a comprehensive and scalable open-source solution for large scale molecular simulations" *Comput. Phys. Commun.* **2010,** *181*, 1477.

117. Apra, E.; Bylaska, E. J.; de Jong, W. A.; Govind, N.; Kowalski, K.; Straatsma, T. P.; Valiev, M.; van Dam, H. J. J.; Wang, D.; Windus, T. L. et al. "NWChem, A computational Chemistry package for parallel computers. Version 6.3", Pacific Northwest National Laboratory, Richland, Washington 993 52-0999, USA, **2013.**

118. "Extensible Computational Chemistry Environment (ECCE), A Problem Solving Environment for Computational Chemistry, Software Version 7.0" (2013), as developed and distributed by Pacific Northwest National Laboratory, P.O. Box 999,

Richland, Washington 99352, USA, and funded by the U.S. Department of Energy, was used to obtain some of these results.

119. Buettner, G. R. The Pecking Order of Free Radicals and Antioxidants: Lipid Peroxidation, α-Tocopherol, and Ascorbate. *Arch. Biochem. Biophys*. **1993**, *300*, 535-543.

120. Iwamura, M.; Inamoto, N. Novel Radical 1,3-Addition to Nitrones. *Bull. Chem. Soc. Jpn.* **1967**, *40*, 702-703.

121. Iwamura, M.; Inamoto, N. Reactions of Nitrones with Free Radicals. I. Radical 1,3-Addition to Nitrones. *Bull. Chem. Soc. Jpn.* **1970**, *43*, 856-860.

122. Janzen, E. G.; Krygsman, P. H.; Lindsay, D. A.; Haire, D. L. Detection of Alkyl, Alkoxyl, and Alkyperoxyl Radicals from The Thermolysis of Azobis(isobutyronitrile) by ESR/Spin Trapping. Evidence for Double Spin Adducts from Liquid-Phase Chromatography and Mass Spectroscopy. *J. Am. Chem. Soc.* **1990**, *112*, 8279.

APPENDIX

Tables of Additional Data from the Calculations

Table A1: The parent nitrone spin traps

Optimized Species[a]	Selected Parameters		[b]Charge Population	Energy (E_h)[c]	Dipole Moment (D)
	Bond lengths (Å)	Bond angles (deg)			
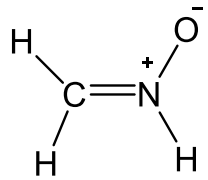 formaldonitrone	CN 1.269 NO 1.254	CNO 128.3 CNH_1 116.5 NCH_2 118.9	C -0.223 O -0.593 N -0.016 H_1 +0.393	SCF -168.80921 $MP2_1$ -169.32379 $MP2_2$ -169.50071 $MP2_3$ -169.55895 DFT -169.69089	4.47
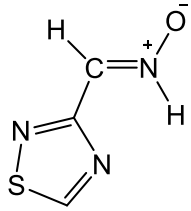 1,2,4 - thiadiazol - 3 -yl nitrone	CN 1.277 NO 1.244	CNO 127.8 CNH_1 116.1 NCS 120.0	C -0.017 O -0.557 N -0.072 H_1 +0.433	SCF -750.95291 $MP2_1$ -752.19826 $MP2_2$ -752.60343 $MP2_3$ -752.81677 DFT -753.46128	5.65
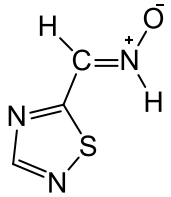 1,2,4 - thiadiazol - 5 - yl nitrone	CN 1.279 NO 1.241	CNO 127.5 CNH_1 117.9 NCS 123.0	C +0.027 O -0.538 N -0.081 H_1 +0.417	SCF -750.94373 $MP2_1$ -752.19170 $MP2_2$ -752.59696 MP_3 -752.81040 DFT -753.45461	1.97

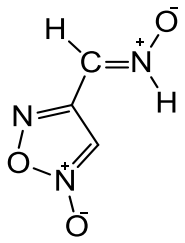 furoxan - 4 - yl nitrone	CN 1.277 NO 1.242	CNO 127.5 CNH_1 117.7 NCS 122.1	C +0.021 O -0.540 N -0.083 H_1 +0.411	SCF -502.97481 $MP2_1$ -504.49516 $MP2_2$ -504.96856 $MP2_3$ -505.13295 DFT -505.53385	1.76
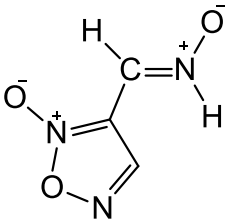 furoxan - 3 - yl nitrone	CN 1.275 NO 1.251	CNO 127.3 CNH_1 118.0 NCS 122.5	C +0.054 O -0.556 N -0.106 H_1 +0.404	SCF -502.97470 $MP2_1$ -504.47422 $MP2_2$ -504.96811 $MP2_3$ -505.13295 DFT -505.53513	4.26
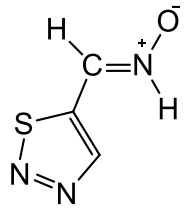 1,2,3 - thiadiazol - 5 - yl nitrone	CN 1.278 NO 1.246	CNO 127.3 CNH_1 117.6 NCS 122.8	C +0.035 O -0.548 N -0.083 H_1 +0.413	SCF -750.89840 $MP2_1$ -752.15743 $MP2_2$ -752.56122 $MP2_3$ -752.69673 DFT -753.41851	0.26

[a]All structures were optimized at the HF/6-31G* level and have no imaginary frequencies

[b]Mulliken population analysis

[c]1 au = 2625.5 kJ/mol. The $MP2_1$, $MP2_2$ and $MP2_3$ energies are single point energies obtained with the cc-pVDZ, cc-pVTZ and cc-pVQZ basis sets respectively using the 6-31G* optimized geometry, *i.e.* MP2/cc-pVDZ//HF/6–31G*, MP2/cc-pVTZ//HF/6–31G* and MP2/cc-pVQZ//HF/6–31G* respectively.

Table A2: Selected biological relevant radicals

Optimized Radical[a]	Selected Parameters		Spin Population	[b]Charge Populations	[c]Energy (E_h)	Dipole (D)
	Bond lengths (Å)	Bond angles (deg)				
•H					SCF -0.49820 $MP2_1$ -0.49927 $MP2_2$ -0.49980 DFT -0.49792	0
•CH_3	CH 1.073	HCH 120.0	C +1.294 H -0.098	C -0.530 H +0.175	SCF -39.63860 $MP2_1$ -39.69002 $MP2_2$ -39.73568 DFT -39.79542	0
•OH	OH 0.958		O +1.056 H -0.056	O -0.457 H + 0.457	SCF -75.22340 $MP2_1$ -75.36660 $MP2_2$ -75.46843 DFT -75.64294	1.94

[a]All structures were optimized at the HF/6-31G* level and have no imaginary frequencies

[b]Mulliken population analysis

[c]1 au = 2625.5 kJ/mol. The $MP2_1$ and $MP2_2$ energies are single point energies obtained with the cc-pVDZ and cc-pVTZ basis sets respectively using the 6-31G* optimized geometry, *i.e.* MP2/cc-pVDZ//HF/6–31G* and MP2/cc-pVTZ//HF/6–31G* respectively.

Table A3: The reaction of new heteroaryl nitrones with •H at the C-site carbon and the O-site oxygen

Table A3a: 1,2,4-thiadiazol-3-yl nitrone

Optimized adducts[a]	Selected parameters			Spin populations	[b]Charge populations	Energy[c] (a.u.)	ΔE^d (kJ/mol)	Dipole moments (D)
	Bond lengths (Å)	Bond angles (deg)	Dihedral angles (deg)					
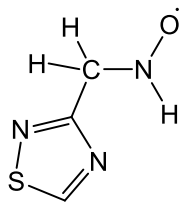	CN 1.441 NO 1.258	CNO 119.5 CNH_1 121.6 NCH_3 109.7 NCH_2 109.7 NCS 111.5	$ONCH_1$ +180.0 $ONCH_3$ +59.0 $ONCH_2$ -59.0 ONCS +180.0	C -0.069 N +0.361 O +0.687 H_1+0.034	C -0.119 N -0.310 O -0.350 H_1 +0.412	SCF -751.55541 $MP2_1$ -752.77293 $MP2_2$ -753.17996 DFT -754.04881	SCF -273.83965 $MP2_1$ -197.9627 $MP2_2$ -201.43099 DFT -235.27106	4.53
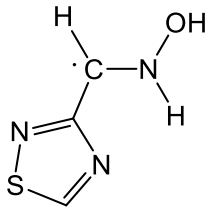	CN 1.352 NO 1.378 OH_2 0.948	CNO 123.0 CNH_1 124.8 NCH_3 118.1 NCS 121.7 NOH_2 106.9	$ONCH_1$ +180.0 $ONCH_3$ 0.0 ONCS +180.0 $CNOH_1$ +180.0	C +0.748 N +0.208 O -0.012 H_1 -0.025 H_2 -0.0006	C -0.013 N -0.384 O -0.577 H_1 +0.428 H_2 +0.464	SCF -751.51998 $MP2_1$ -752.7280 $MP2_2$ -753.13914 DFT -754.01985	SCF -180.81819 $MP2_1$ -79.99899 $MP2_2$ -94.25808 DFT -159.23658	0.62

Table A3b: 1,2,4-thiadiazol-5-yl nitrone

Optimized adducts[a]	Selected parameters			Spin populations	[b]Charge populations	Energy[c] (a.u.)	ΔE^{d} (kJ/mol)	Dipole moments (D)
	Bond lengths (Å)	Bond angles (deg)	Dihedral angles (deg)					
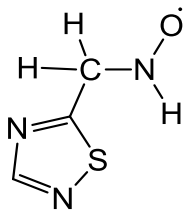	CN 1.445 NO 1.271	CNO 118.0 CNH_1 118.3 NCH_3 107.9 NCH_2 111.3 NCS 112.5	$ONCH_1$+146.1 $ONCH_3$+166.9 $ONCH_2$ +48.4 ONCS -73.7	C -0.033 N +0.254 O +0.769 H_1 -0.018	C -0.141 N -0.330 O -0.294 H_1 +0.387	SCF -751.55709 $MP2_1$-752.76984 $MP2_2$-753.17619 DFT -754.04777	SCF -302.35258 $MP2_1$ -207.07319 $MP2_2$ -208.51984 DFT -250.05262	3.76
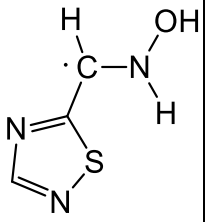	CN 1.399 NO 1.388 OH_2 0.948	CNO 110.6 CNH_1 112.8 NCH_3 118.2 NCS 121.0 NOH_2 104.8	$ONCH_1$+118.9 $ONCH_3$ +0.9 ONCS -177.2 $CNOH_1$-122.8	C +0.034 N +0.045 O +0.043 H_1 0.0 H_2 0.0	C +0.038 N -0.411 O -0.597 H_1 +0.386 H_2 +0.467	SCF -751.54151 MP2 -751.59407 $MP2_2$-753.14303 DFT -754.03515	SCF -261.44729 $MP2_1$2879.91095* $MP2_2$ -121.45826 DFT -216.91881	2.19

Table A3c: Furoxan-4-yl nitrone

Optimized adducts[a]	Selected parameters			Spin populations	[b]Charge populations	Energy[c] (a.u.)	ΔE^{d} (kJ/mol)	Dipole moments (D)
	Bond lengths (Å)	Bond angles (deg)	Dihedral angles (deg)					
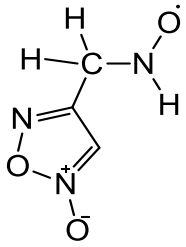	CN 1.450 NO 1.269	CNO 117.7 CNH_1 117.9 NCH_3 112.2 NCH_2 106.2 NCS 110.6	$ONCH_1$+144.6 $ONCH_3$ +85.1 $ONCH_2$ -33.3 ONCS -153.3	C -0.100 N +0.276 O + 0.760 H_1 -0.015	C -0.167 N -0.301 O -0.301 H_1 +0.383	SCF -503.59900 $MP2_1$ -505.01714 $MP2_2$ -505.50841 DFT -506.13304	SCF -330.78675 $MP2_1$ -59.625105 $MP2_2$ -105.12765 DFT -265.88439	2.53
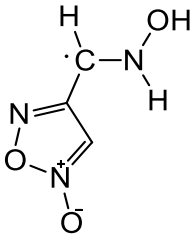	CN 1.406 NO 1.391 OH_2 0.948	CNO 109.9 CNH_1 112.0 NCH_3 118.8 NCS 119.8 NOH_2 104.9	$ONCH_1$+116.9 $ONCH_3$ +12.5 ONCS -167.6 $CNOH_1$ -120.9	C +1.015 N -0.038 O -0.003 H_1 +0.027 H_2 +0.001	C +0.007 N -0.412 O -0.600 H_1 +0.382 H_2 +0.466	SCF -503.58465 $MP2_1$ -504.99882 $MP2_2$ -505.49367 DFT -506.11029	SCF -293.11082 $MP2_1$ -11.525945 $MP2_2$ -66.42778 DFT -206.15426	5.14

Table A3d: Furoxan-3-yl nitrone

Optimized adducts[a]	Selected parameters			Spin populations	[b]Charge populations	Energy[c] (a.u.)	ΔE^{d} (kJ/mol)	Dipole moments (D)
	Bond lengths (Å)	Bond angles (deg)	Dihedral angles (deg)					
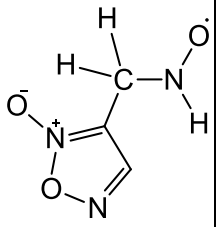	CN 1.446 NO 1.267	CNO 117.9 CNH_1 118.6 NCH_3 107.1 NCH_2 109.4 NCS 112.9	$ONCH_1$+147.4 $ONCH_3$ -50.3 $ONCH_2$ -167.6 ONCS +71.5	C +0.046 N +0.277 O +0.734 H_1 -0.021	C -0.180 N -0.275 O -0.324 H_1 +0.385	SCF -503.60065 $MP2_1$ -505.02015 $MP2_2$ -505.5107 DFT -506.13270	SCF -335.40763 $MP2_1$ -122.50583 $MP2_2$ -112.32152 DFT -261.63108	2.64
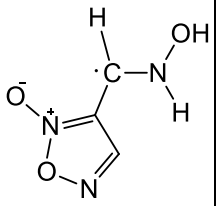	CN 1.356 NO 1.380 OH_2 0.949	CNO 122.4 CNH_1 126.9 NCH_3 117.2 NCS 124.3 NOH_2 107.1	$ONCH_1$+180.0 $ONCH_3$ 0.0 ONCS +180.0 $CNOH_1$+180.0	C +0.739 N +0.165 O -0.011 H_1 -0.022 H_2 -0.0004	C +0.021 N -0.406 O -0.570 H_1 +0.411 H_2 +0.470	SCF -503.56496 $MP2_1$ -504.99118 $MP2_2$ -505.48776 DFT -506.09856	SCF -241.70353 $MP2_1$ -46.445095 $MP2_2$ -52.09255 DFT -171.99651	4.85

Table A3e: 1,2,3-thiadiazol-5-yl nitrone

Optimized adducts[a]	Selected parameters			Spin populations	[b]Charge populations	Energy[c] (a.u.)	ΔE^d (kJ/mol)	Dipole moments (D)
	Bond lengths (Å)	Bond angles (deg)	Dihedral angles (deg)					
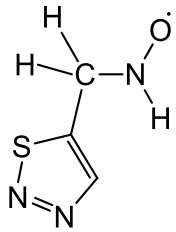	CN 1.448 NO 1.269	CNO 117.5 CNH_1 117.6 NCH_3 106.5 NCH_2 111.1 NCS 110.7	$ONCH_1$ -143.8 $ONCH_3$ +38.1 $ONCH_2$ -78.8 ONCS +158.2	C +0.025 N +0.258 O +0.758 H_1 -0.017	C -0.114 N -0.301 O -0.302 H_1 +0.378	SCF -751.51203 $MP2_1$ -752.71618 $MP2_2$ -753.11723 DFT -754.01087	SCF -303.06147 $MP2_1$ -156.16474 $MP2_2$ -147.55573 DFT -247.95222	2.34
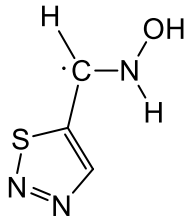	CN 1.410 NO 1.392 OH_2 0.948	CNO 109.6 CNH_1 111.7 NCH_3 117.0 NCS 120.2 NOH_2 104.8	$ONCH_1$+116.5 $ONCH_3$ +13.0 ONCS -167.5 $CNOH_1$ -120.4	C +0.937 N -0.037 O -0.003 H_1 +0.024 H_2 +0.001	C +0.029 N -0.409 O -0.605 H_1 +0.380 H_2 +0.465	SCF -751.50336 $MP2_1$ -752.69053 $MP2_2$ -753.09476 DFT -753.99925	SCF -280.29838 $MP2_1$ -88.82067 $MP2_2$ -88.56074 DFT -217.44391	4.06

[a]All structures were optimized at the HF/6-31G* level and have no imaginary frequencies

[b]Mulliken population analysis

[c]1 au = 2625.5 kJ/mol. The $MP2_1$ and $MP2_2$ energies are single point energies obtained with the cc-pVDZ and cc-pVTZ basis sets respectively at the 6-31G* optimized geometry, *i.e.* MP2/cc-pVDZ//HF/6–31G* and MP2/cc-pVTZ//HF/6–31G* respectively.

[d]ΔE = energy change for gas phase species at equilibrium bond lengths at 0K

$$\Delta E = E_{\text{adduct}} - [E_{\text{new heteroaryl nitrone}} + E_{\text{hydrogen radical}}]$$

Table A4: The reaction of new heteroaryl nitrones with •CH_3 at C- site and O- site

Table A4a: 1,2,4-thiadiazol-3-yl nitrone

Optimized adducts[a]	Selected parameters			Spin populations	[b]Charge populations	Energy[c] (a.u.)	ΔE^d (kJ/mol)	Dipole moments (D)
	Bond lengths (Å)	Bond angles (deg)	Dihedral angles (deg)					
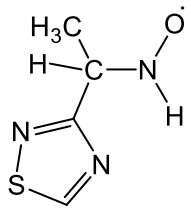	C_1N 1.454 $C_1C_2$1.532 NO 1.266	C_1NO 117.9 $C_1NH_1$118.0 $NC_1C_2$112.2	ONC_1C_2 +70.7 ONC_1H_1 +147.3 NC_1C_2S +24.8 ONC_1H_2 -49.6	C_1 -0.038 N +0.302 O +0.724 H_1 -0.020 C_2 +0.027	C_1 -0.016 N -0.283 O -0.334 H_1 +0.390 C_2 -0.495	SCF-790.59670 $MP2_1$-791.96107 $MP2_2$ -792.40857 DFT -793.33578	SCF-13.626345 $MP2_1$-191.11015 $MP2_2$-182.36723 DFT -207.62454	4.24
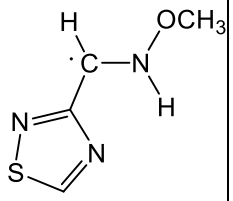	C_1N 1.388 NO 1.390 OC_2 1.402	C_1NO 111.0 NOC_2 110.2 CNH_1 112.4	C_1NOC_2 +127.3 ONC_1S +144.1 ONC_1H_2 -41.5 NOC_2H_4 -179.4 ONC_1H_1 +120.8	C_1 +0.937 N -0.007 O +0.037 C_2 -0.004	C_1 +0.036 N -0.408 O -0.492 C_2 -0.142	SCF -790.57072 $MP2_1$ -791.90729 $MP2_2$ -792.35674 DFT -793.30783	SCF 54.584145 $MP2_1$-49.910755 $MP2_2$-46.287565 DFT-134.241815	1.81

Table A4b: 1,2,4-thiadiazol-5-yl nitrone

Optimized adducts[a]	Selected parameters			Spin populations	[b]Charge populations	Energy[c] (a.u.)	ΔE^d (kJ/mol)	Dipole moments (D)
	Bond lengths (Å)	Bond angles (deg)	Dihedral angles (deg)					
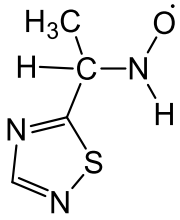	CN 1.458 CC 1.529 NO 1.269	CNO 119.0 CNH_1 117.0 NCC 110.7	ONC_1C_2 +39.1 ONC_1H_1 +143.7 NC_1C_2S +1.7 ONC_1H_2 -82.1	C_1 -0.031 N +0.257 O +0.761 H_1 -0.015 C_2 +0.002	C_1 -0.010 N -0.309 O -0.302 H_1 +0.381 C_2 -0.484	SCF -790.59483 $MP2_1$ -791.95849 $MP2_2$ -792.40549 DFT -793.33476	SCF -32.81875 $MP2_1$-201.55964 $MP2_2$-191.26768 DFT -222.45862	1.38
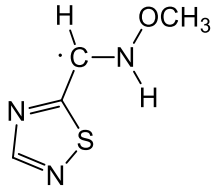	C_1N 1.398 NO 1.384 OC_2 1.405	C_1NO 110.7 NOC_2 110.3 CNH_1 112.9	C_1NOC_2 +118.4 ONC_1S +177.7 ONC_1H_2 +0.4 NOC_2H_4 -179.5 ONC_1H_1 +119.1	C_1 +0.927 N -0.009 O -0.004 C_2 +0.002	C_1 +0.042 N -0.400 O -0.492 C_2 -0.147	SCF -790.57052 $MP2_1$ -791.90136 $MP2_2$ -792.35077 DFT -793.30661	SCF 31.007155 $MP2_1$ -51.56482 $MP2_2$ -47.60032 DFT -148.55079	2.51

Table A4c: Furoxan-4-yl nitrone

Optimized adducts[a]	Selected parameters			Spin populations	[b]Charge populations	Energy[c] (a.u.)	ΔE^d (kJ/mol)	Dipole moments (D)
	Bond lengths (Å)	Bond angles (deg)	Dihedral angles (deg)					
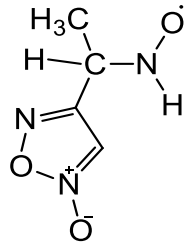	CN 1.454 CC 1.528 NO 1.269	CNO 118.7 CNH_1 117.3 NCC 109.1	ONC_1C_2 +174.4 ONC_1H_1 +145.4 NC_1C_2S -11.8 ONC_1H_2 +54.8	C_1 +0.038 N +0.270 O +0.751 H_1 -0.019 C_2 -0.013	C_1 +0.020 N -0.319 O -0.308 H_1 +0.386 C_2 -0.524	SCF -542.6365 $MP2_1$ -544.20237 $MP2_2$ -544.73582 DFT -545.41698	SCF -60.622795 $MP2_1$-45.132345 $MP2_2$ -82.91329 DFT -230.28261	6.08
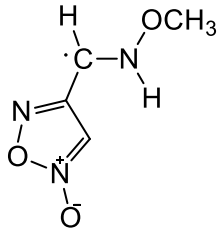	C_1N 1.406 NO 1.387 OC_2 1.404	C_1NO 109.9 NOC_2 110.4 CNH_1 112.0	C_1NOC_2 +116.1 ONC_1S -167.1 ONC_1H_2 +13.1 NOC_2H_4 -179.5 ONC_1H_1 +116.9	C_1 +1.015 N -0.039 O -0.003 C_2 +0.003	C_1 +0.008 N -0.401 O -0.495 C_2 -0.147	SCF -542.61373 $MP2_1$ -544.16534 $MP2_2$ -544.70116 DFT -545.38402	SCF -0.84016 $MP2_1$ 52.08992 $MP2_2$ 8.08654 DFT -143.74613	5.41

Table A4d: Furoxan-3-yl nitrone

Optimized adducts[a]	Selected parameters			Spin populations	[b]Charge populations	Energy[c] (a.u.)	ΔE^{d} (kJ/mol)	Dipole moments (D)
	Bond lengths (Å)	Bond angles (deg)	Dihedral angles (deg)					
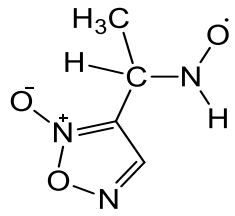	CN 1.446 CC 1.528 NO 1.262	CNO 120.2 CNH_1 119.8 NCC 109.4	ONC_1C_2+175.5 ONC_1H_1 -159.0 NC_1C_2S +10.1 ONC_1H_2 +56.8	C_1 -0.116 N +0.320 O +0.720 H_1 -0.028 C_2 +0.023	C_1 +0.030 N -0.302 O -0.322 H_1 +0.383 C_2 -0.529	SCF -542.6376 $MP2_1$ -544.20364 $MP2_2$ -544.7369 DFT -545.41841	SCF -63.79965 $MP2_1$ -103.4447 $MP2_2$ -86.93031 DFT -230.67643	4.76
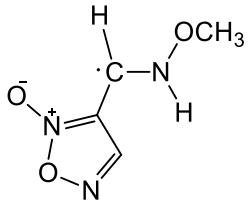	C_1N1.358 NO 1.379 $OC_2$1.400	C_1NO 126.4 NOC_2 116.0 CNH_1 124.7	C_1NOC_2 0.0 ONC_1S +180.0 ONC_1H_2 0.0 NOC_2H_4 -61.9 ONC_1H_1 +180.0	C_1 +0.727 N +0.167 O -0.008 C_2 -0.0008	C_1 +0.018 N -0.393 O -0.447 C_2 -0.200	SCF -542.59225 $MP2_1$ -544.15632 $MP2_2$ -544.69504 DFT -545.37287	SCF 55.266775 $MP2_1$ 20.79396 $MP2_2$ 22.973125 DFT -111.11116	5.51

Table A4e: 1,2,3-thiadiazol-5-yl nitrone

Optimized adducts[a]	Selected parameters			Spin populations	[b]Charge populations	Energy[c] (a.u.)	ΔE^d (kJ/mol)	Dipole moments (D)
	Bond lengths (Å)	Bond angles (deg)	Dihedral angles (deg)					
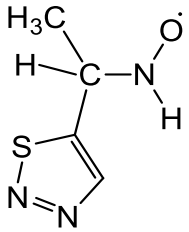	CN 1.459 CC 1.529 NO 1.268	CNO 118.2 CNH_1 117.0 NCC 110.2	ONC_1C_2 +50.5 ONC_1H_1 +143.1 NC_1C_2S +8.0 ONC_1H_2 -69.0	C_1 +0.029 N +0.258 O +0.753 H_1 -0.016 C_2 -0.010	C_1 +0.023 N -0.300 O -0.308 H_1 +0.378 C_2 -0.475	SCF -790.54984 $MP2_1$ -791.90436 $MP2_2$ -792.34702 DFT -793.33476	SCF -33.71142 $MP2_1$-149.41721 $MP2_2$-131.59006 DFT-317.239165	2.03
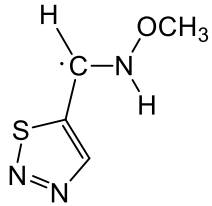	C_1N1.410 NO 1.388 $OC_2$1.404	C_1NO 110.0 NOC_2 110.3 CNH_1 111.6	C_1NOC_2 +116.0 ONC_1S -166.7 ONC_1H_2 +14.0 NOC_2H_4 -179.4 ONC_1H_1 +116.4	C_1 +0.938 N -0.038 O -0.002 C_2 +0.003	C_1 +0.030 N -0.398 O -0.499 C_2 -0.146	SCF -790.53233 $MP2_1$ -791.85703 $MP2_2$ -792.30216 DFT -793.27273	SCF 12.261085 $MP2_1$ -25.15229 $MP2_2$ -13.81013 DFT -154.3794	4.32

[a]All structures were optimized at the HF/6-31G* level and have no imaginary frequencies

[b]Mulliken population analysis

[c]1 au = 2625.5 kJ/mol. The $MP2_1$ and $MP2_2$ energies are single point energies obtained with the cc-pVDZ and cc-pVTZ basis sets respectively at the 6-31G* optimized geometry, *i.e.* MP2/cc-pVDZ//HF/6–31G* and MP2/cc-pVTZ//HF/6–31G* respectively.

[d]$\Delta E = E_{\text{adduct}} - [E_{\text{new heteroaryl nitrone}} + E_{\text{methyl radical}}]$

Table A5: The reaction of new heteroaryl nitrones with •OH at C- site and O- site

Table A5a: 1,2,4-thiadiazol-3-yl nitrone

Optimized adducts[a]	Selected parameters			Spin populations	[b]Charge populations	Energy[c] (a.u.)	ΔE[d] (kJ/mol)	Dipole moments (D)
	Bond lengths (Å)	Bond angles (deg)	Dihedral angles (deg)					
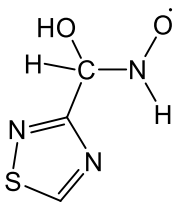	CN 1.429 NO_1 1.274 CO_2 1.274	CNO_1 117.2 CNH_1 117.0 NCO_2 109.4 CO_2H_2 109.7	O_1NCO_2 +77.7 O_1NCH_1 +143.4 NCO_2H_2 -166.2	C -0.014 N +0.224 O_1 +0.791 O_2 +0.009 H_1 -0.014	C +0.317 N -0.305 O_1 -0.291 O_2 -0.731 H_1 +0.396	SCF -826.41068 $MP2_1$-827.81433 $MP2_2$-828.29661 DFT -829.23241	SCF-615.33844 $MP2_1$-654.98349 $MP2_2$ -590.08113 DFT -336.56285	4.46
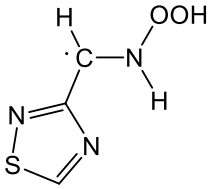	CN 1.391 NO_1 1.359 $O_1O_2$1.403	CNO_1 113.6 NO_1O_2 109.6 $O_1O_2H_4$102.0 CNH_1 114.0	CNO_1O_2 -67.4 $NO_1O_2H_4$-113.9 O_1NCH_1 +127.4 O_1NCH_2 -38.0 O_1NCS +147.6	C +0.956 N -0.005 O_1 -0.013 O_2 +0.038 H_1 +0.001 H_4 -0.002	C +0.023 N -0.348 O_1 -0.226 O_2 -0.453 H_1 +0.390 H_4 +0.460	SCF -826.30472 $MP2_1$-827.69631 $MP2_2$-828.17858 DFT -829.16670	SCF -337.14046 $MP2_1$ -345.12198 $MP2_2$ -280.19336 DFT -164.04124	3.48

Table A5b: 1,2,4-thiadiazol-5-yl nitrone

Optimized adducts[a]	Selected parameters			Spin populations	[b]Charge populations	Energy[c] (a.u.)	ΔE^{d} (kJ/mol)	Dipole moments (D)
	Bond lengths (Å)	Bond angles (deg)	Dihedral angles (deg)					
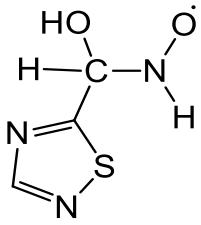	CN 1.436 NO_1 1.266 CO_2 1.389	CNO_1 116.6 CNH_1 120.1 NCO_2 113.4 CO_2H_2 109.4	O_1NCO_2 +64.6 O_1NCH_1 +151.0 NCO_2H_2 -63.9	C -0.022 N +0.287 O_1 +0.738 O_2 +0.015 H_1 -0.021	C +0.362 N -0.290 O_1 -0.324 O_2 -0.743 H_1 +0.394	SCF -826.41356 $MP2_1$ -827.82036 $MP2_2$ -828.30285 DFT -829.24140	SCF -647.00197 $MP2_1$ -688.03853 $MP2_2$ -623.45123 DFT -377.67818	0.68
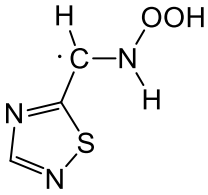	CN 1.392 NO_1 1.375 O_1O_2 1.381	CNO_1 110.5 NO_1O_2 108.1 $O_1O_2H_4$103.5 CNH_1 115.3	CNO_1O_2 +137.0 $NO_1O_2H_4$ -80.0 O_1NCH_1 +122.2 O_1NCH_2 -24.1 O_1NCS +160.8	C +0.893 N +0.013 O_1 +0.016 O_2 -0.009 H_1 +0.011 H_4 -0.0001	C +0.048 N -0.370 O_1 -0.238 O_2 -0.406 H_1 +0.392 H_4 +0.458	SCF -826.30087 $MP2_1$ -827.68721 $MP2_2$ -828.16920 DFT -829.13831	SCF -351.13437 $MP2_1$ -338.45321 $MP2_2$ -272.55316 DFT -107.01538	1.52

Table A5c: Furoxan-4-yl nitrone

Optimized adducts[a]	Selected parameters			Spin populations	[b]Charge populations	Energy[c] (a.u.)	ΔE^{d} (kJ/mol)	Dipole moments (D)
	Bond lengths (Å)	Bond angles (deg)	Dihedral angles (deg)					
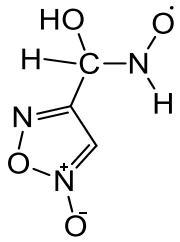	CN 1.454 NO_1 1.267 CO_2 1.377	CNO_1 115.9 CNH_1 118.7 NCO_2 109.9 CO_2H_2 108.6	O_1NCO_2 +53.3 O_1NCH_1 +145.4 NCO_2H_2 -46.6	C +0.035 N +0.275 O_1 +0.735 O_2 +0.0003 H_1 -0.019	C +0.385 N -0.299 O_1 -0.326 O_2 -0.747 H_1 +0.397	SCF -578.45364 $MP2_1$ -580.06375 $MP2_2$ -580.63187 DFT -581.32130	SCF -670.63147 $MP2_1$ -530.32475 $MP2_2$ -511.65744 DFT -379.411005	3.15
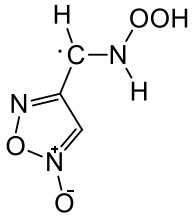	CN 1.393 NO_1 1.360 O_1O_2 1.399	CNO_1 113.7 NO_1O_2 109.4 $O_1O_2H_4$ 102.9 CNH_1 115.7	CNO_1O_2 +70.8 $NO_1O_2H_4$ -110.2 O_1NCH_1 -126.2 O_1NCH_2 +39.9 O_1NCS -149.0	C +2.511 N +3.672 O_1 +4.112 O_2 +4.209 H_1 +0.309 H_4 +0.268	C 0.0101 N -0.3394 O_1 -0.2165 O_2 -0.4482 H_1 0.3813 H_4 0.4653	SCF -578.34597 $MP2_1$ -579.95622 $MP2_2$ -580.52482 DFT -581.21448	SCF -387.94388 $MP2_1$ -248.00473 $MP2_2$ -230.59765 DFT -98.955095	3.55

Table A5d: Furoxan-3-yl nitrone

Optimized adducts[a]	Selected parameters			Spin populations	[b]Charge populations	Energy[c] (a.u.)	ΔE[d] (kJ/mol)	Dipole moments (D)
	Bond lengths (Å)	Bond angles (deg)	Dihedral angles (deg)					
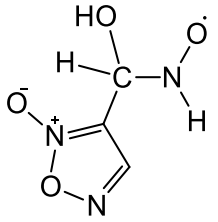	CN 1.458 NO_1 1.268 CO_2 1.377	CNO_1 115.7 CNH_1 118.0 NCO_2 109.5 CO_2H_2 108.5	O_1NCO_2 +50.9 O_1NCH_1 +142.3 NCO_2H_2 -45.3	C +0.050 N +0.263 O_1 +0.740 O_2 -0.002 H_1 -0.017	C +0.384 N -0.297 O_1 -0.324 O_2 -0.743 H_1 +0.395	SCF -578.45405 $MP2_1$ -580.06424 $MP2_2$ -580.63178 DFT -581.32214	SCF -671.99673 $MP2_1$ -586.58921 $MP2_2$ -512.60262 DFT -378.255785	2.52
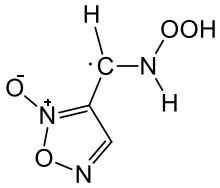	CN 1.363 NO_1 1.384 $O_1O_2$1.391	CNO_1 125.0 NO_1O_2 107.7 $O_1O_2H_4$ 99.9 CNH_1 126.7	CNO_1O_2 0.0 $NO_1O_2H_4$+180.0 O_1NCH_1 +180.0 O_1NCH_2 0.0 O_1NCS +180.0	C +0.762 N +0.130 O_1 -0.009 O_2+0.0002 H_1 -0.019 H_4-0.0005	C +0.042 N -0.409 O_1 -0.224 O_2 -0.428 H_1 +0.411 H_4 +0.485	SCF -578.31658 $MP2_1$ -579.93187 $MP2_2$ -580.50227 DFT -581.18728	SCF -311.06924 $MP2_1$ -239.05178 $MP2_2$ -172.57412 DFT -24.180855	6.68

Table A5e: 1,2,3-thiadiazol-5-yl nitrone

Optimized adducts[a]	Selected parameters			Spin populations	[b]Charge populations	Energy[c] (a.u.)	ΔE[d] (kJ/mol)	Dipole moments (D)
	Bond lengths (Å)	Bond angles (deg)	Dihedral angles (deg)					
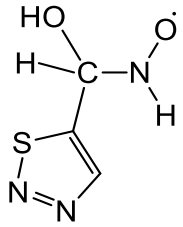	CN 1.443 NO_1 1.273 CO_2 1.388	CNO_1 +116.6 CNH_1 +117.7 NCO_2 +112.9 CO_2H_2 +109.2	O_1NCO_2 +75.2 O_1NCH_1 +142.8 $NCO2H_2$ -66.0	C -0.068 N +0.249 O_1 +0.774 O_2 +0.017 H_1 -0.014	C +0.362 N -0.309 O_1 -0.304 O_2 -0.735 H_1 +0.388	SCF -826.37093 $MP2_1$ -827.76384 $MP2_2$ -828.24107 DFT -829.20130	SCF -654.09082 $MP2_1$ -629.62116 $MP2_2$ -555.08321 DFT -367.17618	3.02
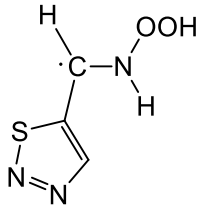	CN NO_1 O_1O_2	CNO_1 NO_1O_2 $O_1O_2H_4$ CNH_1	CNO_1O_2 $NO_1O_2H_4$ O_1NCH_1 O_1NCH_2 O_1NCS	C N O_1 O_2 H_1 H_4	C N O_1 O_2 H_1 H_4	SCF - $MP2_1$ - $MP2_2$ - DFT -829.10257	SCF - $MP2_1$ - $MP2_2$ - DFT -107.96056	-

[a]All structures were optimized at the HF/6-31G* level and have no imaginary frequencies

[b]Mulliken population analysis

[c]1 au = 2625.5 kJ/mol. The $MP2_1$ and $MP2_2$ energies are single point energies obtained with the cc-pVDZ and cc-pVTZ basis sets respectively at the 6-31G* optimized geometry, *i.e.* MP2/cc-pVDZ//HF/6–31G* and MP2/cc-pVTZ//HF/6–31G* respectively.

[d]$\Delta E = E_{\text{adduct}} - [E_{\text{new heteroaryl nitrone}} + E_{\text{hydroxyl radical}}]$

Table 6: The energetic studies of nitrone double adducts

Table A6a: Di •H spin adducts

Optimized adducts[a]	Selected parameters			Charge populations[b]	Energy (a.u.)	ΔE^{d} (kJ/mol)	Dipole moments (D)
	Bond lengths (Å)	Bond angles (deg)	Dihedral angles (deg)				
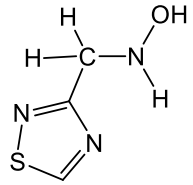 1,2,4-thiadiazol-3-yl nitrone	NO 1.401 CN 1.452 OH_2 0.947	CNO 107.2 CNH_1 108.8 NOH_2 104.5	$CNOH_2$ +122.2 $ONCH_1$ +112.7 ONCS +171.3	C -0.138 N -0.397 O -0.620 H_1 +0.376 H_2 +0.457	SCF -752.14573 $MP2_1$ -753.39683 $MP2_2$ -753.8124 DFT -754.67003	SCF -515.70071 $MP2_1$ -525.17877 $MP2_2$ -549.65368 DFT -558.9952	2.06
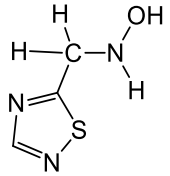 1,2,4-thiadiazol-5-yl nitrone	NO 1.397 CN 1.450 OH_2 0.948	CNO 107.9 CNH_1 109.7 NOH_2 104.7	$CNOH_2$ +123.7 $ONCH_1$ +113.4 ONCS -174.0	C -0.135 N -0.411 O -0.609 H_1 +0.368	SCF -752.14639 $MP2_1$ -753.39737 $MP2_2$ -753.81613 DFT -754.67160	SCF -541.53563 $MP2_1$ -543.81982 $MP2_2$ -576.43378 DFT -580.62932	1.91

				H_2 +0.462			
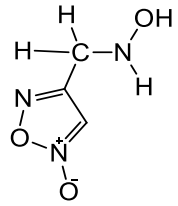 Furoxan-4-yl nitrone	NO 1.398 CN 1.453 OH_2 0.948	CNO 107.0 CNH_1 110.1 NOH_2 104.6	$CNOH_2$ +122.4 $ONCH_1$ +112.7 ONCS +175.5	C -0.147 N -0.382 O -0.616 H_1 +0.358 H_2 +0.465	SCF -504.17685 $MP2_1$ -505.67923 $MP2_2$ -506.18402 DFT -506.75566	SCF -539.90782 $MP2_1$ -487.10902 $MP2_2$ -566.69317 DFT -593.28423	4.60
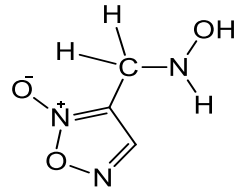 Furoxan-3-yl nitrone	NO 1.398 CN 1.454 OH_2 0.948	CNO 107.2 CNH_1 109.7 NOH_2 104.5	$CNOH_2$ -121.2 $ONCH_1$ -112.9 ONCS -177.6	C -0.116 N -0.372 O -0.620 H_1 +0.357 H_2 +0.465	SCF -504.17701 $MP2_1$ -505.6818 $MP2_2$ -506.18613 DFT -506.75056	SCF -540.616705 $MP2_1$ -548.83452 $MP2_2$ -573.41445 DFT -576.53354	4.37

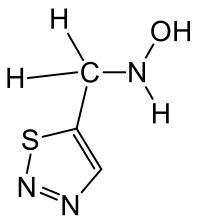 1,2,3-thiadiazol-5-yl nitrone	NO 1.398 CN 1.452 OH_2 0.947	CNO 107.5 CNH_1 109.4 NOH_2 104.7	$CNOH_2$ +124.1 $ONCH_1$ +113.2 ONCS +178.0	C -0.117 N -0.395 O -0.615 H_1 +0.366 H_2 +0.462	SCF -752.10158 $MP2_1$ -753.36426 $MP2_2$ -752.27449* DFT -754.63406	SCF -542.90089 $MP2_1$ -546.86540 $MP2_2$ 3377.30667* DFT -576.84860	3.69

Table A6b: •H + •CH_3 spin adducts

Optimized adducts[a]	Selected parameters			Charge populations[b]	Energy[c] (a.u.)	ΔE[d] (kJ/mol)	Dipole moments (D)
	Bond lengths (Å)	Bond angles (deg)	Dihedral angles (deg)				
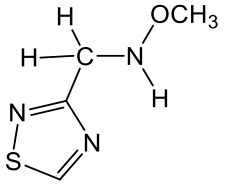 1,2,4-thiadiazol-3-yl nitrone	C_1N 1.452 NO 1.396 OC_2 1.399	C_1NO 107.1 NOC_2 110.1 C_1NH_1 108.8 NC_1S 109.6	C_1NOC_2 +125.6 ONC_1H_1 +112.7 ONC_1S +171.7 $NOCH_3$ -178.7	C_1 -0.137 N -0.383 O -0.513 C_2 -0.134 H_1 +0.375	SCF -791.17431 $MP2_1$ -792.56327 $MP2_2$ -793.01945 DFT -793.94355	SCF -222.1173 $MP2_1$ -461.35286 $MP2_2$ -473.98414 DFT -558.99521	1.96
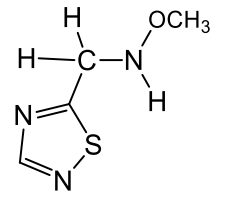 1,2,4-thiadiazol-5-yl nitrone	C_1N 1.450 NO 1.392 OC_2 1.402	C_1NO 107.8 NOC_2 110.2 C_1NH_1 109.7 NC_1S 109.8	C_1NOC_2 -125.9 ONC_1H_1 -113.5 ONC_1S +173.6 $NOCH_3$ +179.0	C_1 -0.135 N -0.398 O -0.502 C_2 -0.141 H_1 +0.366	SCF -791.17523 $MP2_1$ -792.56395 $MP2_2$ -793.01999 DFT -793.94512	SCF -248.63485 $MP2_1$ -480.36148 $MP2_2$ -492.38890 DFT -580.62933	2.19

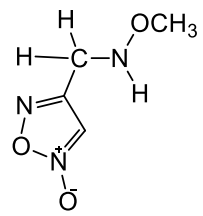 Furoxan-4-yl nitrone	C_1N 1.453 NO 1.393 OC_2 1.403	C_1NO 106.8 NOC_2 110.1 C_1NH_1 110.0 NC_1S 110.1	C_1NOC_2 +125.1 ONC_1H_1 +112.6 ONC1S +176.5 $NOCH_3$ -178.6	C_1 -0.147 N -0.370 O -0.510 C_2 -0.142 H_1 +0.356	SCF -543.20561 $MP2_1$ -544.84553 $MP2_2$ -545.39112 DFT -546.02289	SCF -246.79700 $MP2_1$ -422.91554 $MP2_2$ -491.15491 DFT -593.28424	4.91
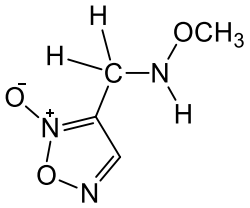 Furoxan-3-yl nitrone	C_1N 1.454 NO 1.393 OC_2 1.403	C_1NO 107.0 NOC_2 110.0 C_1NH_1 109.7 NC_1S 110.4	C_1NOC_2 -123.1 ONC_1H_1 -112.8 ONC_1S -177.0 $NOCH_3$ +178.2	C_1 -0.117 N -0.360 O -0.513 C_2 -0.142 H_1 +0.353	SCF -543.20566 $MP2_1$ -544.84817 $MP2_2$ -545.39334 DFT -546.02435	SCF -247.21708 $MP2_1$ -484.82483 $MP2_2$ -498.16500 DFT -576.53355	4.56
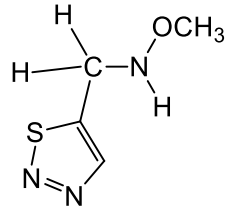 1,2,3-thiadiazol-5-yl nitrone	C_1N NO OC_2	C_1NO NOC_2 C_1NH_1 NC_1S	C_1NOC_2 ONC_1H_1 ONC_1S $NOCH_3$	C_1 N O C_2 H_1	SCF - $MP2_1$ - $MP2_2$ - DFT -793.81042	SCF - $MP2_1$ - $MP2_2$ - DFT -576.84861	-

Table A6c: •CH_3 + •H spin adducts

Optimized adducts[a]	Selected parameters			Charge populations[b]	Energy[c] (a.u.)	ΔE[d] (kJ/mol)	Dipole moments (D)
	Bond lengths (Å)	Bond angles (deg)	Dihedral angles (deg)				
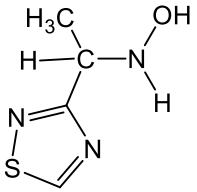 1,2,4-thiadiazol-3-yl nitrone	C_1N 1.458 NO 1.401 C_1C_2 1.532	C_1NO 108.4 NC_1C_2 114.3 $C_1C_2H_3$ 109.9 NOH_2 104.2 C_1NH_1 109.6	ONC_1C_2 +58.1 C_1NOH_2 +121.4 ONC_1H_1 +113.7 $NC_1C_2H_3$ -57.7	C_1 -0.014 C_2 -0.506 N -0.385 O -0.624 H_1 +0.370 H_2 +0.458	SCF -791.18274 $MP2_1$ -792.58298 $MP2_2$ -793.03994 DFT -793.95547	SCF -244.25027 $MP2_1$ -513.10147 $MP2_2$ -527.78064 DFT -527.33168	1.91
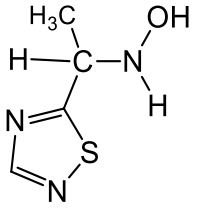 1,2,4-thiadiazol-5-yl nitrone	C_1N 1.457 NO 1.397 C_1C_2 1.527	C_1NO 108.6 NC_1C_2 114.7 $C_1C_2H_3$ 109.4 NOH_2 104.5 C_1NH_1 109.7	ONC_1C_2 +66.6 C_1NOH_2 +123.0 ONC_1H_1 +113.8 $NC_1C_2H_3$ -57.2	C_1 +0.004 C_2 -0.490 N -0.410 O -0.610 H_1 +0.364	SCF -791.18435 $MP2_1$ -792.58498 $MP2_2$ -793.0413 DFT -793.95871	SCF -272.57941 $MP2_1$ -535.57575 $MP2_2$ -548.33830 DFT -553.35038	2.04

				H_2 +0.463			
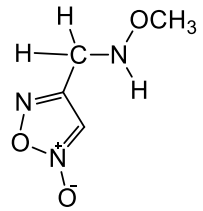 Furoxan-4-yl nitrone	C_1N 1.459 NO 1.398 C_1C_2 1.527	C_1NO 108.2 NC_1C_2 114.8 $C_1C_2H_3$ 109.3 NOH_2 104.6 C_1NH_1 109.4	ONC_1C_2 +62.9 C_1NOH_2 +124.4 ONC_1H_1 +113.4 $NC_1C_2H_3$ -56.7	C_1 -0.004 C_2 -0.500 N -0.399 O -0.611 H_1 +0.364 H_2 +0.462	SCF -543.21796 $MP2_1$ -544.86879 $MP2_2$ -545.41433 DFT -546.03944	SCF -279.221925 $MP2_1$ -483.98467 $MP2_2$ -552.09277 DFT -557.262375	5.03
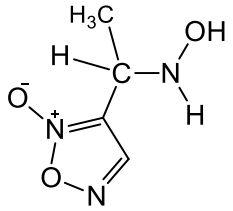 Furoxan-3-yl nitrone	C_1N 1.457 NO 1.387 C_1C_2 1.533	C_1NO 111.4 NC_1C_2 114.3 $C_1C_2H_3$ 114.3 NOH_2 109.2 C_1NH_1 110.8	ONC_1C_2 +76.9 C_1NOH_2 -62.9 ONC_1H_1 +119.5 $NC_1C_2H_3$ -60.8	C_1 +0.012 C_2 -0.523 N -0.378 O -0.590 H_1 +0.348 H_2 +0.442	SCF -543.20754 $MP2_1$ -544.86162 $MP2_2$ -545.40685 DFT -546.03069	SCF -252.15302 $MP2_1$ -520.13780 $MP2_2$ -533.63550 DFT -530.92861	4.85

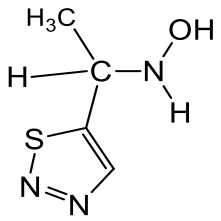 1,2,3-thiadiazol-5-yl nitrone	C_1N 1.458 NO 1.399 C_1C_2 1.529	C_1NO 108.0 NC_1C_2 110.4 $C_1C_2H_3$ 110.0 NOH_2 104.8 C_1NH_1 108.8	ONC_1C_2 -69.0 C_1NOH_2 +124.5 ONC_1H_1 +112.7 $NC_1C_2H_3$ +62.0	C_1 +0.04 C_2 -0.478 N -0.391 O -0.617 H_1 +0.366 H_2 +0.461	SCF -791.13786 $MP2_1$ -792.551 $MP2_2$ -793.00617 DFT -793.41860	SCF -269.53383 $MP2_1$ -536.33714 $MP2_2$ -549.93986 DFT +769.92788*	0.46

Table A6d: di •CH_3 spin adducts

Optimized adducts[a]	Selected parameters			Charge populations[b]	Energy[c] (a.u.)	ΔE[d] (kJ/mol)	Dipole moments (D)
	Bond lengths (Å)	Bond angles (deg)	Dihedral angles (deg)				
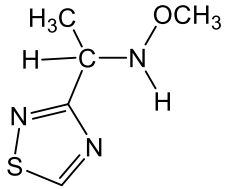 1,2,4-thiadiazol-3-yl nitrone	C_1N 1.459 NO 1.396 OC_3 1.399 C_1C_2 1.532	C_1NO 108.2 NOC_3 109.9 NC_1C_2 114.3 $C_1C_2H_2$ 109.9 OC_3H_3 106.3	C_1NOC_3 +124.3 ONC_1C_2 +58.9 NOC_3H_3 -178.7 $NC_1C_2H_2$ -57.8 ONC_1H_1 +113.8	C_1 -0.013 C_2 -0.504 N -0.371 O -0.514 C_3 -0.133 H_1 +0.368	SCF -830.21125 $MP2_1$ -831.74958 $MP2_2$ -832.24718 DFT -833.22912	SCF +49.51693 $MP2_1$ -449.69564 $MP2_2$ -452.60995 DFT -464.7135	1.80
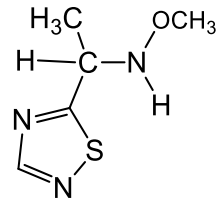 1,2,4-thiadiazol-5-yl nitrone	C_1N 1.457 NO 1.392 OC_3 1.402 C_1C_2 1.527	C_1NO 108.6 NOC_3 110.1 NC_1C_2 114.8 $C_1C_2H_2$ 109.4	C_1NOC_3 +125.0 ONC_1C_2 +67.3 NOC_3H_3 -179.2 $NC_1C_2H_2$ -57.2	C_1 +0.005 C_2 -0.488 N -0.397 O -0.502	SCF -830.21313 $MP2_1$ -831.75174 $MP2_2$ -832.24888 DFT -833.23218	SCF +20.47890 $MP2_1$ -472.59000 $MP2_2$ -474.06028 DFT -490.25962	2.32

		OC_3H_3 106.2	ONC_1H_1 +113.9	C_3 -0.140 H_1 +0.362			
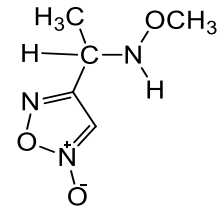 Furoxan-4-yl nitrone	C_1N 1.459 NO 1.394 OC_3 1.403 C_1C_2 1.531	C_1NO 107.9 NOC_3 110.0 NC_1C_2 114.4 $C_1C_2H_2$ 109.6 OC_3H_3 106.2	C_1NOC_3 +123.7 ONC_1C_2 +63.7 NOC_3H_3 -178.9 $NC_1C_2H_2$+113.0 ONC_1H_1 -57.4	C_1 -0.032 C_2 -0.500 N -0.363 O -0.510 C_3 -0.141 H_1 -0.141	SCF -582.24307 $MP2_1$ -584.03147 $MP2_2$ -584.6185 DFT -585.30874	SCF +23.47197 $MP2_1$ -410.28689 $MP2_2$ -468.86179 DFT -483.22328	5.19
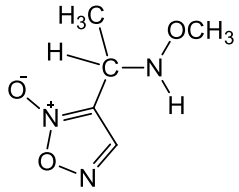 Furoxan-3-yl nitrone	C_1N 1.449 NO 1.393 OC_3 1.404 C_1C_2 1.52	C_1NO 109.7 NOC_3 110.3 NC_1C_2 108.5 $C_1C_2H_2$ 110.9 OC_3H_3 109.6	C_1NOC_3 -122.2 ONC_1C_2 -175.1 NOC_3H_3 +59.3 $NC_1C_2H_2$ -58.2 ONC_1H_1 -115.6	C_1 +0.017 C_2 -0.510 N -0.367 O -0.522 C_3 -0.139 H_1 +0.353	SCF -582.24686 $MP2_1$ -584.03664 $MP2_2$ -584.62351 DFT -585.31344	SCF +13.23252 $MP2_1$ -478.83869 $MP2_2$ -483.19702 DFT -492.20249	5.51

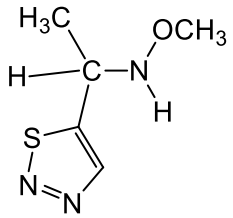 1,2,3-thiadiazol-5-yl nitrone	C_1N 1.459 NO 1.392 OC_3 1.402 C_1C_2 1.529	C_1NO 108.5 NOC_3 110.1 NC_1C_2 114.2 $C_1C_2H_2$ 109.4 OC_3H_3 106.2	C_1NOC_3 +125.6 ONC_1C_2 +61.6 NOC_3H_3 -178.8 $NC_1C_2H_2$ -54.8 ONC_1H_1 +114.1	C_1 +0.04 C_2 -0.506 N -0.385 O -0.507 C_3 -0.140 H_1 +0.361	SCF -830.16683 $MP2_1$ -831.7171 $MP2_2$ -832.21347 DFT -833.19462	SCF 23.025635 $MP2_1$ -471.61857 $MP2_2$ -474.92670 DFT -486.42639	4.29

Table A6e: •H + HO• spin adducts

Optimized adducts[a]	Selected parameters			Charge populations[b]	Energy[c] (a.u.)	ΔE[d] (kJ/mol)	Dipole moments (D)
	Bond lengths (Å)	Bond angles (deg)	Dihedral angles (deg)				
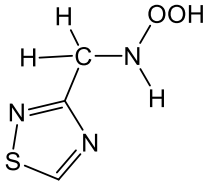 1,2,4-thiadiazol-3-yl nitrone	CN 1.454 NO_1 1.390 O_1O_2 1.381 O_2H_2 0.952	CNO_1 106.1 NO_1O_2 107.8 $O_1O_2H_2$ 103.2	CNO_1O_2 +148.8 O_1NCH_1 +113.8 $NO_1O_2H_2$ -70.7 O_1NCS +172.1	O_1 -0.260 C -0.154 N -0.361 O_2 -0.414 H_1 +0.382 H_2 +0.453	SCF -826.90589 $MP2_1$ -828.34859 $MP2_2$ -828.8375 DFT -829.77255	SCF -607.48819 $MP2_1$ -746.84973 $MP2_2$ -697.93929 DFT -447.41146	3.27

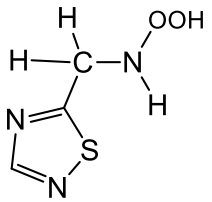 1,2,4-thiadiazol-5-yl nitrone	CN 1.453 NO_1 1.361 O_1O_2 1.403 O_2H_2 0.950	CNO_1 111.5 NO_1O_2 109.2 $O_1O_2H_2$ 101.7	CNO_1O_2 +67.3 O_1NCH_1 -120.5 $NO_1O_2H_2$ +121.7 O_1NCS +161.8	O_1 -0.224 C -0.158 N -0.346 O_2 -0.465 H_1 +0.360 H_2 +0.465	SCF -826.90914 $MP2_1$ -828.35397 $MP2_2$ -828.84264 DFT -829.77668	SCF -640.123155 $MP2_1$ -778.1982 $MP2_2$ -728.42135 DFT -475.76686	3.16
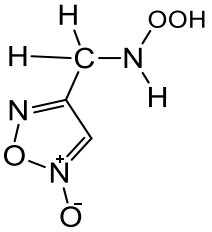 Furoxan-4-yl nitrone	CN 1.452 NO_1 1.361 O_1O_2 1.404 O_2H_2 0.951	CNO_1 112.0 NO_1O_2 109.2 $O_1O_2H_2$ 102.3	CNO_1O_2 +66.5 O_1NCH_1 -120.2 $NO_1O_2H_2$ -127.0 O_1NCS +167.0	O_1 -0.225 C -0.174 N -0.333 O_2 -0.462 H_1 +0.374 H_2 +0.465	SCF -578.94298 $MP2_1$ -580.63937 $MP2_2$ -581.21676 DFT -581.85837	SCF -647.369535 $MP2_1$ -730.78167 $MP2_2$ -735.03761 DFT -482.19933	4.95

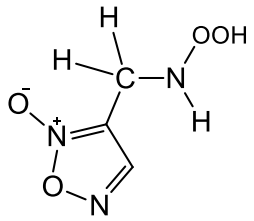 Furoxan-3-yl nitrone	CN 1.454 NO_1 1.362 O_1O_2 1.403 O_2H_2 0.951	CNO_1 111.9 NO_1O_2 109.3 $O_1O_2H_2$ 102.5	CNO_1O_2 -66.8 O_1NCH_1 +119.8 $NO_1O_2H_2$ +122.6 O_1NCS -166.7	O_1 -0.226 C -0.158 N -0.334 O_2 -0.460 H_1 +0.372 H_2 +0.464	SCF -578.94282 $MP2_1$ -580.63984 $MP2_2$ -581.21677 DFT -581.85827	SCF -647.23826 $MP2_1$ -786.99363 $MP2_2$ -736.24534 DFT -478.57614	3.63
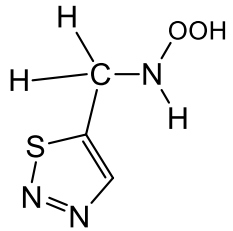 1,2,3-thiadiazol-5-yl nitrone	CN NO_1 O_1O_2 O_2H_2	CNO_1 NO_1O_2 $O_1O_2H_2$	CNO_1O_2 O_1NCH_1 $NO_1O_2H_2$ O_1NCS	O_1 C N O_2 H_1 H_2	SCF - $MP2_1$ - $MP2_2$ - DFT -	SCF - $MP2_1$ - $MP2_2$ - DFT -	-

Table A6f: •OH + •H spin traps

Optimized adducts[a]	Selected parameters			Charge populations[b]	Energy[c] (a.u.)	ΔE[d] (kJ/mol)	Dipole moments (D)
	Bond lengths (Å	Bond angles (deg)	Dihedral angles (deg)				
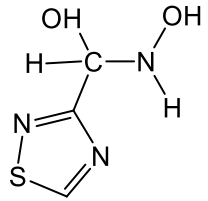 1,2,4-thiadiazol-3-yl nitrone	CN 1.441 NO_1 1.404 CO_2 1.391 O_2H_2 0.950 O_1H_3 0.947	C_1NO_1 106.8 NCO_2 113.1 CO_2H_2 108.0 CNH_1 108.6 NO_1H_3 104.7	CNO_1H_3 +122.2 O_1NCO_2 +56.8 NCO_2H_2 -56.0 O_1NCH_1 +112.5	O_1 -0.641 C +0.300 N -0.390 O_2 -0.744 H_1 +0.381 H_2 +0.467 H_3 +0.465	SCF -827.00376 $MP2_1$ -828.44645 $MP2_2$ -828.93855 DFT -829.86184	SCF -864.445875 $MP2_1$-1003.78116 $MP2_2$ -963.24607 DFT -681.84235	1.77
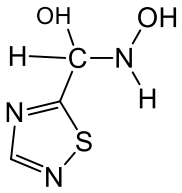 1,2,4-thiadiazol-5-yl nitrone	CN 1.444 NO_1 1.383 CO_2 1.371 O_2H_2 0.951	C_1NO_1 111.6 NCO_2 111.1 CO_2H_2 108.4 CNH_1 112.2	CNO_1H_3 +57.6 O_1NCO_2 +67.7 NCO_2H_2 +56.5 O_1NCH_1 -121.8	O_1 -0.587 C +0.324 N -0.357 O_2 -0.706	SCF -826.98912 $MP2_1$ -828.43533 $MP2_2$ -828.92734 DFT -829.84962	SCF -850.110645 $MP2_1$ -991.80888 $MP2_2$ -950.79070 DFT -667.270825	2.30

	O_1H_3 0.953	NO_1H_3 109.2		H_1 +0.356 H_2 +0.470 H_3 +0.434			
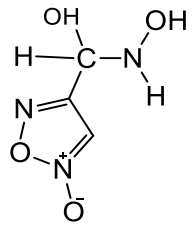 Furoxan-4-yl nitrone	CN 1.442 NO_1 1.401 CO_2 1.390 O_2H_2 0.950 O_1H_3 0.948	C_1NO_1 106.5 NCO_2 113.3 CO_2H_2 108.5 CNH_1 109.4 NO_1H_3 104.8	CNO_1H_3 +123.1 O_1NCO_2 +57.8 NCO_2H_2 -57.1 O_1NCH_1 +112.5	O_1 -0.637 C +0.317 N -0.368 O_2 -0.752 H_1 +0.365 H_2 +0.477 H_3 +0.472	SCF -579.03794 $MP2_1$ -580.73184 $MP2_2$ -581.31275 DFT -582.24759	SCF -896.687015 $MP2_1$ -973.56166 $MP2_2$ -987.05935 DFT -1504.09644	5.79
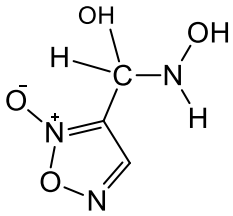 Furoxan-3-yl nitrone	CN 1.428 NO_1 1.386 CO_2 1.393 O_2H_2 0.953 O_1H_3 0.953	C_1NO_1 109.8 NCO_2 109.6 CO_2H_2 110.3 CNH_1 109.3 NO_1H_3 107.6	CNO_1H_3 -55.4 O_1NCO_2 +66.7 NCO_2H_2 +173.3 O_1NCH_1 +117.5	O_1 -0.600 C +0.354 N -0.365 O_2 -0.777 H_1 +0.358 H_2 +0.460	SCF -579.03666 $MP2_1$ -580.73192 $MP2_2$ -581.31199 DFT -581.94381	SCF -893.61518 $MP2_1$-1028.7497 $MP2_2$ -986.24545 DFT -703.16141	2.09

				H_3 +0.494			
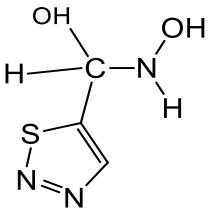 1,2,3-thiadiazol-5-yl nitrone	CN 1.440 NO_1 1.401 CO_2 1.391 O_2H_2 0.949 O_1H_3 0.947	C_1NO_1 106.8 NCO_2 113.5 CO_2H_2 108.7 CNH_1 108.8 NO_1H_3 104.9	CNO_1H_3 +124.2 O_1NCO_2 +58.5 NCO_2H_2 -60.8 O_1NCH_1 +112.7	O_1 -0.634 C +0.369 N -0.385 O_2 -0.754 H_1 +0.370 H_2 +0.473 H_3 +0.467	SCF -826.96191 $MP2_1$ -828.41642 $MP2_2$ -828.90696 DFT -829.82980	SCF -897.68471 $MP2_1$-1032.13656 $MP2_2$ -991.12888 DFT -710.01397	5.17

Table A6g: •CH_3 + •OH spin adducts

Optimized adducts[a]	Selected parameters			Charge populations[b]	Energy[c] (a.u.)	ΔE[d] (kJ/mol)	Dipole moments (D)
	Bond lengths (Å)	Bond angles (deg)	Dihedral angles (deg)				
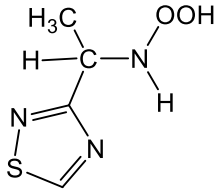 1,2,4-thiadiazol-3-yl nitrone	C_1N 1.462 NO_1 1.365 O_1O_2 1.404 C_1C_2 1.525	C_1NO 112.8 NC_1C_2 110.4 NO_1O_2 109.8 $O_1O_2H_2$ 102.6	$C_1NO_1O_2$ +67.0 $O_1NC_1H_1$ -119.2 $NO_1O_2H_2$ -118.6 $O_1NC_1C_2$ +60.8	O_1 -0.233 C_1 -0.025 N -0.314 O_2 -0.466 H_1 +0.369 H_2 +0.459 C_2 -0.483	SCF -865.94315 $MP2_1$ -867.53918 $MP2_2$ -868.06903 DFT -869.06181	SCF -336.69412 $MP2_1$ -746.42965 $MP2_2$ -686.54200 DFT -425.77734	2.78
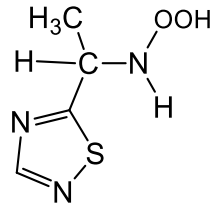 1,2,4-thiadiazol-5-yl nitrone	C_1N 1.461 NO_1 1.362 O_1O_2 1.403 C_1C_2 1.529	C_1NO 112.6 NC_1C_2 110.7 NO_1O_2 109.4 $O_1O_2H_2$ 101.8	$C_1NO_1O_2$ +65.2 $O_1NC_1H_1$ -120.1 $NO_1O_2H_2$ +119.8 $O_1NC_1C_2$ +52.5	O_1 -0.228 C_1 -0.019 N -0.337 O_2 -0.466	SCF -865.94652 $MP2_1$ -867.54168 $MP2_2$ -868.07195 DFT -869.05792	SCF -369.644145 $MP2_1$ -770.21668 $MP2_2$ -711.19544 DFT -433.07623	2.84

				H_1 +0.359 H_2 +0.465 C_2 -0.4844			
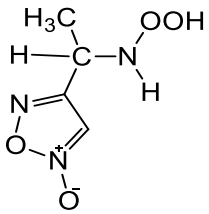 Furoxan-4-yl nitrone	C_1N 1.459 NO_1 1.361 O_1O_2 1.405 C_1C_2 1.529	C_1NO 113.0 NC_1C_2 110.5 NO_1O_2 109.0 $O_1O_2H_2$ 102.2	$C_1NO_1O_2$ +66.8 $O_1NC_1H_1$ -119.8 $NO_1O_2H_2$ -130.2 $O_1NC_1C_2$ +58.5	O_1 -0.229 C_1 -0.0363 N -0.325 O_2 -0.463 H_1 +0.373 H_2 +0.465 C_2 -0.483	SCF -617.97987 $MP2_1$ -619.8256 $MP2_2$ -620.44471 DFT -546.03944*	SCF -375.60403 $MP2_1$ -718.91441 $MP2_2$ -714.24102 DFT -	5.14
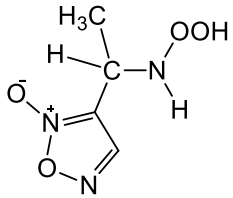 Furoxan-3-yl nitrone	C_1N 1.456 NO_1 1.366 O_1O_2 1.402 C_1C_2 1.529	C_1NO 112.1 NC_1C_2 108.6 NO_1O_2 109.6 $O_1O_2H_2$ 101.7	$C_1NO_1O_2$ -66.6 $O_1NC_1H_1$ +119.9 $NO_1O_2H_2$ -121.8 $O_1NC_1C_2$ +170.3	O_1 -0.239 C_1 -0.003 N -0.347 O_2 -0.457 H_1 +0.365 H_2 +0.467 C_2 -0.517	SCF -617.98311 $MP2_1$ -619.82824 $MP2_2$ -620.44766 DFT -621.46768	SCF -384.399455 $MP2_1$ -780.8237 $MP2_2$ -723.16772 DFT-1297.49585*	6.53

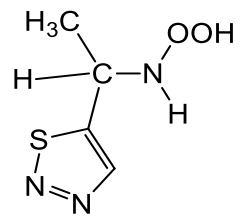 1,2,3-thiadiazol-5-yl nitrone	C_1N 1.462 NO_1 1.384 O_1O_2 1.382 C_1C_2 1.528	C_1NO 109.8 NC_1C_2 114.0 NO_1O_2 107.7 $O_1O_2H_2$ 103.2	$C_1NO_1O_2$ +96.3 $O_1NC_1H_1$ +114.3 $NO_1O_2H_2$ +75.6 $O_1NC_1C_2$ +62.5	O_1 -0.249 C_1 +0.028 N -0.371 O_2 -0.417 H_1 +0.371 H_2 +0.457 C_2 -0.511	SCF -865.89919 $MP2_1$ -867.5037 $MP2_2$ -868.03245 DFT -869.01864	SCF -364.393145 $MP2_1$ -760.47608 $MP2_2$ -701.32356 DFT -424.727135	3.34

Table A6h: •OH + •CH_3 spin adducts

Optimized adducts[a]	Selected parameters			Charge populations[b]	Energy[c] (a.u.)	ΔE[d] (kJ/mol)	Dipole moments (D)
	Bond lengths (Å)	Bond angles (deg)	Dihedral angles (deg)				
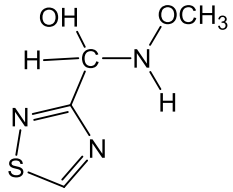 1,2,4-thiadiazol-3-yl nitrone	C_1N 1.441 NO_1 1.399 C_1O_2 1.392 O_1C_2 1.402	C_1NO_1 106.7 NO_1C_2 110.3 NC_1O_2 113.2	$C_1NO_1C_2$+125.1 $O_1NC_1H_1$+112.6 $O_1NC_1O_2$ +57.7 $NC_1O_2H_2$ -55.2	O_1 -0.535 C_1 +0.303 N -0.376 O_2 -0.746 H_1 +0.379 H_2 +0.466 C_2 -0.138	SCF -866.03236 $MP2_1$ -867.61288 $MP2_2$ -868.14558 DFT -869.13521	SCF -570.914975 $MP2_1$ -939.92900 $MP2_2$ -887.52402 DFT -618.48904	1.75
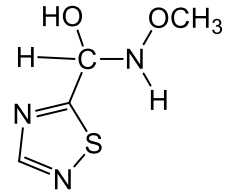 1,2,4-thiadiazol-5-yl nitrone	C_1N 1.442 NO_1 1.395 C_1O_2 1.383 O_1C_2 1.404	C_1NO_1 107.1 NO_1C_2 110.4 NC_1O_2 113.7	$C_1NO_1C_2$+128.1 $O_1NC_1H_1$ +112.8 $O_1NC_1O_2$ +64.6 $NC_1O_2H_2$ -63.819	O_1 -0.521 C_1 +0.337 N -0.395 O_2 -0.720	SCF -866.02962 $MP2_1$ -867.61098 $MP2_2$ -868.14369 DFT -869.13454	SCF -587.823195 $MP2_1$ -952.16383 $MP2_2$ -899.54881 DFT-634.242035	3.60

				H_1 +0.370 H_2 +0.464 C_2 -0.145			
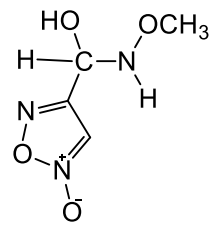 Furoxan-4-yl nitrone	C_1N 1.441 NO_1 1.396 C_1O_2 1.391 O_1C_2 1.405	C_1NO_1 106.3 NO_1C_2 110.3 NC_1O_2 113.3	$C_1NO_1C_2$ +126.7 $O_1NC_1H_1$ +112.6 $O_1NC_1O_2$ +58.6 $NC_1O_2H_2$ -56.3	O_1 -0.534 C_1 +0.319 N -0.356 O_2 -0.754 H_1 +0.362 H_2 +0.475 C_2 -0.145	SCF -618.06674 $MP2_1$ -619.89814 $MP2_2$ -620.51987 DFT -621.21798	SCF -603.681215 $MP2_1$ -909.36818 $MP2_2$ -911.57360 DFT -645.26914	6.13
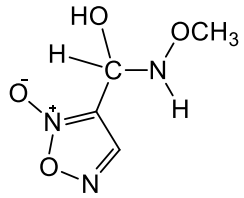 Furoxan-3-yl nitrone	C_1N 1.451 NO_1 1.388 C_1O_2 1.388 O_1C_2 1.403	C_1NO_1 108.8 NO_1C_2 110.8 NC_1O_2 107.5	$C_1NO_1C_2$ -115.1 $O_1NC_1H_1$ -114.4 $O_1NC_1O_2$ -172.6 $NC_1O_2H_2$ -59.3	O_1 -0.509 C_1 +0.322 N -0.379 O_2 -0.747 H_1 +0.359	SCF -618.06293 $MP2_1$ -619.89488 $MP2_2$ -620.51702 DFT -621.21299	SCF -593.966865 $MP2_1$ -955.78702 $MP2_2$ -905.2724 DFT -628.80725	5.38

				H_2 +0.4643 C_2 -0.1402			
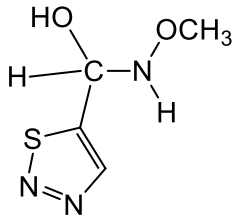 1,2,3-thiadiazol-5-yl nitrone	C_1N 1.441 NO_1 1.396 C_1O_2 1.389 O_1C_2 1.404	C_1NO_1 106.8 NO_1C_2 110.4 NC_1O_2 113.6	$C_1NO_1C_2$ 128.1 $O_1NC_1H_1$ 112.9 $O_1NC_1O_2$ +59.4 $NC_1O_2H_2$ -58.9	O_1 -0.529 C_1 +0.368 N -0.378 O_2 -0.749 H_1 +0.369 H_2 +0.470 C_2 -0.144	SCF -865.99065 $MP2_1$ -867.58307 $MP2_2$ -868.11419 DFT -869.10347	SCF -604.521375 $MP2_1$ -968.86201 $MP2_2$ -915.93193 DFT -647.44830	5.29

Table A6i: Di •OH spin adducts

Optimized adducts[a]	Selected parameters			Charge populations[b]	Energy[c] (a.u.)	ΔE[d] (kJ/mol)	Dipole moments (D)
	Bond lengths (Å)	Bond angles (deg)	Dihedral angles (deg)				
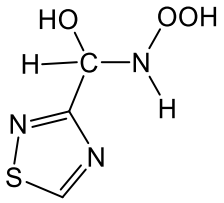 1,2,4-thiadiazol-3-yl nitrone	CN 1.449 NO_1 1.362 CO_2 1.385 O_1O_3 1.400	CNO_1 113.3 NO_1O_3 110.4 $O_1O_3H_2$ 103.0 NCO_2 107.9 CO_2H_3 108.3	CNO_1O_3 +71.7 $NO_1O_3H_2$ -107.7 O_1NCO_2 +161.4 NCO_2H_3 -49.3 O_1NCH_1 -123.4	O_1 -0.231 C +0.310 N -0.360 O_2 -0.731 O_3 -0.461	SCF -901.76282 $MP2_1$ -903.40002 $MP2_2$ -903.96529 DFT -904.96554	SCF -953.345305 $MP2_1$-1230.20428 $MP2_2$ -1115.8375 DFT -573.35407	2.06
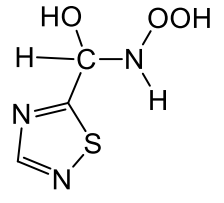 1,2,4-thiadiazol-5-yl nitrone	CN 1.448 NO_1 1.369 CO_2 1.383 $O_1O_3$1.402	CNO_1 110.0 NO_1O_3 110.0 $O_1O_3H_2$ 101.9 NCO_2 111.0 CO_2H_3 109.5	CNO_1O_3 +68.9 $NO_1O_3H_2$ +114.1 O_1NCO_2 +69.6 NCO_2H_3 -56.3 O_1NCH_1 -120.3	O_1 -0.251 C +0.357 N -0.332 O_2 -0.751 O_3 -0.462	SCF -901.76535 $MP2_1$ -903.40222 $MP2_2$ -903.96805 DFT -904.96419	SCF -984.08991 $MP2_1$-1253.20366 $MP2_2$-1140.07086 DFT -587.32435	3.60

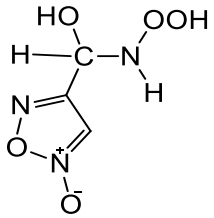 Furoxan-4-yl nitrone	CN 1.455 NO_1 1.368 CO_2 1.381 O_1O_3 1.403	CNO_1 110.0 NO_1O_3 109.8 $O_1O_3H_2$ 101.9 NCO_2 110.1 CO_2H_3 109.2	CNO_1O_3 +68.1 $NO_1O_3H_2$ +116.6 O_1NCO_2 +63.3 NCO_2H_3 -55.0 O_1NCH_1 -119.5	O_1 -0.251 C +0.339 N -0.326 O_2 -0.745 O_3 -0.461	SCF -653.79778 $MP2_1$ -655.68546 $MP2_2$ -656.34039 DFT -657.04745	SCF -987.634335 $MP2_1$-1200.11605 $MP2_2$-1142.01374 DFT -597.87886	5.83
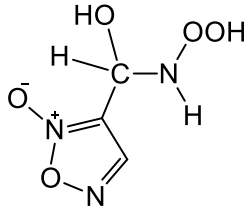 Furoxan-3-yl nitrone	CN 1.449 NO_1 1.362 CO_2 1.387 O_1O_3 1.405	CNO_1 112.0 NO_1O_3 109.8 $O_1O_3H_2$ 102.4 NCO_2 113.4 CO_2H_3 109.0	CNO_1O_3 -63.3 $NO_1O_3H_2$ -118.6 O_1NCO_2 +90.3 NCO_2H_3 -73.7 O_1NCH_1 +120.1	O_1 -0.218 C +0.323 N -0.348 O_2 -0.731 O_3 -0.480	SCF -653.79602 $MP2_1$ -655.6862 $MP2_2$ -656.33952 DFT -657.04763	SCF -983.30226 $MP2_1$-1257.03689 $MP2_2$-1140.91103 DFT -594.99081	6.71
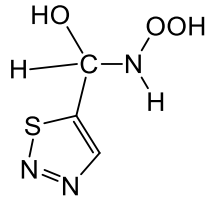 1,2,3-thiadiazol-5-yl nitrone	CN 1.445 NO_1 1.387 CO_2 1.388 O_1O_3 1.382	CNO_1 108.3 NO_1O_3 107.9 $O_1O_3H_2$ 103.2 NCO_2 113.6 CO_2H_3 108.9	CNO_1O_3 +98.2 $NO_1O_3H_2$ +77.6 O_1NCO_2 +60.6 NCO_2H_3 -67.0 O_1NCH_1 +113.0	O_1 -0.266 C +0.354 N -0.364 O_2 -0.744 O_3 -0.415	SCF -901.72202 $MP2_1$ -903.36877 $MP2_2$ -903.93222 DFT -904.92959	SCF -989.34091 $MP2_1$-1255.35657 $MP2_2$-1139.83457 DFT -591.26260	4.07

[a]All structures were optimized at the HF/6-31G* level and have no imaginary frequencies

[b]Mulliken population analysis

[c]1 au = 2625.5 kJ/mol. The $MP2_1$ and $MP2_2$ energies are single point energies obtained with the cc-pVDZ and cc-pVTZ basis sets respectively using the 6-31G* optimized geometry, *i.e.* MP2/cc-pVDZ//HF/6–31G* and MP2/cc-pVTZ//HF/6–31G* respectively.

[d]$\Delta E = E_{\text{adduct}} - [E_{\text{new heteroaryl nitrone}} + E_{\text{radical 1}} + E_{\text{radical 2}}]$

Table A7: Energetics of the addition reactions of DMPO, PBN and FxBN with •OH

[a]Nitrone	ΔE (kJ/mol)				$^{d}t_{1/2}$ (s)	$^{d}k_{ST}*10^{9}$ ($dm^{3}mol^{-1}s^{-1}$)
	DFT		HF			
	Monoadduct[b]	Diadduct[c]	Monoadduct[b]	Diadduct[c]		
DMPO	-1123.81	-571.73	-628.14	-935.92	3300.0	3.6
PBN	+5940.85	+5739.95	+5471.65	+5195.04	36.0	2.6
FxBN	-1548.71	-1847.18	-698.44	-979.83	7560.0	12.2

[a]All structures were optimized and their energies were obtained at the DFT/m06/6-31G* and HF/6-31G* levels and have no imaginary frequencies

[b]$\Delta E = E_{\text{adduct}} - [E_{\text{nitrone}} + E_{\text{OH radical}}]$

[c]$\Delta E = E_{\text{adduct}} - [E_{\text{nitrone}} + E_{\text{OH radical}} + E_{\text{OH radical}}]$

[d]Experimental data obtained from Barriga *et al.*[64]

Table A8: Molecular energies of DMPO, PBN and FxBN spin traps and adducts at DFT/m06/6-31* and HF/6-31G* levels

	Molecular energy, E_h (hartree)	
Molecule	DFT	HF
•OH	-75.642945	-75.22340
DMPO	-364.922063	-362.841659
PBN	-560.110596	-556.831192
FxBN	-662.659219	-659.102469
DMPO-OH	-440.993092	-438.304334
PBN-OH	-633.490532	-629.970314
FxBN-OH	-738.892104	-734.591920
DMPO-diOH	-516.425738	-513.644974
PBN-diOH	-709.210005	-705.299281
FxBN-diOH	-814.648744	-809.922508

VITA

EYRAM AKOSUA ASEMPA

EDUCATION

MSc. Chemistry, East Tennessee State University (ETSU), Johnson City, Tennessee (2014-2016)

B.Sc. Chemistry, (First Class Honor) Kwame Nkrumah University of Science and Technology, Ghana, West Africa (2009-2013)

EXPERIENCE

Graduate Teaching Assistant, Chemistry Department, College of Arts and Sciences, East Tennessee State University, Johnson City Tennessee (2014-2016)

Teaching Assistant, Chemistry Department, College of Science, Kwame Nkrumah University of Science and technology, Kumasi, Ghana (2013-2014)

PUBLICATIONS

R. Tia, E. Asempa, E. Adei, "Computational Studies of the Reactivity, Regio-Selectivity and Stereo-Selectivity of Pericyclic Diels-Alder Reactions of Substituted Cyclobutenones", *J. Theor. Comput. Sci.* (2014) 1:114.

E. Asempa, Scott J. Kirkby, "Computational Studies of Spin Trapping of Biologically Relevant Radicals by New Heteroaryl Nitrones", Abstracts,

71st Southwest/67th Southeast Joint Regional Meeting of the American Chemical Society, Memphis, Tennessee, United States, 4-7 November 2015 (2015) COMP-15, American Chemical Society, Washington, D.C.

E. Asempa, Scott J. Kirkby, "Computational Studies of Spin Trapping of Biologically Relevant Radicals by New Heteroaryl Nitrones", Abstracts of Papers, 251st ACS National Meeting, San Diego, CA, United States, 13-17 March 2016 (2016), COMP-514, American Chemical Society, Washington D.C.

E. Asempa, Scott J. Kirkby, "Computational Studies of Spin Trapping of Biologically Relevant Radicals by New Heteroaryl Nitrones," Abstract 81, 2016 Appalachian Student Research Forum, ETSU, Johnson City, Tennessee, 6-7 April 2016.

GRANT Applied for and awarded

Eyram Asempa and Scott Kirkby, ETSU School of Graduate Studies and ETSU Graduate Council Research Grant (2015-2016) "Computational Studies of the Spin Trapping of Biologically Relevant Radicals by New Heteroaryl Nitrones": $800